NTNU

Norwegian University of
Science and Technology

Process simulation and evaluation of options for heat and power generation on offshore oil and gas installations

Jonas Brenntrø

Master of Energy and Environmental Engineering
Submission date: June 2016
Supervisor: Lars Olof Nord, EPT

Norwegian University of Science and Technology
Department of Energy and Process Engineering

NTNU

Norwegian University
of Science and Technology

Department of Energy
and Process Engineering

EPT-M-2016-22

MASTER THESIS

for

student Jonas Brenntrø

Spring 2016

Process simulation and evaluation of options for heat and power generation on offshore oil and gas installations

Background and objective

On offshore oil and gas installations the power demand is high. Process heat is also needed. In addition, the power plant should be flexible to be able to adjust to the needs of the oil and gas processes on the platform or FPSO both short and long term. The current dominating technology is based on simple cycle gas turbines. Other options currently installed on the Norwegian continental shelf includes gas turbines with waste heat recovery units (WHRU), electricity from onshore, and combined cycle plants with steam bottoming cycle.

The overall objective of the Master's thesis is to make detailed process models of different designs for generation of both heat and power on offshore installations and subsequently simulate the process and generate results such as power and heat output, plant efficiency and CO_2 emissions. The work should build on the specialization project completed in December 2015. Emphasis should be put on off-design operation to evaluate the flexibility and efficency of the designs seen over the full platform lifetime. How is the CO_2 emitted change when evaluating the full platform lifetime with different heat and power loads compared to just considering the design-point case? Investigate how different designs and selection of design-point can give lower CO_2 emissions and allow for more flexible operation.

The following tasks are to be considered:

1. Literature study on off-design process modeling and simulation and electrification of the Norwegian continental shelf.
2. Build up process models of the selected cycles with a focus on off-design models and operational flexibility.
3. Model validation with industrial or literature data.
4. Quasi-dynamic simulations for different operating scenarios to consider the full platform lifetime. Modification of the design and the design point to achieve the lowest CO_2 emissions over the lifetime and allow for flexible operation to changes in heat and power demand.
5. Sensitivity analysis to investigate which input parameters effect the results the most.

Within 14 days of receiving the written text on the master thesis, the candidate shall submit a research plan for his project to the department.

When the thesis is evaluated, emphasis is put on processing of the results, and that they are presented in tabular and/or graphic form in a clear manner, and that they are analyzed carefully.

The thesis should be formulated as a research report in English with summary, conclusion, literature references, table of contents etc. During the preparation of the text, the candidate should make an effort to produce a well-structured and easily readable report. In order to ease the evaluation of the thesis, it is important that the cross-references are correct. In the making of the report, strong emphasis should be placed on both a thorough discussion of the results and an orderly presentation.

The candidate is requested to initiate and keep close contact with his/her academic supervisor(s) throughout the working period. The candidate must follow the rules and regulations of NTNU as well as passive directions given by the Department of Energy and Process Engineering.

Risk assessment of the candidate's work shall be carried out according to the department's procedures. The risk assessment must be documented and included as part of the final report. Events related to the candidate's work adversely affecting the health, safety or security, must be documented and included as part of the final report. If the documentation on risk assessment represents a large number of pages, the full version is to be submitted electronically to the supervisor and an excerpt is included in the report.

Pursuant to "Regulations concerning the supplementary provisions to the technology study program/Master of Science" at NTNU §20, the Department reserves the permission to utilize all the results and data for teaching and research purposes as well as in future publications.

The final report is to be submitted digitally in DAIM. Based on an agreement with the supervisor, the final report and other material and documents may be given to the supervisor in digital format.

☐ Work to be done in lab (Water power lab, Fluids engineering lab, Thermal engineering lab)
☐ Field work

Department of Energy and Process Engineering, 13. January 2016

Olav Bolland
Department Head

Lars Nord
Academic Supervisor

Preface

This master thesis was written at the Department of Energy and Process Engineering, Faculty of Engineering Science and Technology at the Norwegian University of Science and Technology, NTNU, as a fulfilment of a Master of Science degree in Energy and Environmental Engineering. It was written during the spring of 2016 under the guidance of my supervisor, Associate Professor Lars O. Nord and with the help of PhD Candidate Luca Riboldi.

I would like to thank Lars O. Nord for help and expertise during the months it took to write this thesis.

Trondheim, 8-June-2016

Jonas Brenntrø

Abstract

In the efforts of trying to reduce global greenhouse gas emissions, the Norwegian oil and gas industry is looking for ways to improve efficiencies when supplying heat and power offshore. By making a scenario of a platform with set heat and power requirements, this thesis tries to answer the question, "*What are good options for heat and power generation offshore and how do they perform in a lifetime analysis?*"

To answer that question, the modelled platform scenario had varying ambient temperature according to North Sea weather data, and a typical heat and power profile, with a maximum power requirement of 60 MW and a maximum heat requirement of 22 MW. The platform's lifetime was assumed to be 20 years. 7 different cases were modelled and tested in the process simulation software, Ebsilon Professional, with the VTU gas turbine library. To evaluate the designs, focus was put upon lifetime CO_2 emissions and flexibility.

A case of two GE LM2500+G4 with WHRUs, the most common power technology used offshore, gave a total lifetime emission of 3.99 mega tonnes CO_2. The best alternative for the modelled platform were thought to be a combination of a simple cycle and a combined cycle: One LM2500+G4 giving off heat to a WHRU while another LM2500+G4 providing heat to an OTSG that drives a steam extraction cycle. It had high flexibility and low lifetime emissions of 3.20 mega tonnes CO_2.

A case of electrifying the platform was also evaluated, with using a gas boiler to provide process heat. It was found that the results were highly dependent on assumed associated emission ratings to onshore electric power. With an assumption of marginal power coming from EU and predicted future emission rates, the electrification case gave off 3.60 mega tonnes CO_2. The longer a platform operates or the later it is built; the more favourable electrification becomes due to predicted cleaner electric energy in the future.

Sammendrag

I arbeidet med å prøve å redusere de globale klimagassutslippene, er den norske olje- og gassindustrien på jakt etter måter å forbedre effektiviteten av prosessvarme og strøm offshore. Ved å lage et scenario av en plattform med ett sett varme og strømforbruk, forsøker oppgaven å svare på spørsmålet: "*Hva er gode alternativer for varme og kraftproduksjon offshore og hvordan yter de i en livsløpsanalyse*?"

For å svare på spørsmålet, hadde den modellert plattformen en varierende omgivelsestemperatur i henhold til værdata fra Nordsjøen, og en typisk varme og strøm profil, med maksimalt effektbehov på 60 MW og et maksimalt varmekrav på 22 MW. Plattformens levetid ble antatt å være 20 år. 7 forskjellige 'cases' ble modellert og testet i simuleringsprogrammet Ebsilon Professional, med VTU's gassturbinbibliotek. For å evaluere designene, ble livstid CO2-utslipp og fleksibilitet primært evaluert.

En 'case' med to GE LM2500+G4 med WHRUs, den vanligste kraftteknologien som brukes offshore, ga en total levetidsutslipp på 3,99 megatonn CO2. Det beste alternativet for den modellerte plattformen ble antatt å være en kombinasjon av en enkel syklus og en kombinert syklus: en LM2500+G4 som avgir varme til en WHRU mens en annen LM2500+G4 avgir varme fram eksosen til en OTSG som driver en dampsyklus med dampekstraksjon. Den hadde høy fleksibilitet og lave levetidsutslipp på 3,20 megatonn CO2.

Elektrifisering av plattformen ble også vurdert, med hjelp av en gasskjele for prosessvarme. Resultatene var svært avhengig av antagelser av de tilhørende CO_2-utslippene av den landbasert elektriske kraften. Med en forutsetning at den marginale kraften kommer fra EU og at elektrisk energi blir renere i framtiden, ga elektrifiseringscasen ett utslipp på 3,60 megatonn CO_2. Jo lengre en plattform er i drift eller hvor senere den er bygget; desto mer gunstig ble elektrifisering på grunn antatt renere elektrisk energi i fremtiden.

Table of Contents

Nomenclature

AC	Alternating current		
CAPEX	Capital expenditure		
CC	Combined cycle		
CCGT	Combined cycle gas turbine, same as CC		
CCHP	Combined cycle heat and power		
CCS	Carbon capture and storage		
CHP	Combined heat and power		
CV	Control volume		
DC	Direct currrent		
ER	Emission rate		$kgCO_2/MWh$
ETS	Emission Trading System		
EU	European Union		
EU	European Union		
EUF	Energy utilization factor		-
GE	General electric		
GGE	Greenhouse gas emissions		
GT	Gas turbine		
HP	High pressure		bar
HRSG	Heat recovery steam generator		
HVAC	High voltage alternating current		
HVDC	High voltage direct current		
IEA	International Energy Agency		
LCA	Life cycle analysis		
LHV	Lower heating value of fuel		J/kg
LP	Low pressure		bar
Mt	Mega tonnes		10^9 kg
NCS	Norwegian continental shelf		
NEEDS	New Energy Externalities Development for Sustainability		
NG	Natural gas		
NO_X	Nitrogen oxides, primarily NO and NO_2		
OPEX	Operational expenditure		
OSTG	Once through steam generator		
RH	Relative humidity		-, %
ST	Steam generator		
TIT	Temperature inlet turbine		
TL	Transmission losses		
VOC	Volatile organic compounds		
WEO	World Energy Outlook		
WETO	World Energy Technology Outlook		
WHRU	Waste heat recovery unit		
Latin letters			
A	Area		m^2
c_p	Specific heat capacity		J/kg k

E	Energy		J
g	Gravitation constant	~9.81	m/s^2
h	Specific enthalpy		J/kg
H	Head		J/kg
m	Mass		kg
M	Molecular weight		kg/kmol
$\dot{m}$	Mass flow		kg/s
n	Polytropic exponent		
Q	Heat duty		J
$\dot{Q}$	Heat flow		J/s, W
R	Specific gas constant		
R_0	Gas constant	8314	J/kmol k
s	Specific entropy		J/kg k
S	Entropy		J/k
T	Temperature		K
t	Time, time period		s, h, year
U	Internal energy		J
U	Heat transfer coefficient		W/m^2K
u	Specific internal energy		J/kg
v	Relative velocity		m/s
v	Specific volume		m^3/kg
$\dot{V}$	Volume flow		m^3/s
W	Work		J
w	Specific work		J/kg
$\dot{W}$	Work per second, power		W
x	steam quality		-
Z	Compressibility function		-
Greek letters			
Δ	Delta, change from one state to another		
η	Efficiency		-
κ	Specific heat ratio, isentropic exponent		-
κ_T	Isentropic temperature exponent		-
κ_V	Isentropic volume exponent		-
ρ	Density		kg/m^3
σ	Irreversibilities, entropy change		J/K
Subscripts			
0	Reference value		
1	Stage 1 or input		
2	Stage 2 or exit		
b	Boundary		
C	Cold		
c	Carnot		
crit	Critical condition		
CV	Control volume		
e	Component number, exit		
el	electrical		

fg	Fluid/gas, phase transition		
g	Gas		
GT	Gas turbine		
H	Hot		
h.e.	Heat exchanger		
i	Component number, in		
int rev	Internal reversible process		
j	Component number		
l	Liquid		
lm	Logarithmic mean		
p	Polytropic		
pinch	Pinchpoint		
rev cycle	Reversible cycle		
s	Isentropic		
sat	Saturated vapour or liquid		
ST	Steam turbine		
steam	Steam in the Rankine cycle		
T	Temperature		
v	Specific volume		

1. Introduction

1.1 Background

The reduction of greenhouse gas emissions (GGE) to avoid having a higher global warming than a 2 °C increase within the year 2100, calls for stricter emission reductions in Norway and EU. [1] One of the central ways to reduce national emissions is to find and consider more efficient and environmentally-friendly alternatives for providing heat and power on the North Continental Shelf (NSC).

The Norwegian petroleum industry is one of the world-leading petroleum industries when it comes to environmental and climate standards. But still there are room for improvements. In 2013, GGE from petroleum activities corresponded to about 13.5 million tons CO_2 equivalents. That is about 25 % of Norway's total GGE. Comparatively, Norway's transport sector accounts for roughly 32 %. Of those CO_2 equivalents emitted from the petroleum industry, about 81 % came from gas turbines in 2015, mainly to produce power. [2] Considering that only 45 % of the estimated total recoverable resources on the NCS has been produced so far and that Norway expects to keep producing oil and gas for the foreseeable future, there are large incentives to reduce emissions from power production offshore. [3]

One of the most promising power technologies to improve efficiencies and reduce emissions offshore, is the use of steam bottoming cycles. A lot of research has been performed trying to increasing the efficiency of power production offshore by the use of this technology. To this date there are only 3 offshore facilities that have installed combined-cycle gas turbines in the world, all 3 are currently operating in Norway on the Oseberg, Snorre and Eldfisk fields. Carbon separation from produced gas and storage is also a technology used to reduce global emissions. The Sleipner Vest field and the Snøhvit field combined stores about 1.7 million tonnes CO_2 annually. Some of the major incentives Norway use upon operators on the NCS to utilize more efficient technologies to reduce emissions are CO_2 taxation and the EU Emissions Trading System. [4] The average cost of CO_2 emissions offshore in 2015 were about 500 NOK per tonne CO_2.

Another way to reduce emissions offshore is to electrify platforms with onshore power by subsea cables, assuming that the energy coming from land comes from clean sources. But many platforms use heat recovered from the gas turbine flue gas for process heat. Then it is important

to find good alternatives for providing necessary process heat offshore in case of onshore electricity.

This thesis will study the heat and power production offshore using the three currently most prominent heat and power technologies offshore; the simple gas turbine cycle, the combined cycle and electrification.

1.2 Objectives

The objective of this thesis was to find and study different alternatives for supplying heat and power offshore and make detailed process models and quasi-dynamic simulations. Accordingly, the research question was:

"What are good options for heat and power generation offshore and how do they perform in a lifetime analysis?"

To answer that, results, such as lifetime CO_2 emissions, flexibility and sensitivity were used in evaluating the performance of the different technologies. To do so, a model of an offshore platform with set requirements of power and process heat were made and different technological alternatives where evaluated while serving the platforms needs. First the most common way to generate heat and power offshore was investigated: Simple cycle gas turbines with WHRUs. It was then compared with different steam bottoming technologies with steam extraction and backpressure. At last simulations of offshore electrification were performed. Ebsilon Professional [5] was used combined with the VTU gas turbine library [6] to perform the simulations. To compare the different alternatives for heat and power offshore following tasks were concluded:

1. Literature study on relevant technologies for power and heat supply and off-design process modelling and electrification of the NCS.
2. Building of process models with focus on off-design flexibility.
3. Validation with literature data.
4. Quasi-dynamic lifetime simulations, design screening and optimization of the best suited designs.
5. Sensitivity analysis of the chosen designs.

A qualitatively literature study of weights, flexibility and responsiveness were done to compare the different technologies as well as the lifetime efficiencies and CO_2 emissions.

1.3 Contributions

The main contributions to this study was simulations of models considered for off-design operations, done in Ebsilon Professional. Lifetime simulations made in EbsScript simulated varying ambient temperatures, heat loads and power loads. First a simple cycle with two LM2500+G4 gas turbines to provide power and WHRUs attached to provide process heat was simulated. Then it was compared with gas turbines with steam bottoming cycle technology and steam extraction or backpressure to provide heat. In the case of electrification of the platform, emission ratings associated with onshore power were predicted and used, and a gas boiler provided process heat. Table 1.1 below gives an overview of the simulated cases in this thesis.

Table 1.1 Overview of the simulated cases with a short description and gas turbines used.

Case	Short description	Gas turbines used
1a	Simple cycle with WHRU	2x LM2500+G4
1b	Simple cycle with WHRU, different GTs.	1x LM2500+G4 1x LM6000PF S25
2a	Combine cycle with steam extraction	1x LM2500+G4 1x LM2500PJ
2b	Combined cycle with steam extraction and separated GT with WHRU	2x LM2500+G4
2c	Combined cycle with backpressure	1x LM2500+G4 1x LM2500+
2d	Combined cycle with a gas boiler	1x LM6000PF S25
3	Electrification from onshore with a gas boiler	-

1.4 Limitations and assumptions

Due to the restricted time and resources, following limitations apply:

- Dynamical behaviour not included.
- Regular offshore process restrictions were followed but only a limited weight and area assessment of equipment were included.
- Simplifications were done in modelling of the designs but it was tried to keep the simulations reflective and conservative comparing to real life designs.
- Primarily CO_2 was considered when looking at GGE, while NO_X reduction was reduced by using DLE-technology gas turbines.
- Economic costs of different technologies were largely not evaluated.

- Socio-economic costs and life cycle assessment (LCA) CO_2 costs were assumed negligible after de-commissioning and recycling.
- Focus on global, not national GGE in case of electrification.
- Mainly assumed EU marginal power while evaluating electric CO_2 emissions.
- Bottlenecks in the power grid when supplying onshore power were not considered.

1.5 Risk assessment

No field work or laboratory work was done in relation with this thesis. Therefore, no risk assessment was performed.

2 Heat and power generation offshore

It is more than 50 years ago since the Norwegian petroleum history started and it has played a key role in the welfare development in Norway. [7] Since production started it is estimated that over 50 % of the estimated total recoverable resources still remains. Oil and gas production in Norway had its peak in 2001 but, because of new smaller fields combined with some of the larger fields are getting nearer the end of their lifetimes, the production has remained stable the last years and is predicted to remain relatively stable in the years to come, as seen in Figure 2.1. Already existing activity is what will keep the production steady even though the decreased oil prices the recent year has postponed many recent investments on the NCS. [8]

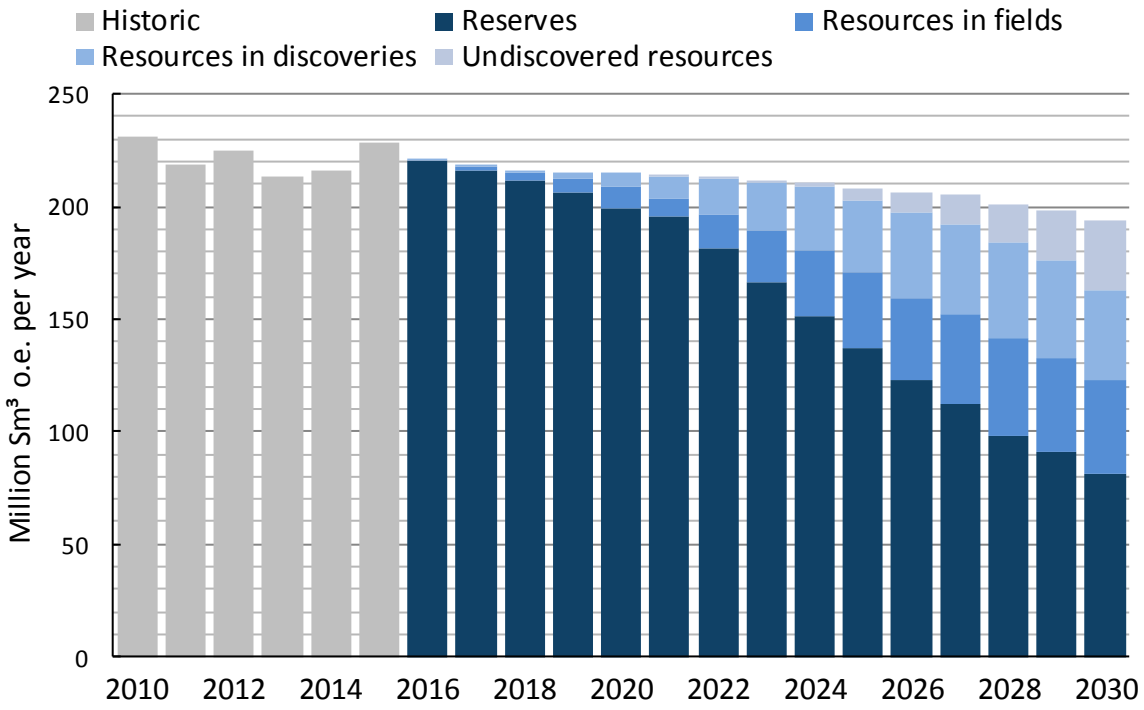

Figure 2.1 Oil and gas production history and forecast on the North continental shelf, 2010-2030. [8]

To maintain the predicted oil and gas production in Norway, while also taking care of the environment and meeting national and global emissions goals to reduce global warming, better energy efficiency and better solutions for producing power offshore is needed. The next sub-chapter will look into emissions to air from the offshore petroleum industry. It will try to show why energy efficiency and better solutions for producing power offshore is an important part for the future oil and gas industry.

2.1 Greenhouse gas emissions to air

This thesis will mainly focus on CO_2-emissions, which is the primary air emissions from power production offshore, along with NO_X. CO_2 emissions are the main contribution related to the greenhouse effect and global warming and ocean acidification. [9] NO_X on the other side, affects ecosystems and wildlife more directly by acidification of soil and river systems. [2] Although NO_X-emissions are not directly accounted for in this thesis it is minimized by utilizing DLE (Dry Low Emissions) gas turbine technology, which will be looked more into in when discussing power technologies in chapter 4.

From 1990 to 2006 the CO_2 emissions per produced oil equivalent on the North Continental Shelf (NCS) was reduced by 20 %, mainly due to reduced flaring and increased energy efficiency. The introduction of the CO_2 tax in 199 have helped increase energy efficiency, as well as general technology advancements. [10] But because of increased activity, and the increased gas production and compression, the total CO_2 emissions in the Norwegian petroleum sector has increased, as shown in Figure 2.2 below.

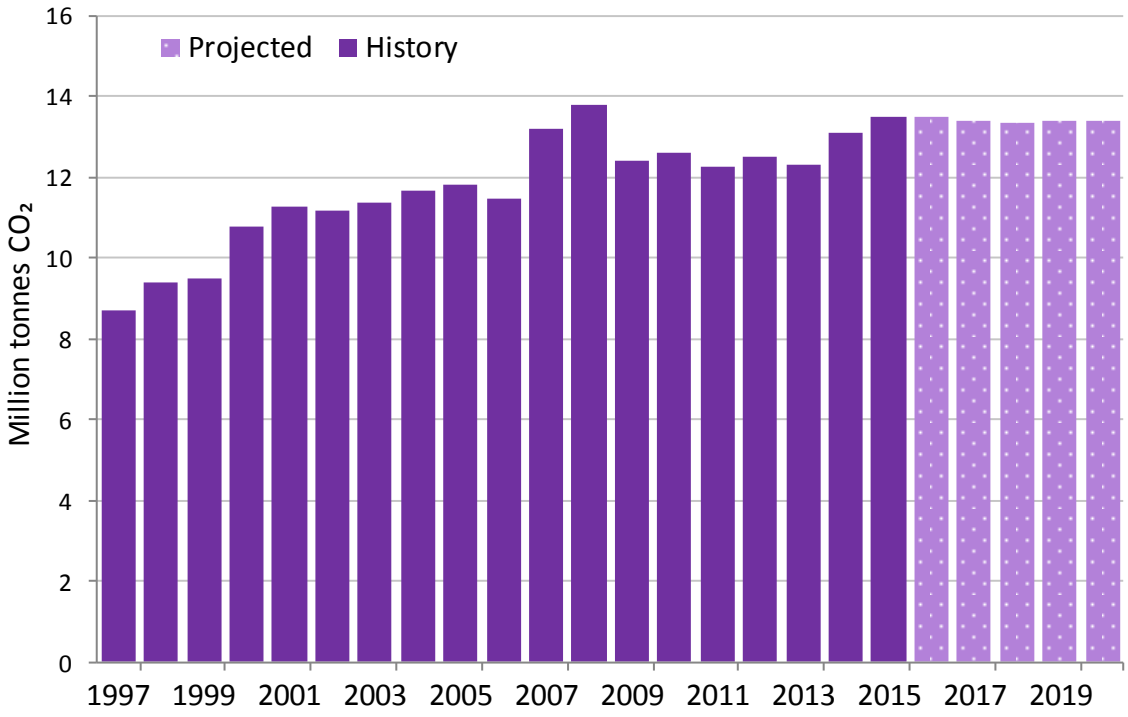

Figure 2.2 Historical and projected emissions of CO_2 from the Norwegian petroleum sector, 1997-2020. [2]

Before a discovery can be developed offshore, a plan for development and operation (PDO) must be in order, which have to include an overview of energy use as well as an assessment of use of power from shore instead of power production offshore. After that, the main instruments

in use to reduce GGE offshore are the carbon tax and the EU emission trading system. Both of these systems apply to the petroleum sector while most other industries have to only use on or the other.

The carbon tax from 1991 was almost doubled from 0.49 NOK/Sm^3 in 2012 to 0.96 NOK/Sm^3 in 2013, and is in 2016 at 1.02 NOK/Sm^3. The price for other liquid fuels, like condensate or oil, is the same at 1.02 NOK/l. The reason for taxing CO_2 by fuel usage is because it is much easier to measure than the CO_2 contents in the exhaust gas, and can be calculated by formula (2.1) below. The tax is an equivalent of 436 NOK per tonne CO_2. [2]

$$CO_{2,tax} = Sm3 \cdot l \tag{2.1}$$

Norway joined the European emission trading system (EU ETS) in 2008. It is a 'cap and trade' system where the total emitted CO_2 within the system is limited and reduced every year in accordance with GGE and global warming goals. If a company or installation emits more or less than the allotted emissions the exceeding amounts can be sold or bought in the EU ETS. Depending on industries activities, allowances can be allotted free of charge or bought and traded. Heat and power generation offshore are not given free of charge and in 2015 the price were between 50 and 80 NOK per tonne CO_2. Including the Norwegian CO_2-tax, that gives a total price of ca. 500 NOK per tonne CO_2. [2]

The cap and trade system gives an economical dynamical incentive to reduce emissions if CO_2 prices are high. That way, CO_2 emissions will be reduced where it is most cost effective first while where it is harder to reduce emissions will have to bear the cost. But due to recession or a too high emissions cap, the EU ETS has been constrained the last year by a surplus of allowances that has kept the price too low to incentivise low-carbon investments. To rectify that situation and increase market stability, the EU agreed in 2015 to introduce a Market Stability Reserve that allows reduction of allowances. [1]

That also rectifies another important problem which comes when reducing CO_2 emissions one place within the EU ETS: When reducing the emissions at one place it only frees up allowances, reduces the CO_2 price and moves the emissions somewhere else within EU. That argues for reducing CO_2 emission on the NCS only reduces national emissions levels while not effecting EU and global emissions and does not reduce global warming. But by introducing the Market Stability Reserve ensures that developments reducing CO_2 emissions lead to a lower market

price which then again can potentially induce a more ambitious CO_2 policy and globally lower the CO_2 emissions. [11]

Figure 2.3 shows the source of CO_2 emissions offshore. It shows that GTs for power production and direct drive is the major emission source with 81.1 % of total petroleum emissions in 2015. Therefore, a good way to reduce emissions is to increase efficiencies of power production offshore and consider different alternatives.

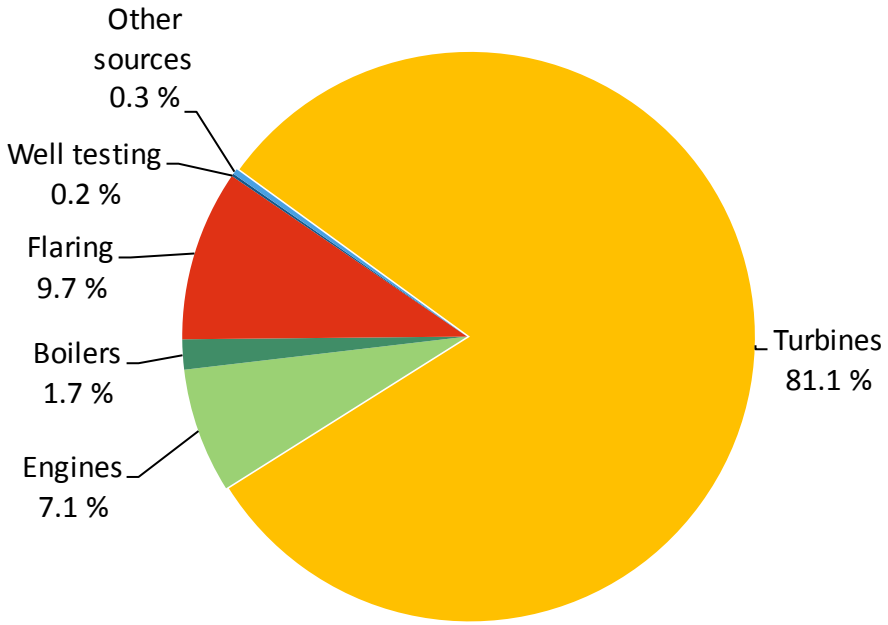

Figure 2.3 CO_2 emissions by category from petroleum activities in 2015. Total emissions: 13.484 million tonnes CO_2. [2]

The Norwegian petroleum sector is world leading in uses to reduce greenhouse gas emissions and emissions per unit oil is lower than in any other petroleum producing countries. As well as having more efficient equipment and better energy managements systems, the Sleipner Vest field, the Gudrun field and Snøhvit on Melkøya all separates CO_2 from produced natural gas and store it in formations or returns it back to the fields. When it comes to supplying more environmentally friendly power, CCGT plants are installed on the Oseberg, Snorre and Eldfisk fields. And Ormen Lange, Snøhvit, Troll 1, Valhall and Goliat are already supplied by onshore power while Martin Linge, Johan Sverdrup and the Utsira High formation will be fitted with onshore power in the future. Before going more deeply into the different prominent technologies for providing power, an overview of heat and power generation restrictions will be looked more into.

2.2 Heat and power generation offshore

The need of power and heat on an offshore platform is highly dependent on what type of field is being developed. It can vary if the field is primary an oil or gas field, characteristics of the oil and gas extracted, what topside processing is required, and injection, export and compression needs. The heat and power intensity, the energy needed to extract per unit oil or gas, is also likely to increase over time as the field develops, as illustrated in Figure 2.4. Platforms can have a large variation in power demand while platforms that for example export gas is more likely to have a more stable power need. Therefore, it is important that the heat and power production on a platform is flexible and can adapt. Some of the largest power and heat consumers on a platform can include oil and gas injections into the well, separation, recompression, export pumps and treatment of oil, gas condensate and water.

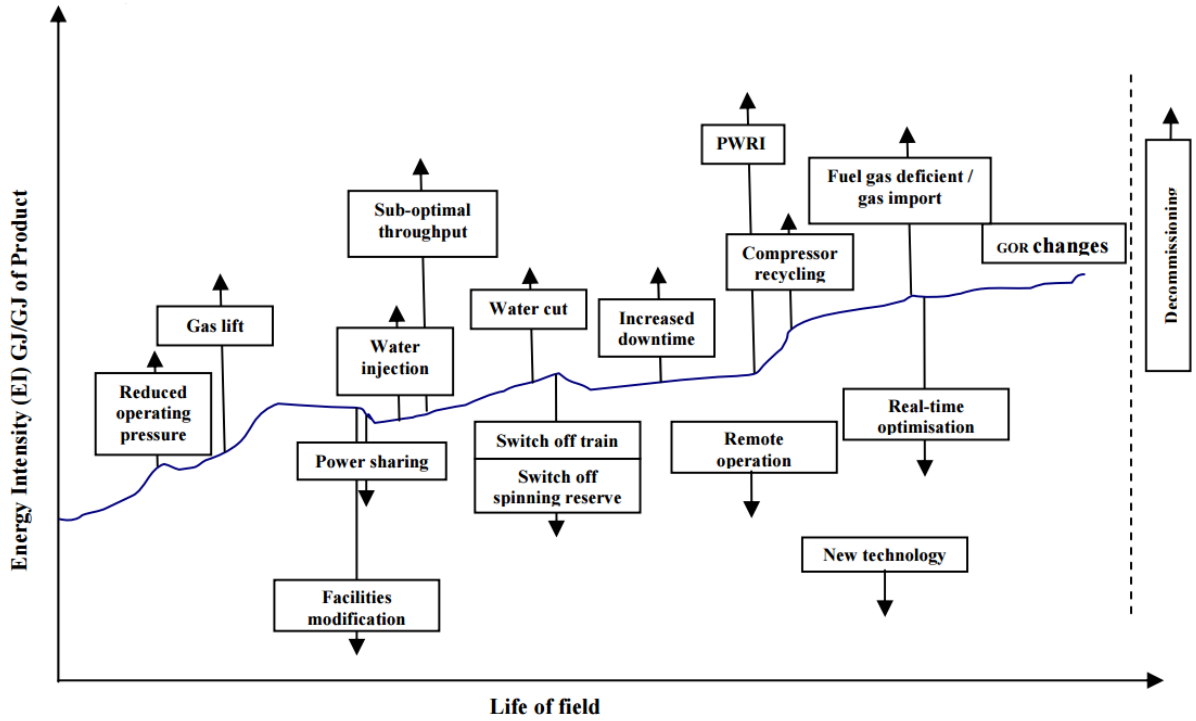

Figure 2.4 A purely illustrative rendering of key events and the change of energy intensity in a field's lifetime. [12]

While energy intensity normally increases during the life of a field, oil and gas production usually goes up to a plateau at maximum production, stays there for a while, and then decreases to the end of the field's life when production is not high enough to justify operating the field any longer. A typical production profile can be seen in Figure 2.5 where produced water, sand and solids are also included. The combination of increase in energy intensity and the production profile give power profiles that are usually high in the start of a fields lifetime and then plateaus

to a lower power demand to the end of a field's life time, which will be discussed more in the model description in chapter 5.

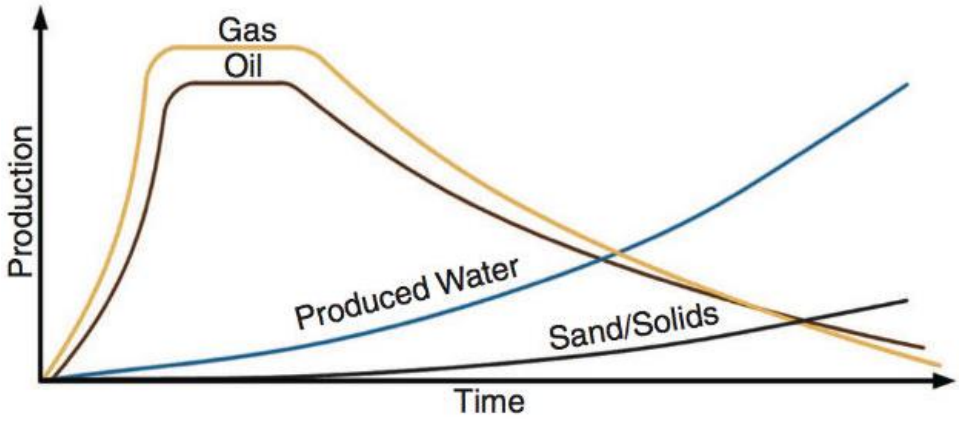

Figure 2.5 An illustrative typical oil well production profile. [13]

Most of the process heat needed offshore is also highly dependent on oil and gas production as it is mostly used to stabilize condensate, separate the crude oil and dehydrate gas. Energy intensity for heat is also likely to rise due to higher amounts of produced water, especially on gas fields, but not to the same degree as the energy intensity for power. Table 2.1 show the most common process heat needs and the temperature ranges.

Table 2.1 Overview of where process heat is commonly needed offshore and its temperature. Crude oil separation is usually the largest heat consumer. [14, 15]

Process heat	**Temperature [°C]**
Gas dehydration, glycol reboiling	205
Condensate stabilization column	180-200
Crude oil separation	45-90
Fuel gas heating	40-60

Ideally, power production offshore requires high power to weight ratios and compact technology, due to the high expenses and limited space on instalments offshore. Robustness, reliability, easy maintenance, flexibility, fast start-up times are also variables greatly desired due to operation costs, high production costs during failure and variable heat and power loads. All these traits make aeroderivative gas turbines ideal for offshore power production and it is the reason why it is the number one power technology in use offshore. Recently higher efficiency has become more into focus due to emissions concerns and that is the primary reason why modifications and alternatives to gas turbines are being looked into. [16, 17] Process heat can easily be produced when a WHRU is attached to the exhaust of a gas turbine and is viewed upon as a major energy saving. Gas turbines usually use gas processed at the platform but that

is not always accessible, especially during the commissioning of a platform, therefore many gas turbines are dual-fuel turbines and can utilize for example diesel as a secondary fuel.

Due to the increased CO_2 taxation, technologies to enhance the efficiencies and reduce emissions offshore has been made more economically feasible, like the steam bottoming cycle. Despite all the work that has been done to find alternatives, the steam cycle still remains the obvious choice as the bottoming cycle for gas turbines onshore but it is also currently the most prominent bottoming technology offshore. [18] It takes heat from the gas turbine flue gas and use it to produce steam in a heat recovery steam generator. Then the superheated steam is let through a steam turbine and the energy in the steam is transformed to mechanical energy that can be utilized in a generator. That way the power production increases without affecting the gas turbine to a large degree, and the net efficiency increases. Yet the increased efficiency of a combined cycle and reduced emission taxes have to be weighted in opposition of higher instalments costs, lower power to weight ratios and the risk of less proven technology and potentially lower flexibility. Therefore, it is important with thorough research in the use of steam bottoming cycle so those risks can be lowered and variables like power to weight ratios can be increased. Another possible option for reducing emissions offshore on the NCS is electrification from onshore.

2.3 Electrification

By the use of subsea direct current or alternating current power technology, energy can be transferred from land to offshore platforms. A large fraction of onsite CO_2 emissions can be reduced by laying cables from shore to offshore platforms instead of using gas turbines onsite. In that case gas or electrical burners can be used to provide heat. Especially in Norway it seems like a good idea to replace gas turbines that burn fossil fuel with hydropower and 'clean' energy. But the electrification is more complicated than that and this sub-chapter will try to go through the most important factors such as abatement costs, where the extra produced power will come from and electrical emission ratings (ER, g CO_2/kWh).

Most research about current planned electrification projects conclude that the abatement cost of CO_2 is higher than the current price of 500 NOK per tonne. [19-21] Even though it may make sense on a national level to reduce GGE by considerable expensive electrification, one can argue that the resources could be spent much better and reduce a lot more global GGE other places or other countries with much lower CO_2 prices. That could also give a higher effect on reducing the EU ETS CO_2 price and bring about a lower emission cap. Some of the money

could instead of electrification also be spent on research which could benefit several parts of the world to reduce emissions.

It is also important to consider where the extra produced power to supply offshore platforms would come from. There is two ways to consider it. Either the power comes from the average Norwegian el.mix (electrical mix) by all the power plants produce slightly more power or it has to come marginally from a specific power source. Norway has well developed hydro power with few places left to expand and the variation of power produced every year is mostly due to rainfall. Therefore, this thesis argues that most power provided to electrification would either have to be imported from Europe or a reduction in export of power, with both having the same conclusions that more power has to be produced in less clean European power plants. A way to counteract this is to build wind power or CCGT power plants specifically because of offshore electrification. But if it is economically feasible to build new power plants it is likely to be built regardless of offshore electrification.

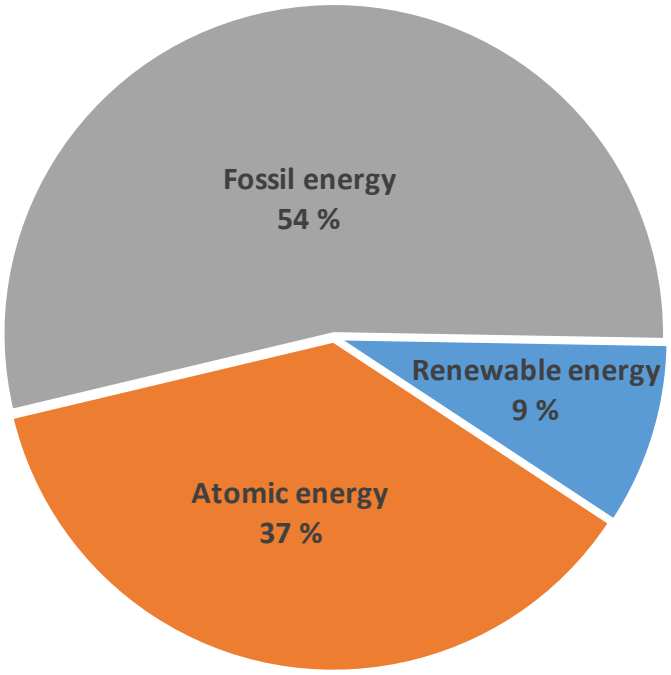

Figure 2.6 Trade declaration of electrical energy bought in Norway in 2014 without paying for guarantees of origin. [22]

Even though 98 % of the power generated in Norway is from renewable energy sources, far from the majority of the energy used in Norway is considered clean anymore due to the implementation and selling of green energy licenses abroad. Of the 132.2 TWh issued green energy licenses in 2014, only 19 TWh was bought in Norway. The resulting energy make-up

provided to Norwegian energy consumers can be seen in Figure 2.6. [22] Theoretically, offshore platforms can buy green energy at an increased cost, which may increase the price and development of environmentally friendly power alternatives. But the use and sale of green licenses and its importance is considered arbitrary by the author, or else most the Norwegian power consumption must be seen as heavily polluting according to Figure 2.6 and Norwegian emissions have to be adjusted accordingly.

It is also important to include the change in CO_2 prices and electrical emission ratings during the full lifetime of a project. Even if the ER is high now and CO_2 prices are low, it is likely to change because of the goal of reducing GGE every year. WEO 2015's most modest scenarios predict a EU ETS carbon pricing from 75NOK/tonne in 2014 to 251 NOK/tonne in 2030 and 335 NOK/tonne in 2040. And the ER is expected to drop from its current 520 g/kWh globally to 350 g/kWh globally in 2040. [1]

Chapter 5.3 will go through emissions related to electrifications used in this thesis while chapter 4 will go more in depth about the technical aspects of electrification and the other power cycles. But first some theory will be introduced in chapter 3 to better understand the calculations and principles underlying the power technologies evaluated.

3 Theory

This chapter covers essential thermodynamic theory and equations used in the different components and processes encountered in this project. Most of the calculations were either used to calculate results from the simulation outputs, control and check the results from the simulations to make sure they were thermodynamically possible and to calculate values and design points for certain components. This project is not extensive enough to include the derivation of all the formulas used. If deeper understandings of the theory in this chapter is wanted, the textbooks used in the different subchapters provide a great overview of detailed thermodynamic principles and process engineering.

3.1 Laws of thermodynamics

Principles of Engineering Thermodynamics by Moran and Shapiro [23] were used as source and to validate the thermodynamics theory presented here. The first and second law of thermodynamics provide the back bone of the understanding of the processes simulated.

3.1.1 3.1.1 First law of thermodynamics

The first law of thermodynamics, or the law of conservation of energy, is essential for calculating results and to check if any impossible calculations are being performed like more energy coming out of a control volume than energy coming in, at steady state. It is shown in equation (3.1) and says that the change in kinetic, potential or internal energy per unit time in a closed system is equal to heat going in or work going out of the system.

$$\frac{dE}{dt} = \dot{E}_{kinetic} + \dot{E}_{potential} + \dot{U} = \dot{Q} - \dot{W} \tag{3.1}$$

Conservation of mass in a control volume is important in most process calculations. The change in mass within a control volume must be equal to the sum of mass flows going into the system and mass flows going out of the system(3.2).

$$\frac{dm_{cv}}{dt} = \sum_i \dot{m}_i - \sum_e \dot{m}_e \tag{3.2}$$

The definition of enthalpy is shown below. Since enthalpy is not directly measurable but calculated from other data, a reference state has to be used if one is not only interested in enthalpy change. Enthalpy is often read from tables and often different tables uses different reference states, which is important to consider.

$$h = u + pv \tag{3.3}$$

$$W = \int_{V1}^{V2} p dV \tag{3.4}$$

Equation (3.4) shows work by expansive or compressive work. It can be used to expend the work term in (3.1) as shown in (3.5). It is also used to calculate compression and expansion work in equation (3.21).

$$\dot{W} = \dot{W}_{CV} + \dot{m}_e(p_e v_e) - \dot{m}_e(p_i v_i) \tag{3.5}$$

By expanding the work term and then combining it with the definition of enthalpy in (3.3) we get the energy balance equation in (3.6) which states that the change in energy is equal to heat going in minus work going out plus the change of enthalpy, kinetic energy and potential energy of streams going in and out of the system [23]. At steady-state, when there are no changes in time, the equation must be equal to zero. In most processing calculations the terms for kinetic and potential energy can be neglected.

$$\frac{dE_{cv}}{dt} = \dot{Q}_{cv} - \dot{W}_{cv} + \sum_i \dot{m}_i(h_i + \frac{V_i^2}{2} + gz_i) - \sum_e \dot{m}_e(h_e + \frac{V_e^2}{2} + gz_e) \tag{3.6}$$

3.1.2 3.1.2 Second law of thermodynamics

The Kelvin-Plank statement of the second law of thermodynamics explains losses involved in thermodynamic processes and the exchange of heat:

> *"It is impossible for any system to operate in a thermodynamic cycle and deliver a net amount of energy by work to its surroundings while receiving energy by heat transfer from a single thermal reservoir"[23]*

In simpler terms it means that it's impossible to get more energy out of a cycle than what is put in. The best case scenario is a reversible cycle with no losses, usually called the Carnot cycle. The Carnot efficiency is shown in (3.7) below and is used to determine how far the efficiency of a process is from a cycle without any losses and it can help to identify irreversibilities in the process.

$$\eta_C = \left(\frac{W_{cycle}}{Q_H}\right)_{\substack{rev \\ cycle}} = \left(1 - \frac{Q_C}{Q_H}\right)_{\substack{rev \\ cycle}} = 1 - \frac{T_C}{T_H} \tag{3.7}$$

Entropy is a property much like enthalpy but used to evaluate losses and irreversibilities in processes. It has to be calculated from other measurable properties and a reference state is needed when looking at absolute entropy. The change in entropy is defined by equation (3.8). The last term, σ, identifies losses and it would be zero if the process was internally reversible.

$$S_2 - S_1 = \int_1^2 \left(\frac{\delta Q}{T} \right)_b + \sigma \tag{3.8}$$

The change of entropy in a control volume over time is shown in (3.9) and includes entropies of masses going in and out of the CV. The change will be zero if the process is at a steady state. [23]

$$\frac{dS_{cv}}{dt} = \sum_j \frac{\dot{Q}_j}{T_j} + \sum_i \dot{m}_i s_i - \sum_e \dot{m}_e s_e + \dot{\sigma}_{cv} \tag{3.9}$$

3.2 Compression and expansion

This subchapter will cover the compression and expansion theory used for calculating performance of compressors and turbines, which was used in this thesis to validate and control the performance of the gas turbines and steam turbines used in Ebsilon professional and the VTU library. [6] Even though the gas turbine components used function more like a 'black box' with only inputs and outputs with compression, combustion, heat exchanging and expansion going on inside it, the theory can still be used to validate the results to a certain degree and check if power and heat outputs are reasonable. It will focus on real gas polytropic case but will include differences to isentropic calculations, which were used for the steam turbines. Most of the theory is based on *Gas Turbine* Theory by Saravanamutto [17] and information from Lars. E. Bakken [24].

The main difference between isentropic and polytropic calculations is the temperature and volume exponents in use, κ_T and κ_v for the isentropic case which can be used interchangeably with n_T and n_v for the polytropic efficiency case. (3.11) show how to use the polytropic exponent instead of κ which would be used in the isentropic case. κ_T and κ_v would be calculated in the same was as n_T and n_v in, (3.15) and (3.20) respectively, only with isentropic calculations instead of using polytropic efficiency, η_p. For ideal gas; $\kappa_T = \kappa_v = \kappa$ and $n_T = n_v = n$.

Most of the theory will be showed for a compression process. The main difference between expansion and compression processes is that usually only a general polytropic exponent, n, is

used for expansion processes and that some of the formulas for calculating power and head is altered to give positive values for both compression and expansion.

The generalized polytropic process is shown in (3.10) and the use of *n*, the polytropic exponent, in (3.11) and κ in (3.12). Equation (3.11) shows the main difference between calculating with polytropic exponents and isentropic exponents.

$$pv^n = const \tag{3.10}$$

$$\frac{n-1}{n} = \frac{\kappa - 1}{\kappa \eta_p} \tag{3.11}$$

$$\kappa \equiv \frac{c_p}{c_v} \tag{3.12}$$

By utilizing the real gas formula (3.13) into the general polytropic process (3.10);

$$pv = ZRT \tag{3.13}$$

one can calculate the temperature after a compression or expansion in formula (3.14).

$$T_2 = T_1 \left(\frac{p_2}{p_1} \right)^{\frac{n-1}{n}} \left(\frac{Z_1}{Z_2} \right) = T_1 \left(\frac{p_2}{p_1} \right)^{\frac{n_T - 1}{n_T}} \tag{3.14}$$

From that one can obtain the polytropic temperature exponent which varies with temperature, pressure and changes in temperature and pressure along the given polytropic efficiency curve:

$$n_T = \frac{1}{1 - \frac{p}{T} \left(\frac{\partial T}{\partial p} \right)_{\eta_p}} \tag{3.15}$$

The average polytropic temperature exponent is defined;

$$n_T = \frac{n_{T1} + 2n_{Tm} + n_{T2}}{4} \tag{3.16}$$

where

$$T_m = \frac{T_1 + T_2}{2} \tag{3.17}$$

and

$$p_m = \sqrt{p_1 p_2} \tag{3.18}$$

The polytropic volume exponent can be found the same way but more directly from the polytropic process;

$$pv^{n_v} = const \tag{3.19}$$

which gives:

$$n_v = -\frac{v}{p}\left(\frac{\partial p}{\partial v}\right)_{\eta_p} \tag{3.20}$$

When calculating the polytropic head, the exponent is assumed constant to be able to make an analytical calculation:

$$H_p = \int_1^2 v dp \approx \frac{n_v}{n_v - 1}\left[p_2 v_2 - p_1 v_1\right] \tag{3.21}$$

By using (3.19) and (3.13) we get an approximate solution:

$$H_p \approx f \frac{n_v}{n_v - 1} \frac{Z_1 R_0 T_1}{M}\left[\left(\frac{p_2}{p_1}\right)^{\frac{n_v - 1}{n_v}} - 1\right] \tag{3.22}$$

A correction factor *f* is used in (3.22) to account for the change in the volume exponent along the compression path, according to Schultz procedure [25], which is assumed equal for both isentropic and polytropic calculations:

$$f = \frac{h_{2,s} - h_1}{\frac{\kappa_v}{\kappa_v - 1}\left[p_2 v_2 - p_1 v_1\right]} \tag{3.23}$$

The definition of polytropic and isentropic efficiency can then at last be used to calculate the real head:

$$H = \frac{H_p}{\eta_p} = \frac{H_s}{\eta_s} \tag{3.24}$$

Schultz method [25] is extensively used in the industry when more accurate calculations are needed for performance analysis which uses compressibility functions *X* and *Y* as well as the familiar compressibility factor, *Z*, to determine more accurate exponents. It will not be gone further into because of the scope of this project but it is something the reader should be aware of.

3.3 Heat transfer

Only simple heat transfer calculations were performed in this project to check and control the performance of the different heat exchanger components used, based on the overall heat transfer coefficient, transfer area and the logarithmic temperature difference shown in equation (3.25). For the design point of heat recovery units and heat exchangers, pressure drop and minimum pinch point were used to limit the size and weight, which will be discussed more in chapter 4.2.4. The heat transfer equations are based on *Principles of Heat and Mass Transfer* by Incropera et.al [26].

$$Q = UA\Delta T_{lm} \tag{3.25}$$

The logarithmic mean temperature difference is calculated by the following equation, where ΔT_H is the temperature difference of the hot fluid in and cold fluid out and ΔT_C is the temperature difference of the hot fluid out and cold fluid in:

$$\Delta T_{lm} = \frac{\Delta T_H - \Delta T_C}{\ln\left(\frac{\Delta T_H}{\Delta T_C}\right)} \tag{3.26}$$

The ΔT_{lm} is governed by the temperature difference and thereby also by the pinch point, which will be most used in this project. The pinch point in a heat exchanger is the minimum temperature difference between the two fluids in the unit. In the industry when designing heat exchangers, the *UA* value is often used to define the size of heat exchanger needed for defined fluids, pressure losses, mass flows and either temperatures or heat transferred. When the required *UA* is known, the size of the heat exchanger can be calculated from known heat transfer coefficients, material thermal conductivity and thickness, inner and outer diameters, size and efficiency of fins and expected fouling.

It is also important to avoid vibrations in a heat exchanger which is a risk when velocities through it are too high. Therefore, it was checked that not too high volume flows were passed through the heat exchangers relative to design point volume flow.

A somewhat simpler way to calculate heat transferred is shown in (3.27) where one assume no heat is lost to the surroundings, i.e. $\eta_{h.e.} = 1$. When calculating for fluids or at low pressures it is often safe to assume close to constant c_p which can simplify the calculation. It was used to calculate the mass flows in some of the process heat cycles.

$$\dot{Q} = \dot{m}(h_2 - h_1) \approx \dot{m} c_p (T_2 - T_1) \tag{3.27}$$

For a heat exchanger with phase change like a once through steam generator, OTSG, one can divide the heat calculation into three parts; superheater, evaporator and economizer:

$$\dot{Q} = \dot{m}\left((h_e - h_{sat})_{superheater} + (h_{fg})_{evaporator} + (h_{sat} - h_i)_{economizer} \right) \tag{3.28}$$

The efficiency of a WHRU or HRSG is shown below, where the heat extracted is compared to ambient conditions.

$$\eta_{WHRU/HRSG} = \left(\frac{h_i - h_e}{h_i - h_{ambient}} \right)_{fluegas} \tag{3.29}$$

If one assumes a complete combustion the heat added to a cycle can be calculated by taking the lower heating value multiplied by the fuel mass flow:

$$\dot{Q} = \dot{m}_{fuel} LHV \tag{3.30}$$

3.4 Power outputs and efficiencies

Here the formulas for calculating the different efficiencies, that has not already been shown previous in this chapter, shown and explained. First off is the power required or gained by compressing or expanding a fluid:

$$\dot{W}_{fluid} = \dot{m}H = \dot{m}H_p\eta_p = \dot{m}H_s\eta_s \tag{3.31}$$

The shaft power output of a gas turbine can be calculated by taking the enthalpy difference over the turbine multiplied with the mass flow of air and fuel and then subtracting the enthalpy difference over the compressor multiplied with the air flow in, shown in (3.32).

$$\dot{W}_{GT,shaft} = \dot{W}_{turbine} - \dot{W}_{compressor} = \dot{m}_3(h_3 - h_4) - \dot{m}_1(h_2 - h_1) \tag{3.32}$$

The total electrical power output can be calculated by the shaft power multiplied by the mechanic and generator efficiency:

$$\dot{W}_{GT} = \dot{W}_{GT,shaft}\eta_{GT,gen}\eta_{GT,mech} \tag{3.33}$$

A steam turbine without reheating and with one or more outputs for steam extraction can be calculated by (3.34).

$$\dot{W}_{ST,shaft} = \dot{m}_i h_i - \sum_e \dot{m}_e h_e \tag{3.34}$$

Total electrical output of the steam turbine is calculated similarly to the gas turbine:

$$\dot{W}_{ST} = \dot{W}_{ST,shaft}\eta_{ST,gen}\eta_{ST,mech} \tag{3.35}$$

Steam quality, *x*, is calculated by gas (steam) mass flow divided by total mass flow. It is used to check there is not too much liquid going out of a steam turbine, which can damage it.

$$x = \frac{\dot{m}_g}{\dot{m}_g + \dot{m}_l} \tag{3.36}$$

Calculating the power required to drive a pump for liquid fluids is similar to calculating power required for a fluid in (3.31), the difference is that the efficiency of the motor has to be included. The head and efficiency of the pump can be calculated isentropic or polytropic.

$$\dot{W}_{pump} = \dot{m} H_{pump}\eta_{pump}\eta_{motor} \tag{3.37}$$

The efficiency of a gas turbine is calculated by the power output divided by the total lower heating value of the fuel used:

$$\eta_{GT} = \frac{\dot{W}_{GT}}{\dot{m}_{fuel} LHV} \tag{3.38}$$

Calculating the efficiency of the steam turbine cycle is similar. The difference is that one has to use the remaining heat in the exhaust not already used in the gas turbine as a basis for available energy:

$$\eta_{ST} = \frac{\dot{W}_{ST}}{\dot{m}_{fuel} LHV(1 - \eta_{GT})} \tag{3.39}$$

To get the total plant power output the power from the gas and steam turbines is taken and power used for pumps and other auxiliary power uses are subtracted, as shown below.

$$\dot{W}_{net} = \dot{W}_{GT} + \dot{W}_{ST} - \sum \dot{W}_{aux} \tag{3.40}$$

And the net plant efficiency is achieved by the net power output divided by the energy in the fuel used:

$$\eta_{net} = \frac{\dot{W}_{net}}{\dot{m}_{fuel} LHV} \tag{3.41}$$

At last the heat utilized in different processes in a combined heat and power plant is included in the energy utilization factor, *EUF* or total efficiency, η_{tot}:

$$EUF = \eta_{tot} = \frac{\dot{W}_{net,plant} + \dot{Q}_{process}}{\dot{m}_{fuel} LHV_{fuel}} \tag{3.42}$$

In the same way total lifetime efficiency can be calculated by taking total energy output divided by total energy input:

$$EUF_{lifetime} = \frac{\sum \left(\dot{W}_{net} + \dot{Q}_{process} \right)}{LVH_{fuel} \sum \dot{m}_{fuel}} \tag{3.43}$$

In the case of electrification, transmission losses, *TL*, due to resistive and inductive losses have to be included in the calculations to get a full overview of power produced versus power needed at the platform with related emissions. As seen in (3.44) any eventual extra auxiliary loses to produce heat has to be included with the original power need at the platform and divided by 1-*TL* to get the power produced on an onshore power plant.

$$\dot{W}_{el,produced} = \frac{(\dot{W}_{el,needed} + \dot{W}_{aux,losses})}{1 - TL} \tag{3.44}$$

To get the correct power output in the combined cycle cases, an iterative method had to be carried out to select to correct gas turbine load which gave a correct heat extraction and a total correct power output from the gas turbine(s) and steam turbine. To minimize each iteration an approximation to Euler's' method was used. First the boundary condition was checked to see if one of the GTs or both had to be in operation. Then the next iteration of gas turbine power output was set to current power output minus the error times a step size. Euler's method can be seen in equation (3.45) and the approximation made can be seen in (3.46).

$$y_{n+1} = y_n + hy'(t) \tag{3.45}$$

$$\dot{W}_{GT,n+1} = \dot{W}_{GT,n} + h(\dot{W}_{tot,goal} - \dot{W}_{net}) \tag{3.46}$$

The step size in the approximation was set to GT power output then stepwise lowered at certain iterations to always reach a solution in the cases were there were no convergence with the original step size:

$$h = \left[\left(\frac{\dot{W}_{GT1} + \dot{W}_{GT2}}{\dot{W}_{net}} \approx 0.7 \right)_{n<6}, \quad [0.4]_{6<n<15}, \quad [0.2]_{14<n} \right] \tag{3.47}$$

3.5 CO_2 emissions

Emissions rates or *ER* is calculated by taking the CO_2 emitted divided by the total power produced, or total CO_2 emitted divided with energy produced during a time period as shown in (3.48).

$$ER = \frac{\dot{m}_{CO_2,exhaust}}{\dot{W}_{net}} = \frac{m_{CO_2,exhaust}}{W_{net}} \tag{3.48}$$

Total CO_2 emissions, m_{CO2}, produced can be calculated by taking the exhaust mass flow multiplied with CO_2 mass fraction times a time interval, at steady state. At a quasi-dynamic simulations, with a series of alternating steady states, total CO_2 can be calculated by summing the CO_2 emitted at each steady state interval, as shown in equation (3.49).

$$m_{CO_2,tot} = \sum_i \dot{m}_{co_2,i} t_i \tag{3.49}$$

Total emissions from onshore power were calculated in the same way, but by using emission ratings, *ER*, multiplied with produced electrical energy on shore:

$$m_{co_2} = \sum_i ER_i W_{el,produced,i} \tag{3.50}$$

Before introducing modelling methodology used in the simulations in chapter 5, an overview will be given in chapter 4 which make use of the theory in this chapter to make more complex power and heat cycles.

4 Heat and power technologies and components

Before modelling, simulating and producing results, it is important to understand how thermodynamic theory gone through in chapter 3 can be utilized to create more advanced heat and power cycles. It is also essential to understand how different cycles work together and how each component functions with its limitations and how its performance affect the whole power cycle to achieve reliable results. This chapter covers the major components and thermodynamic cycles used in this study.

4.1 Gas turbine and waste heat recovery

The first process and the base case of this study is a simple gas turbine that provides the required power and a WHRU that provides the process heat needed from the flue gas. The thermodynamic name for the simple gas turbine cycle is the Brayton cycle which will be explained first.

4.1.1 Brayton cycle

The Brayton cycle, or the gas turbine cycle, is shown below in Figure 4.1. It is a relatively compact, low weight and efficient power cycle which is what makes it popular offshore. It basically consists of a compressor where air goes in and a heat source, usually a combustion chamber, and then a turbine to drive the compressor and to supply work.

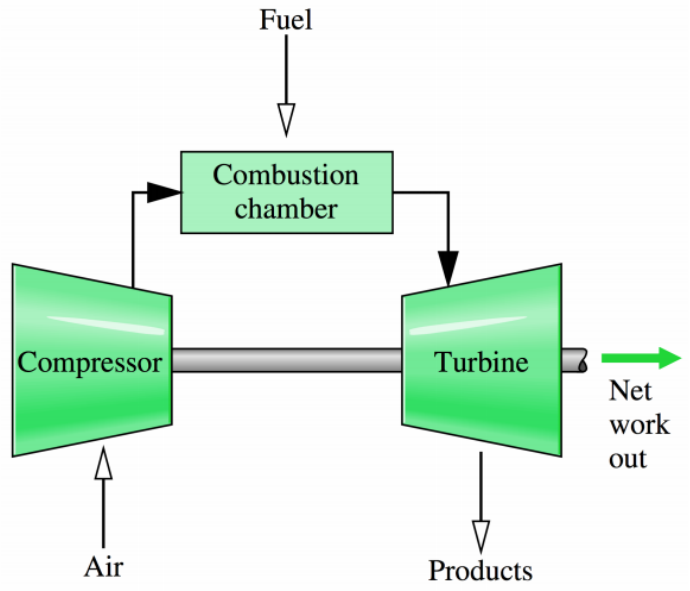

Figure 4.1 Illustrative figure of a Brayton cycle showing the air going into the compressor, heated in the combustion chamber and then expanded through the turbine. [23]

In Figure 4.2 a temperature-entropy diagram is shown of a basic Brayton cycle. T-s diagrams are a good tool for showing heat transfer and irreversibilities in processes. In this diagram we have following changes of state:

- 1-2s: In the isentropic case air comes in at 1 at ambient temperature and pressure, and the pressure and temperature increases through the compressor to 2s.
- 1-2: Here the real compression process is shown with losses. The air gets compressed to the same pressure because of the set pressure ratio of the compressor but the losses isentropic losses are introduced as an increase in temperature and entropy. The temperature achieved after compression can be calculated by formula (3.14) and the power consumed by (3.24).
- 2-3: Heat is added in the combustion chamber at a constant pressure which increases the temperature and entropy. At a complete combustion the heat added and temperature before expansion can be calculated by equation (3.30)
- 3-4s: Isentropic expansion of the air and combustion products through the turbine down to ambient pressure or back pressure.
- 3-4: Irreversible real expansion of the flue gas to ambient or back pressure. By using the expansion versions of equation (3.14) and (3.24), and subtracting the power needed in point 1-2, one can calculate the power net gain from the cycle. [23]

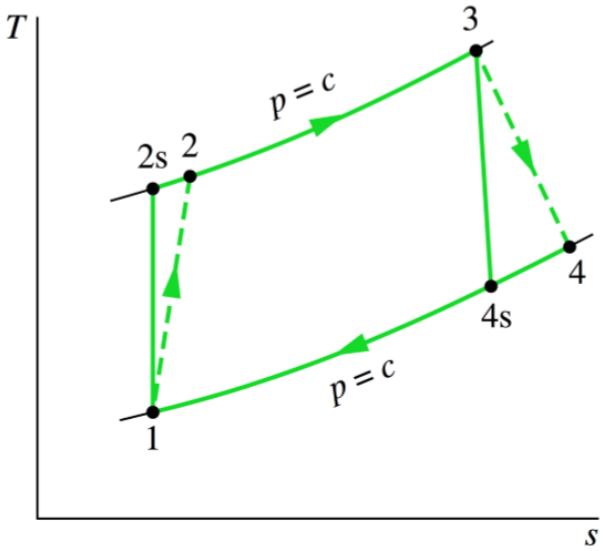

Figure 4.2 T-s diagram of a typical Brayton cycle showing the difference of a isentropic and real cycle. [23]

4.1.2 Gas turbine

The gas turbine is the most important component in this study and Figure 4.2 shows an ideal cycle with only entropy losses. Real gas turbines also have losses like pressure drop in the combustion chamber and at inlet and outlet because of filters or heat exchangers, which is not included in the simple Brayton cycle. In a modern gas turbine, the current efficiency limiting factor is mainly the temperature out of the combustion chamber because of material properties and degradation of the first turbine blades, where the temperature is the highest. By increasing the turbine inlet temperature (TIT) the efficiency of a gas turbine increases because of the diverging constant pressure lines as the temperature increases. Improvement in cooling and material technology has been the main reason for increase in efficiency as it allows for higher TIT. For that purpose, it is common to use air, water or steam cooling with different configurations to increase the maximum temperature.

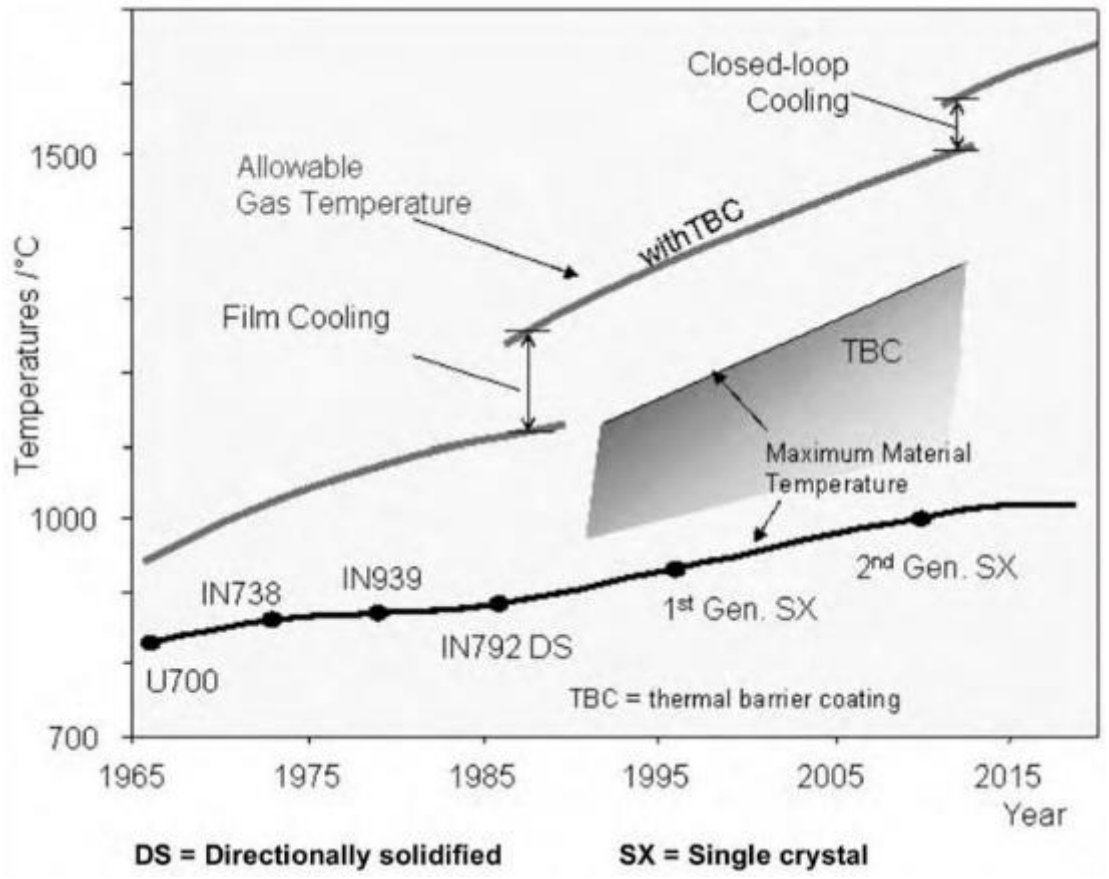

Figure 4.3 Historical technological improvements that have led to higher gas turbine efficiencies. [27]

NO_x emission from combustion is dependent on temperature and the time the gas stays at a certain temperature. The longer the gas is hot or the higher the temperature, the more NO_X is formed. One way to control the temperature is the control the air/fuel ratio, as seen in Figure

4.4. [17] With a low air/fuel ratio combustion isn't completed and there are high CO (VOC, volatile organic compounds) emissions. Slightly above stoichiometric ratio it has a near to complete combustion and the temperatures run very high which produces NO_X emissions. At higher air fuel ratios, it has a lower combustion temperature but it's still a near to complete combustion, which gives low values for both NO_X and CO emissions. At even higher air fuel ratios the temperature gets even lower and the combustion is less complete and CO emissions raises.

To reduce NO_X emissions DLE (dry low emissions) technology have been in use since the year 2000 on the NCS. It reduces the NO_X emissions by controlling the time and temperature by a large amount of nozzles instead of SAC (single annular combustion) turbines. [28]

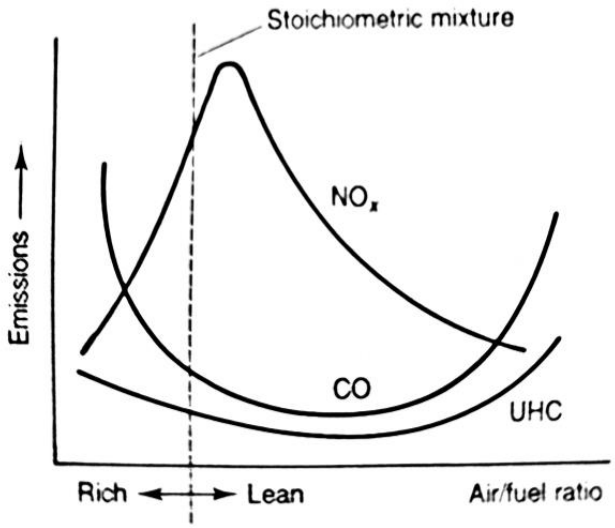

Figure 4.4 Emissions of a gas turbine, showing the trade-off between NO_X and VOCs (carbon mono oxide and Unburnt Hydrogen Carbons) at different air/fuel ratios. [17]

Gas turbines can be based on aeroderivative or industrial designs. Aeroderivative turbines are based on flight engines and are what is used offshore because of their low size and mass compared to industrial designs. They also have the advantage of being reliable and easier to service because of their origin and designs. The main difference between a jet engine and an aeroderivative turbine used for power generation is an extra power turbine, usually on a different shaft than the compressor and high pressure turbine, mounted at the end which delivers power to a generator instead of propulsion.

The gas turbine used as a model in the base case in this study is the GE LM2500+ G4, shown in Figure 4.5. It is based on the most common gas turbine offshore, the LM2500, with a proven

reliability and it can deliver up to 35 MW power, dependent on configuration and ambient conditions. It is a derivate from the CF6 aircraft engine family and the LM2500 engine designs has over 51 million operating hours world-wide. [16] Thus it fulfils the requirements of power production offshore with a proven reliability, low weight to power ratio, relatively good efficiency, easy and fast adjustment to power load.

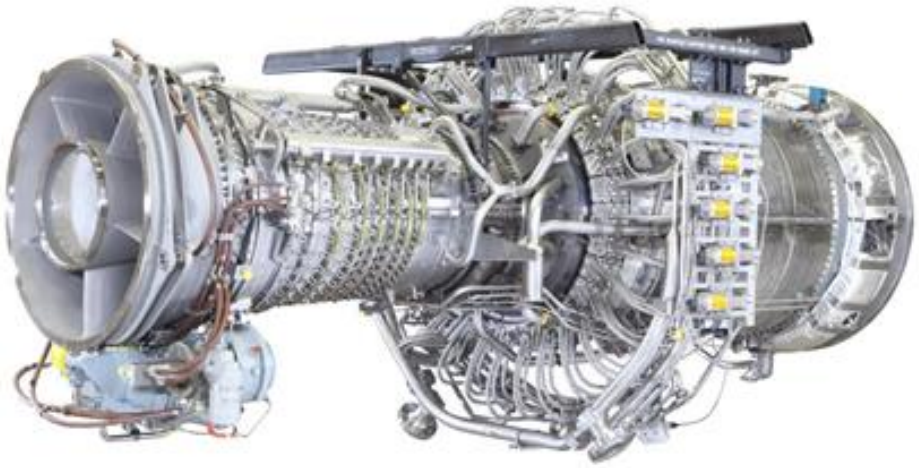

Figure 4.5 A gas turbine of the GE LM2500 family. The wider mid-section large amount of tubes in the middle shows the advanced DLE system with its many nozzles lowering NO_X emissions. [28, 29]

Modern gas turbines are usually operated off-design by the use of variable guide-vanes to increase off-design performance and by controlling the TIT by adjusting the fuel into the combustion chamber. When producing power most turbines are run at fixed speeds set according to the generator and frequency of the power grid. Figure 4.6 shows the combined off-design operations of a compressor and a turbine, giving the characteristics of a normal simple gas turbine without using VIGV. It is plotted with the pressure ratio of the compressor versus the non-dimensional mass flow through the simple gas turbine, while the mass flow of the fuel added is assumed equal to the mass flow bled out of the compressor. By comparing the power need of the compressor, the output of the turbine and power load at set speed, the graph shown can be obtained. At fixed constant speed the gas turbine efficiency characteristics will follow the near vertical lines and will be designed to go through the centre of the efficiency contours. [17] A gas turbine's power output and efficiency is in the same way related to ambient pressure, ambient temperature and relative humidity, which all change the mass flow due to swallowing capacity and the fuel needed to reach the desired TIT.

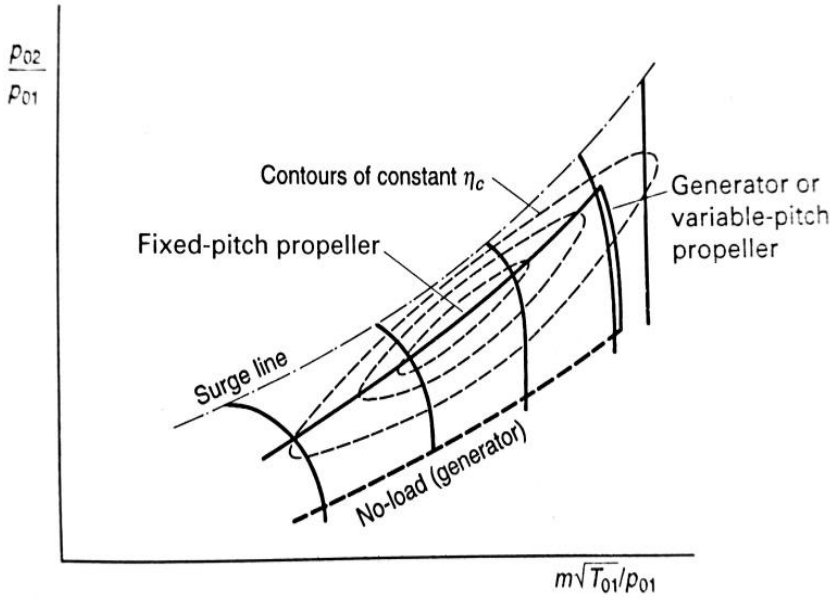

Figure 4.6 Combined off-design efficiencies curves of compression and expansion resulting in the efficiency curves of a simple gas turbine. [17]

Figure 4.7 shows a single-lift skid for a fast installation of a gas turbine. It includes a gas turbine, starter equipment, fuel system, bearing lube oil system, driven equipment and a generator. Inlet air filters, potential WHRU and exhaust stack is installed on top of it. A LM2500G4+ skid with all the equipment except a WHRU weighs about 150 tonnes. [30, 31]

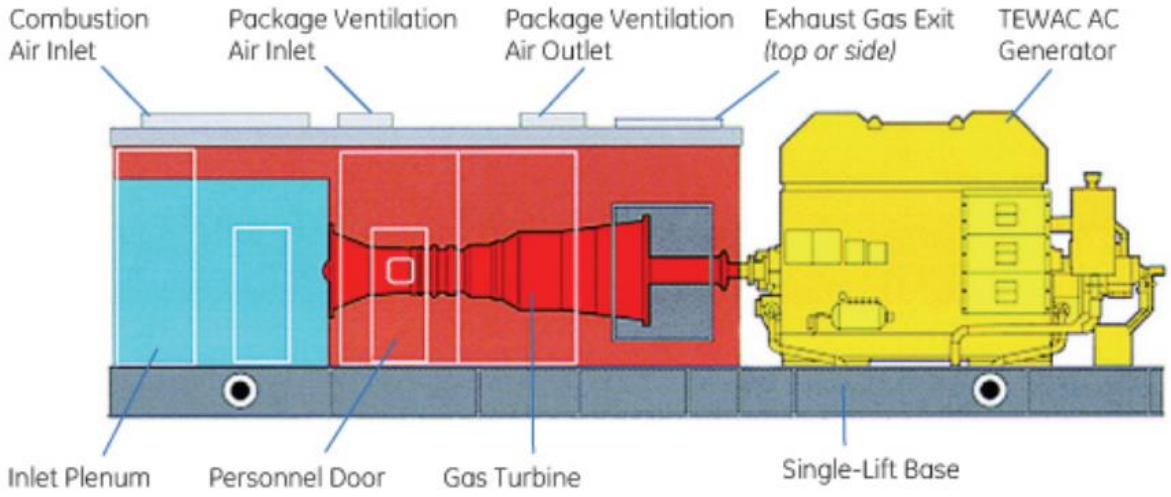

Figure 4.7 Overview of a single-lift gas turbine skid, excluding the air filters and any WHRUs. [30]

4.1.3 Waste heat recovery unit

The WHRU is the heat exchanger mounted after the gas turbine and it takes out heat from the exhaust gas and delivers it to where it is needed through a heat carrier system. The heat is transferred by hot flue gas traveling through banks of tubes with fluids inside the tubes at lower temperatures, extracting the heat. In this study an economizer is used as a WHRU to heat pressurized water which is then transported to where heat is needed in the different processes. The WHRU is designed to minimize pressure loss of the flue gas while being compact. The flue gas outlet temperature is one of the limitations of WHRUs because of the dew point of sulphuric acid which is depended of the partial pressure of sulphur in the exhaust. [27] It is normally not a problem in a WHRU due to process heat temperature usually is above 100 °C.

Due to the set UA values of the waste heat recovery unit transferred heat in off-design operation is mostly dependent on volume flows and temperatures of the flows coming in. If the process heat temperature requirements are set, then the heat transferred can be controlled by by-passing a part of the flue gas to achieve required process heat temperature at set heat requirement. The pressure drop over the WHRU is proportional to the velocity (and subsequently volume flow) squared and will change the backpressure of the gas turbine and its efficiency. The selecting of design point and how pressure drop and minimum pinch point temperature affect the WHRU size will be discussed more in chapter 4.2.4.

To reduce the size and weight of the WHRU package a WHRU can be installed with an integrated exhaust bypass which is ideal for offshore platforms. Halvorsen group did a 20 MW WHRU offshore retrofit installation that weighed about 70 tonnes and the same weight is assumed for the WHRU used in this study, which brings up the total assumed weight of a single gas turbine including WHRU up to ca. 220 tonnes. [32]

4.2 Combined cycle heat and power

By combining the Brayton cycle from the previous subchapter with a steam cycle, we get the combined cycle. In a combined cycle heat left in the exhaust gas from the gas turbine is utilized to generate superheated steam that can be let through a steam turbine to provide extra power. In that way the efficiency goes up and the *ER* is reduced.

4.2.1 Rankine cycle

The Rankine cycle is the thermodynamic name for the simplified steam cycle shown in Figure 4.8. First, steam at a chosen temperature and pressure is generated in a boiler by a heat source, in this study warm exhaust gas, and goes into the steam turbine. In the turbine the steam is

expanded down to a low pressure, usually below atmosphere pressure, and the power generated, W_t, is utilized in a power generator.

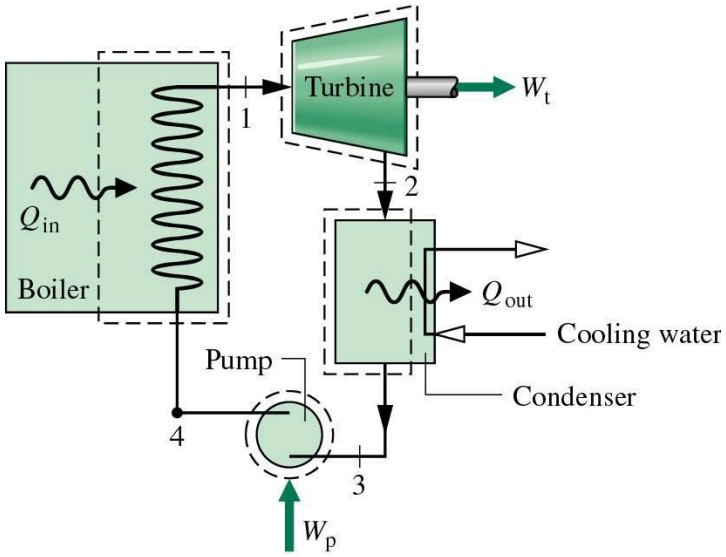

Figure 4.8 Diagram of a Rankine cycle with the key components: steam boiler, turbine, condenser and pump. [23]

The limiting factor of the condensing pressure out of the steam turbine is the temperature of the available cooling and the size of the condenser. Traditionally it has been more likely to choose a higher pressure out of the steam turbine offshore than onshore, relative to the temperature of the cooling water, to reduce the size of the condenser. But studies have found that choosing a lower condensing pressure, of around 0.04 bar is more power/weight efficient. [33] Another limiting factor is the steam quality out of the turbine, as too much and too large water droplets at the exit of the steam turbine will lead to erosion and degeneration of the turbine [34]. Moran and Shapiro says that a common practice is to have a minimum steam quality of x=0.9 while other studies suggest steam quality down to x=0.88 is not uncommon [35]. Figure 4.9 shows with the difference between path 1-2 and 1'-2' how important superheat is to achieve a high power output while having a high steam quality out of the turbine. At higher pressure; higher steam temperatures or lower condensation pressures are required to have a sufficiently high steam quality.

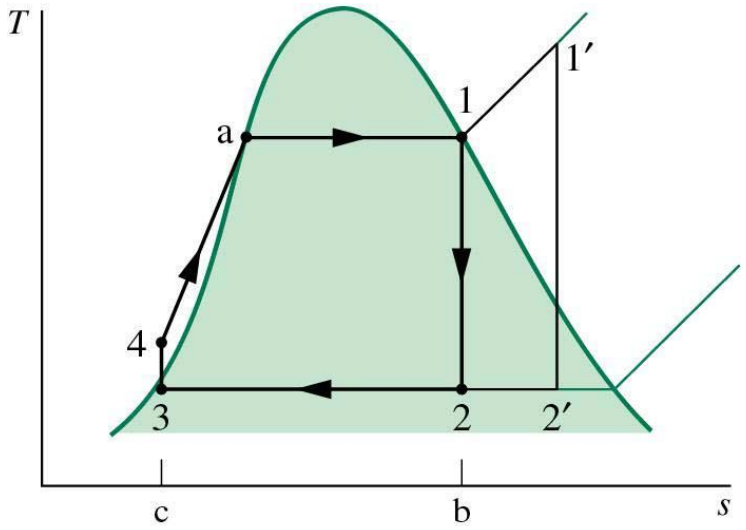

Figure 4.9 T-s diagram of a Rankine cycle showing the different stages of expansion, condensing, pumping and heating the water/steam. [23]

After the steam is condensed at a selected pressure based on saturation temperature, from 2' to 3, the water is pumped isentropically to point 4 shown in the figure above. Then the water is heated at constant pressure in the economizer between 4-a, then evaporated in the evaporator between a-1 and lastly superheated between 1-1', following the heat transfer equation (3.28).

There are many technologies to improve the performance of a Rankine cycle, like reheating or regenerative feed water heating. But because of offshore weight and footprint constraints and the low pressure, this study will not include more advanced options of the Rankine cycle.

4.2.2 Combined cycle

The combined cycle is simply a combined Brayton and Rankine cycle, where the remaining heat in the exhaust from the gas turbine is utilized in a steam cycle, as shown in Figure 4.10. The benefits of a combined cycle, as already mentioned, are higher efficiencies and higher utilization of the heating value of the fuel. By utilizing a HRSG as a heat exchanger instead of a smaller WHRU one can expect a higher back pressure of the gas turbine and therefore a slightly lower efficiency of the gas turbine, but the extra power from the steam turbine more than makes up for that. The largest disadvantage of a combined cycle offshore is the extra footprint and weight required and lower power to weight ratio. Another disadvantage is the slower start-up times till full power and lower flexibility in operation.

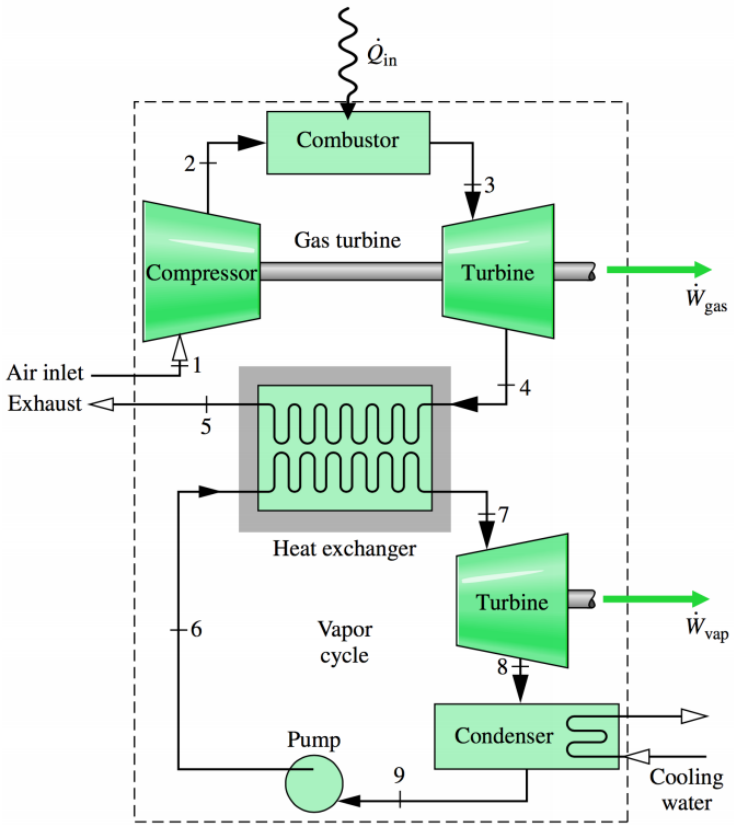

Figure 4.10 Combined gas turbine-steam cycle where the heat from the gas turbine flue gas is utilized in a steam turbine. [23]

4.2.3 Steam extraction and back-pressure

To supply process heat in the combined cycle the two most common ways are to either extract steam from the steam turbine or have a higher back-pressure out of the steam turbine Steam extraction is done by having one or several extra outlet at a stage of the steam turbine that give a desired saturation pressure, as shown in Figure 4.11. A back-pressure steam cycle will look equal to Figure 4.8 but the steam exit pressure out of the turbine will be considerably higher and a part or most of the remaining condensation heat will supply process heat instead of going to the cooling water. At high process heat temperatures needed steam extraction is generally the best way to provide heat due to the low efficiencies at high back-pressure. Back-pressure steam cycle can be the best choice when a lot of process heat is needed at lower temperatures,

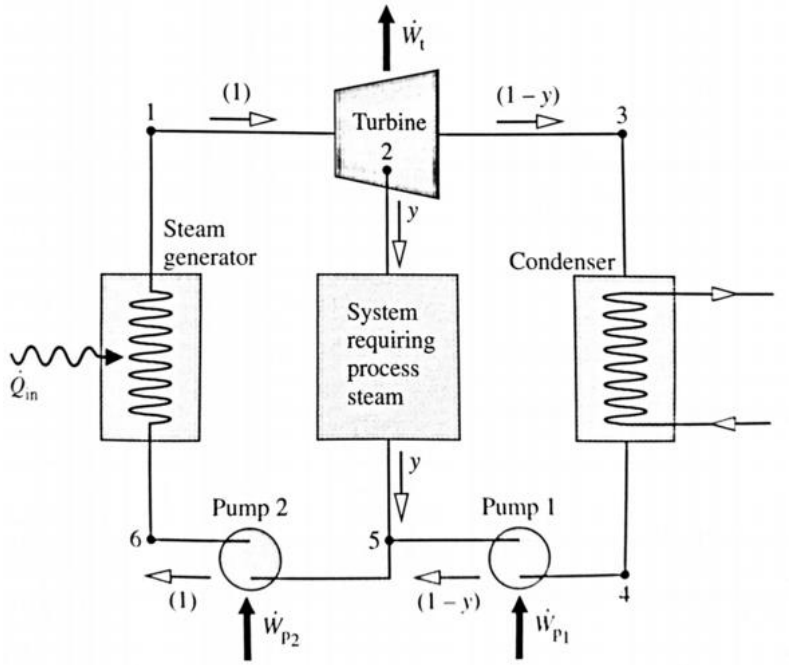

Figure 4.11 Steam extraction providing process heat in a steam cycle. [23]

4.2.4 Once through steam generator

The HRSG is the first component after the gas turbine in the combined cycle. It can be fired or unfired, have several or only one pressure level. A HRSG is designed to maximize heat extraction from the flue gas by minimizing the pinch point while also keeping the pressure loss of the flue gas relatively low to increase the efficiency of the gas turbine. Both minimum pinch point and pressure loss is directly related to the size and weight of a HRSG which both have to compromise for size and weight. A normal pressure loss is between 25 to 30 mbar [27]. Offshore the pinch point and pressure loss is more likely to be chosen at higher values than onshore to reduce size and weight. And the pinch point temperature for a HRSG is normally between 8-35 kelvin, while being in the upper temperature range offshore [18, 33].

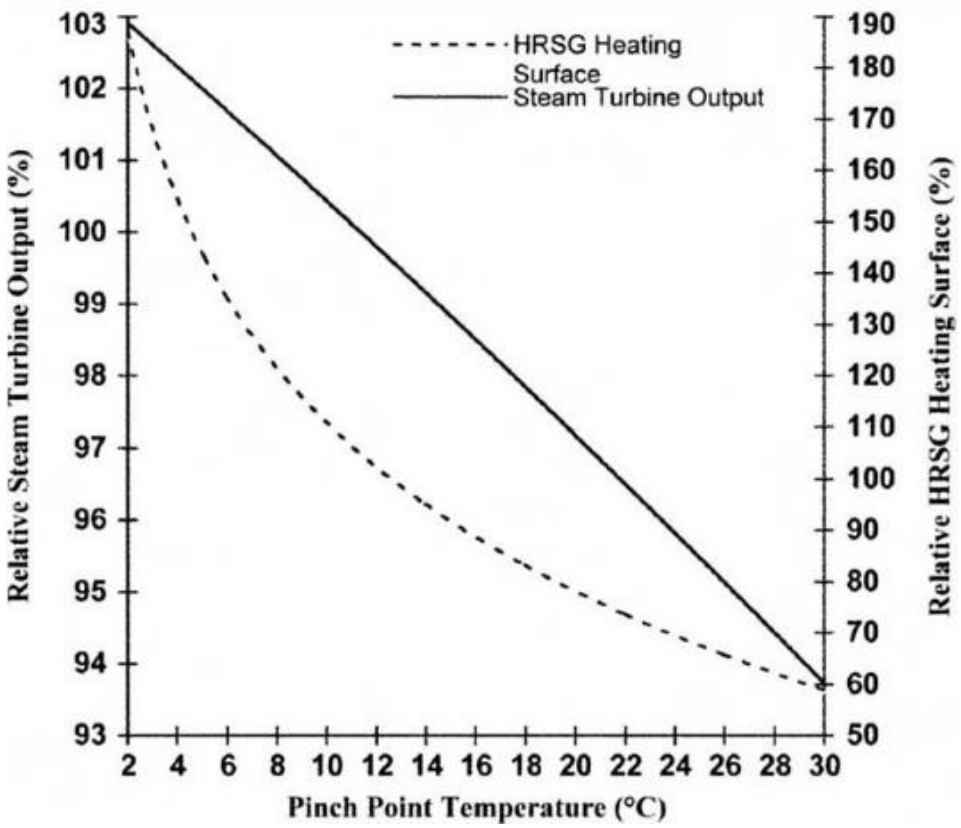

Figure 4.12 Showing the relation between pinch point temperature in a HRSG, steam turbine power output and HRSG size. [27]

Figure 4.12 and Figure 4.13 shows the relation between pinch point temperature, pressure loss, HRSG surface area and relative steam turbine output. That makes flue gas pressure loss in the HRSG and minimum pinch point good indicators of HRSG design and size. Considering a constant heat exchange surface thickness in the HRSG, the weight of the HRSG can be assumed proportional to the surface area.

There are two main configurations of HRSGs used, vertical or horizontal layout. In a horizontal layout the tubes are mounted vertical and natural convection provides circulation of the water. In a vertical WHRU the exhaust goes through the tube bundles vertically while the tubes are horizontal and therefore it requires circulation pumps to keep the flow. That makes it possible to have smaller diameter pipes. The main advantage of a vertical heat recovery unit is that it requires smaller footprint area but while it reaches higher vertically instead, which is valuable off-shore where area is limited. [27]

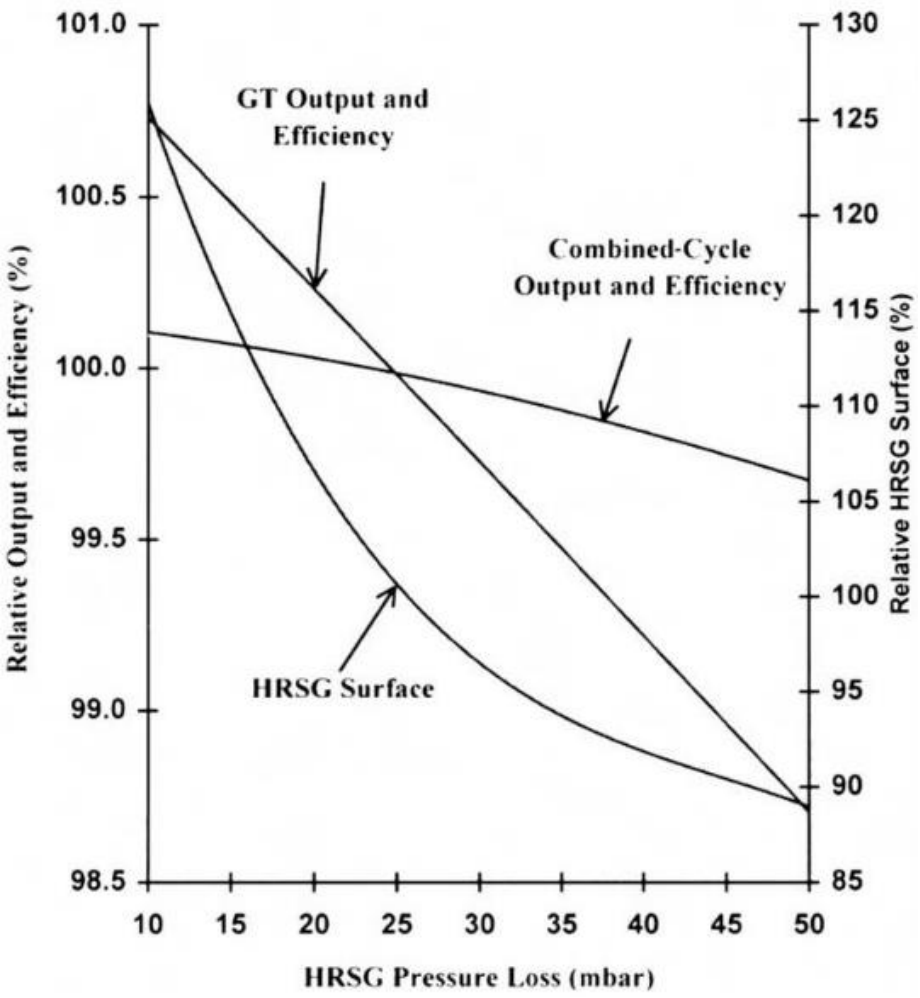

Figure 4.13 Showing the relation between flue gas pressure loss in a HRSG, HRSG size, steam turbine power output and efficiency. [27]

A once through steam generator, OTSG, at a single pressure has the recent years proven to be a good compromise between weight and efficiency for offshore installations and has been used in several studies [33, 36, 37]. By avoiding steam drums and the bypass stack, the size can be reduced. And its flexibility by not having clearly defined zones for economizer, evaporator and superheater, are also a clear advantage for offshore use. The main disadvantages of a single pressure OTSG without a by-pass valve is the increased cost of materials that need to be able to handle higher temperatures for it to be able to run dry and a reduced efficiency compared to a normal HRSG with drums and several pressure levels. But offshore, the reduced area and footprint is valuable. [36] Figure 4.14 shows the benefits of a HRSG with several pressures with a lower temperature difference and thereby higher efficiency.

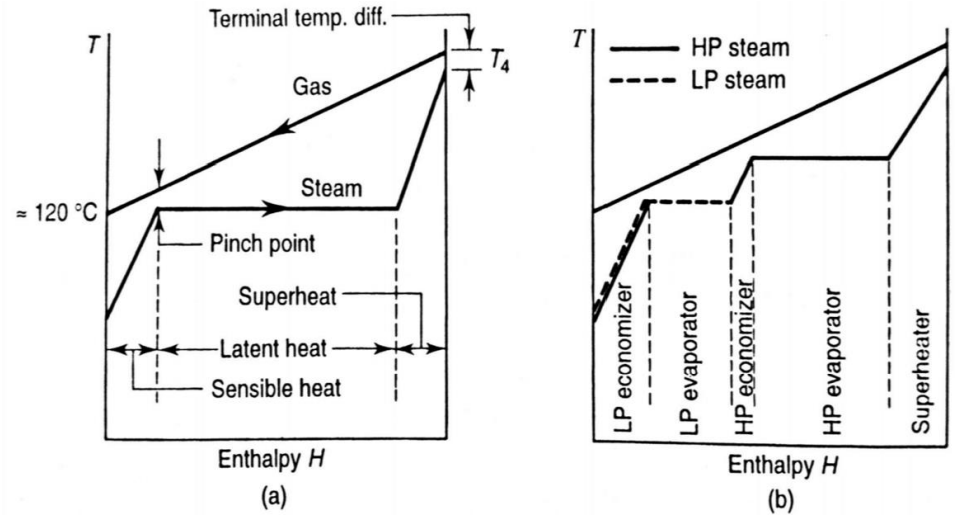

Figure 4.14 q-T diagrams of single (a) and dual pressure (b) HRSG. [17]

As the heat transfer of the water side is much higher than the gas side the temperature of the tubes in the HRSG will be close to equal to the temperature of the water. It is therefore important to consider the inlet temperature and the dew point of sulphuric acid which may be a problem if the feed water temperature falls below 50 °C, dependent on the fuel burned in the gas turbine. [27] This is usually not a problem for natural gas as it is usually processed and contain low fractions of SO_2.

At off-design the pressure loss through the OTSG will depend upon the volume flow going through it, as with the WHRU. Because there are no drums and the regulation of the feed water through the OTSG is designed to let the areas of where evaporation occurs and superheating begins be able to flow through the different regions depending on flows and temperatures of flue gas and feed water. The superheat temperature also has to be considered at off-design according to material selection so the temperature does not reach too high values and can damage equipment. [38]

4.2.5 Steam turbine

There exist a large number of different designs and types of steam turbines on the market due to its wide use in the power industry, as shown in Figure 4.15. The most common used in the power industry is the condensing steam turbine which have very low exit pressure and can allow for a small amount of water formation. Some of the requirements of a modern steam turbine are high efficiencies over a large operation window, short start-up times and short installation times. There are ways to modify and optimize a steam turbine with for example reheating at several stages. In this study a standard simple steam turbine was utilized in Ebsilon

Professional, and in the case of steam extraction; two separate steam turbine components were used. No steam reheating or regenerative feed water heating were utilized in the simulations due to the weight and space limiting factors offshore. [23, 27]

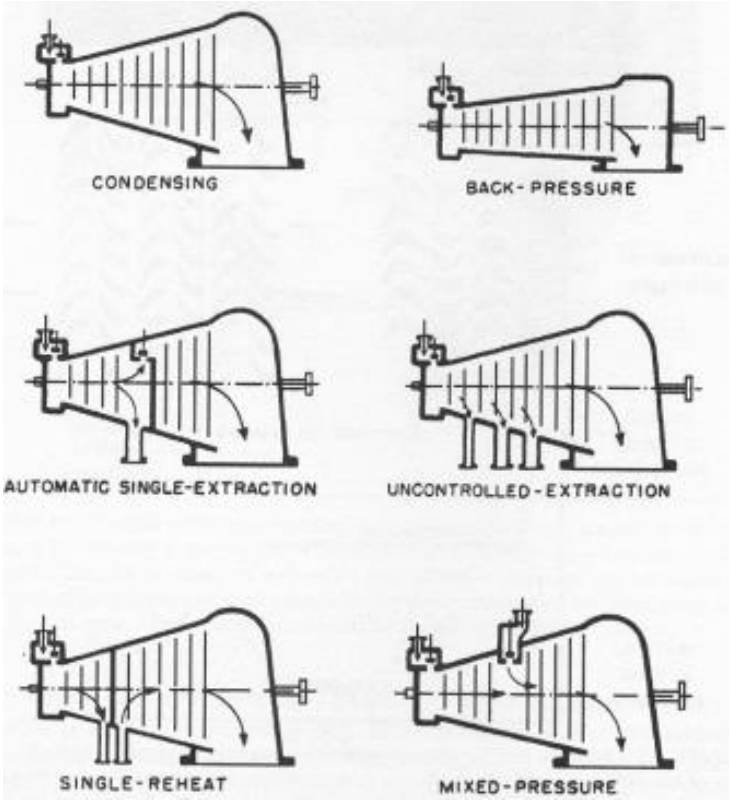

Figure 4.15 Showing 6 of the most common steam turbines used in the industry. [18]

To operate a steam turbine most efficiently at off design it is common to use sliding steam pressure by the use of Stodola's cone law or the Law of the Ellipse, shown in equation (4.1). [18] The inlet pressure is governed by the turbine's swallowing capacity and by adjusting the pressure a near constant volume flow can be kept through the turbine resulting in high off design efficiencies. [27]

$$\frac{\dot{m}}{\dot{m}_0} = \frac{p_i}{p_{i,0}} \sqrt{\frac{p_{i,0} v_{i,0}}{p_i v_i}} \sqrt{\frac{1 - \left[\frac{p_e}{p_i}\right]^{\frac{n+1}{n}}}{1 - \left[\frac{p_e,0}{p_i,0}\right]^{\frac{n+1}{n}}}} \tag{4.1}$$

A steam cycle can be operated at constant pressure by having a valve before the turbine inlet to regulate the pressure, which is often desirable at 50 % pressure and load to avoid having to low saturation temperatures in the HRSG, as shown in Figure 4.16.

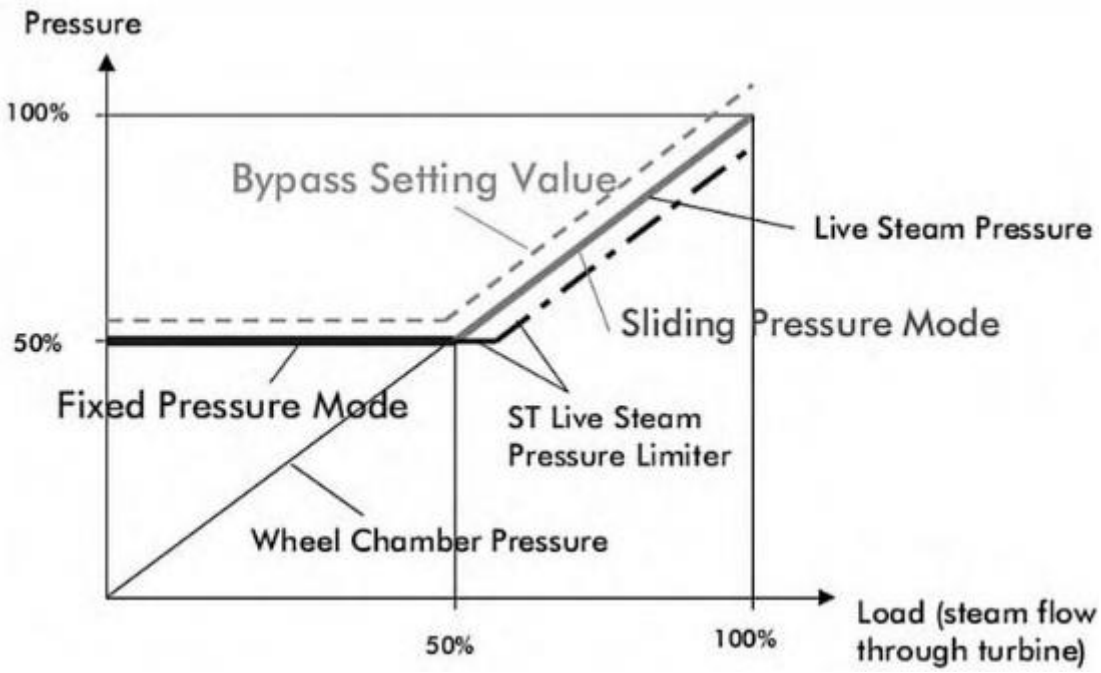

Figure 4.16 Off design controlling of a steam turbine with sliding pressure operation down to 50 % load and fixed pressure mode at lower loads. A bypass valve is used to prevent too high volume flows at a certain load. [27]

Figure 4.17 show how the extraction pressure can be set constant at lower loads to maintain a correct saturation temperature for the process heat. By having a throttle before the inlet of the turbine after the extraction the back and extraction pressure of the first turbine remains constant.

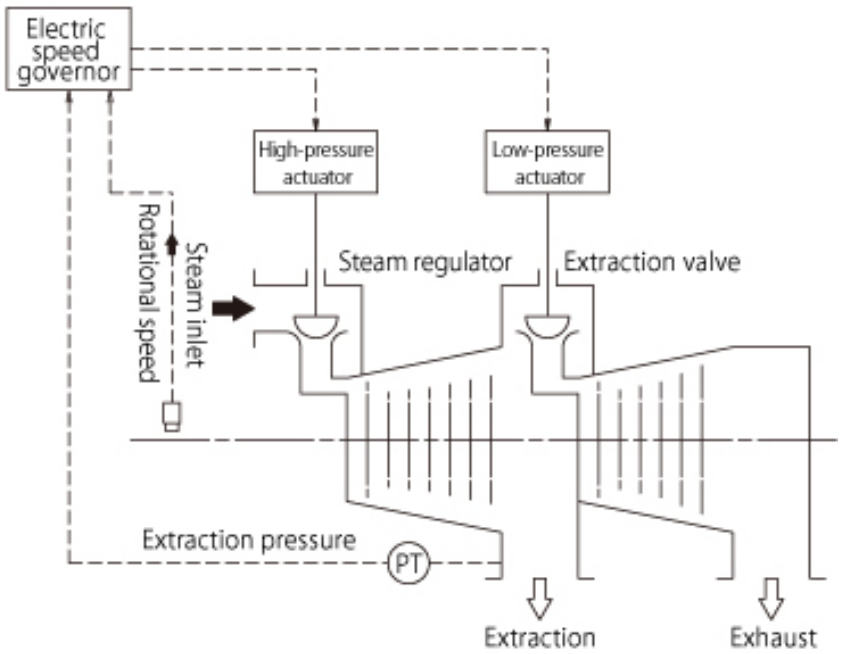

Figure 4.17 Illustration of how swallowing capacity and inlet pressures can be controlled at constant high pressure and constant steam extraction pressure. [39]

4.2.6 Condenser and deaerator

Because of the low and relatively steady temperature of the sea water at the NCS it is common to use a direct water cooling shell and tube condenser where salt water flows inside the tube bundles and water condenses on the outside. Offshore, the condensing pressure usually is chosen larger relative to the temperature of the cooling water than onshore to save space and weight. A condenser also has to be designed to be able to take by-pass steam during steam cycle start-up and load rejection during a steam cycle trip. [40]

Inert gases, like oxygen, in the condenser lowers the partial steam pressure and saturation temperature and will have dramatic effect on the performance of the condenser. Also, presence of O_2 and CO_2 dissolved in the feed water will increase corrosion in the system. Therefore, it is important with a de-aerator to remove inert gases that leaks into the system because of the under pressure. [18, 36]

A combined deaerating condenser has been used in recent studies [33] but little research was found on the subject. But by combining both into a single unit space and weight could be saved. The principles of a deaerator is shown in Figure 4.18 where the condensate is heated to decrease the solubility of the gases even more and where the gases are carried away on a flow of steam through the air vent [36].

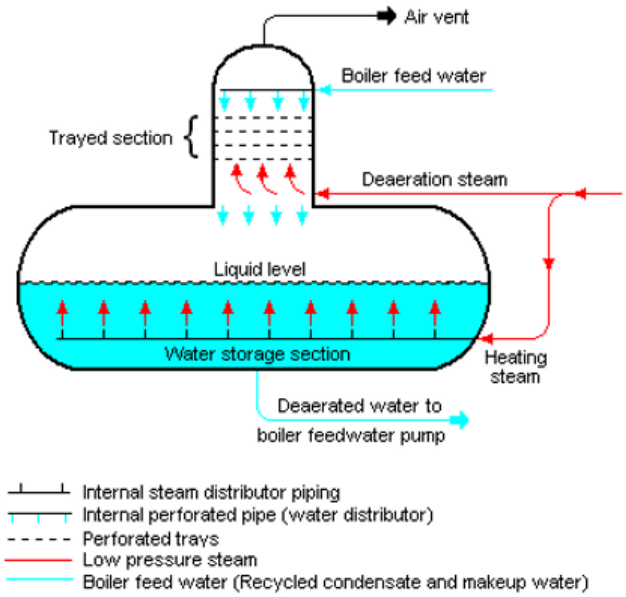

Figure 4.18 Principles of a deaerator. [18]

4.2.7 Pumps

The major pump work in a combined cycle is by the lifting of sea water for the condenser and the high pressure pumps for the feed water. Due to the importance of these pumps it is normal

to have reserve pumps in case of failure or maintenance. To efficiently regulate a pump frequency transformers are used to adjust its speed running at off-design.

4.2.8 Feed water treatment and supply

To supply feed water to process heat and steam cycle on an offshore platform, salt water either has to be desalinated and treated on-site or it can be transported from shore. And for an OTSG the water requirements are stricter as there are no drums that can be opened and cleaned. [36] However, as this study does not go in-depth into weight and space considerations offshore, water treatment was not researched. But it is important to remember the extra space and weight requirement for a combined cycle also includes tanks for storing make-up water and facilities for water treatment.

4.3 Electrification and gas burner for heat supply

This thesis will not go deeply into the technicalities of electrification and electrical power supply. But generally to supply electrical power to an offshore platform, high voltage subsea cables are used. For distances below 150-200 km high voltage alternating current (HVAC) is normally used. [19] Then the voltage can be transformed to the optimal voltage onshore and the cables can go directly to a platform before the voltage is transformed down for use and possibly distributed to platforms nearby. For longer distances from shore HVDC (high voltage direct current) is used to avoid unacceptable transmission losses. Then a larger rectifying and transformer station is required onshore as well as more equipment offshore to invert the power back to AC. Then an own hub platform might be used to invert and distribute the power to nearby platforms, as seen in Figure 4.19 of the planned Utsira High electrification. Research for mounting subsea transformers on the seabed is also conducted to save platform weight and space. [19]

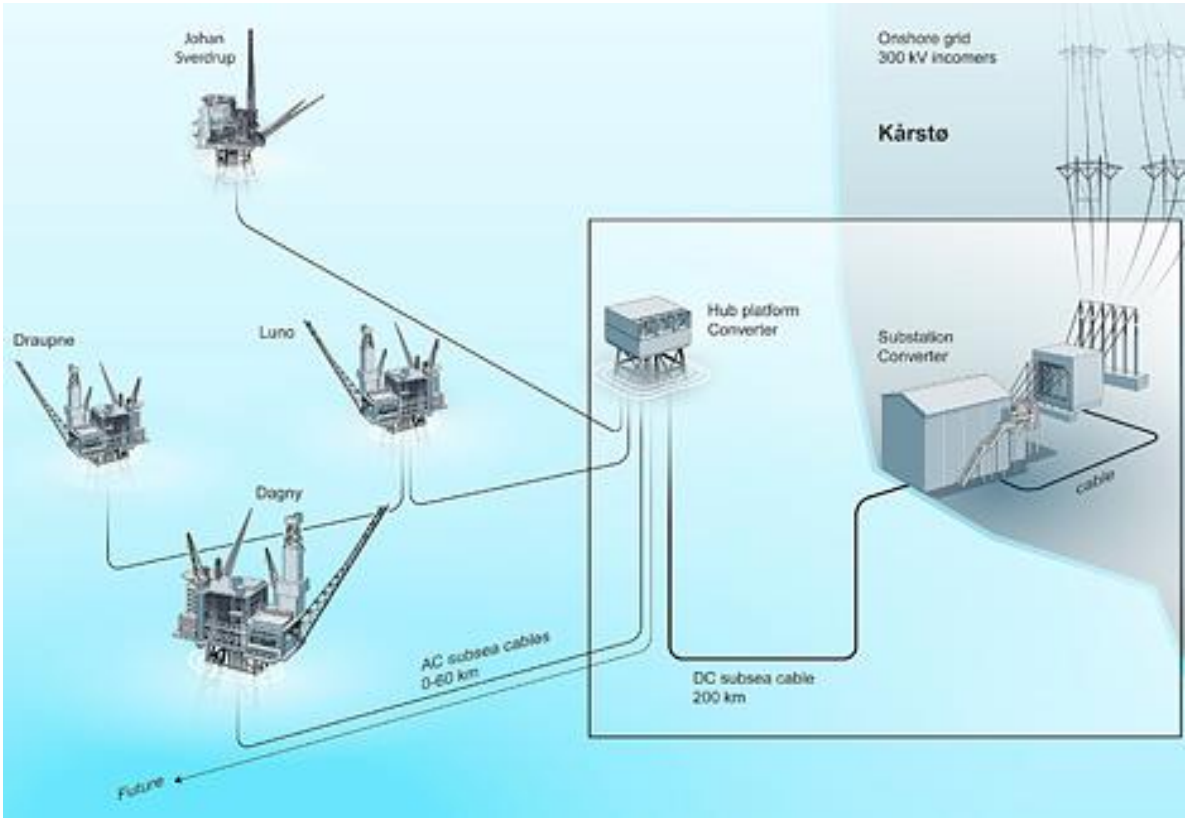

Figure 4.19 Sketch of the Utsira High electrification project. A power station on shore rectifies HVAC to HVDC. A central power hub platform receives the HVDC cables from shore and inverts it back to HVAC before providing platforms in the area with onshore power. Power is then transformed down to normal voltage AC on each platform. [41]

It is more economically beneficial if there are more than one operator in an offshore area to share to infrastructure cost of electrification. There is also a distinction of part or full electrification of a platform. In a part electrification only power turbines and convenient exchangeable power equipment are replaced while some compressors and other equipment may still be driven by gas turbines. [19]

One of the benefits of electrification is the highly flexible load runtime and high responsiveness that comes with electric power. The platform may in that regard optimize efficiency and reduce losses without having to consider minimum load and most efficient load sharing between turbines.

To provide process heat during electrification of an offshore platform a gas or electrical boiler is a good alternative to provide heat. Industrial gas boilers are optimized to deliver heat and have very high efficiencies above 90 %. A gas or oil boiler work much like a HRSG with dedicated areas of the tube banks as economizer, evaporator and superheater. The tube banks are usually arranged around the flame and along the flue gas path to absorb radiation and convective heat transfer. After the economizer the remaining heat in the flue gas is used to heat

up the incoming air. Figure 4.20 shows an example of an industrial gas/oil boiler from Hoval that can deliver up to 21 MW of heat with an efficiency of 91.5 %. [42]

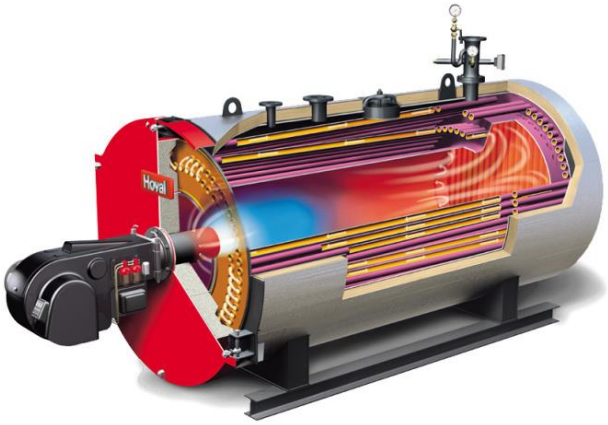

Figure 4.20 An example of an industrial gas boiler. [42]

5 Model description/methodology

Now that the theory and how it can be used to create different power and heat cycles have been gone through, it is time to look at runtime conditions, limitations and design parameters used to simulate a platform's power and heat need before doing lifetime simulations and model screening.

To evaluate the different options, it was assumed that a platform would be operated for 20 years with a varying heat and power demand and quasi-dynamic simulations were done to that affect. That mean that after deciding the design point for various components the simulations were run many times at different ambient temperatures, power demands and heat demands at steady state and the CO_2 emissions were calculated according to how long each period lasted, according to equation (3.49) and (3.50).

5.1 Weather and temperature profiles

Ambient conditions can have a large impact on performance and CO_2 emissions throughout the lifetime of power generation as it directly affects the performance of gas turbines, as discussed in chapter 4.1. It was chosen to use data from the North Sea in the simulations, specifically from the Sleipner A weather station which had monthly average temperatures for most of the months the last 10 years, as shown in Figure 5.1 below.

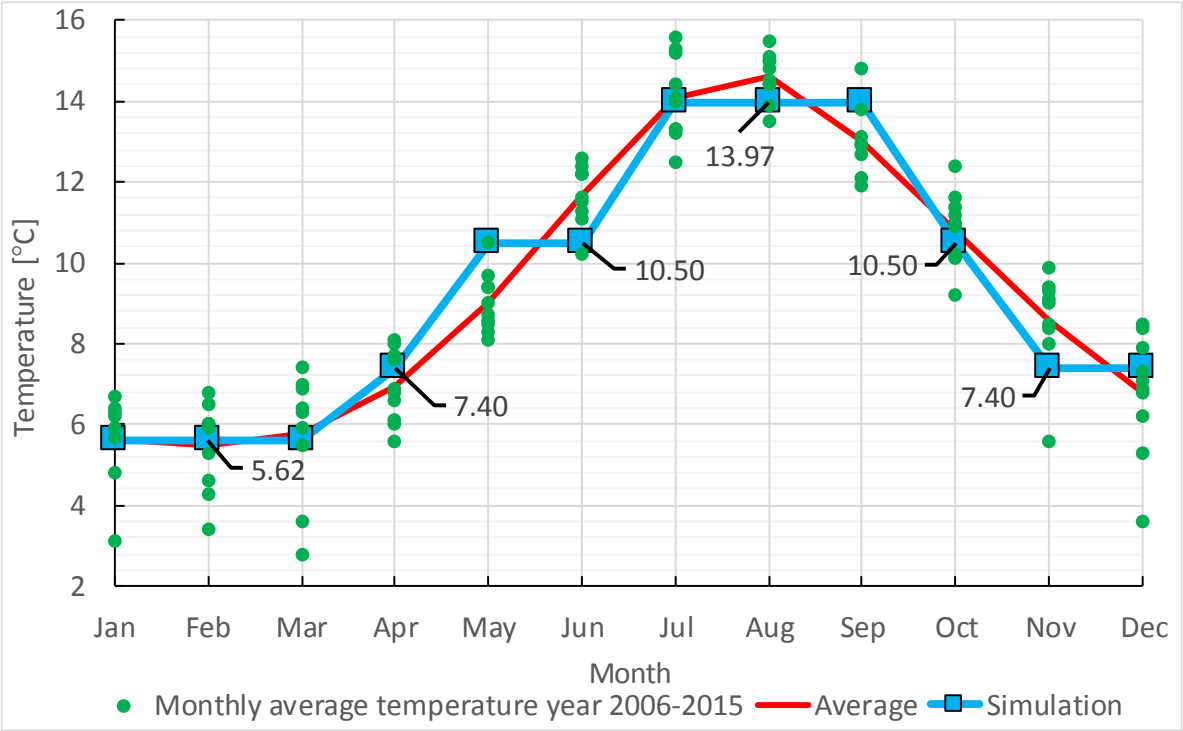

Figure 5.1 Monthly temperatures at Sleipner A weather station. [43]

To simplify the simulations and reduce time needed for running a lifetime model simulation it was chosen to use 4 different temperatures throughout the year. The temperatures were chosen based on the average of the mean temperatures for the respective months. 5.62 °C for the 3 coldest months, 7.40 °C for 3 next to coldest months, 10.50 °C for the next to warmest months and 13.97 °C for the 3 warmest months, as shown in the figure. Practically it means that in the lifetime model simulations, the year was divided into 4 parts and each quarter used the same temperatures every year.

The monthly pressure data obtained from Sleipner A did not have any clear relation to the seasons and therefore ambient pressure in the simulations were set to a constant value. The average pressure data from sea level was 1.0107 bar. The weather station also had pressure data at platform level a few months which were 0.0104 bar lower than the sea level measurements. Therefore, it was chosen to use a constant ambient pressure of 1.00 bar in the simulations.

Table 5.1 Pressure and relative humidity data from Sleipner A. [43]

Average pressure at sea level [bar]	1.0107
Pressure difference between sea and platform [bar]	0.0104
Ambient pressure used in the simulation [bar]	1.00
Average RH, used in the simulations [%]	82.8

The relative humidity data seemed to coincide with the seasons a bit more but the data was limited with only 5 measurements the last 10 years at Sleipner A so it was chosen to kept constant with an ambient relative humidity of 82.8 %.

Sea temperatures were also researched and found but they coincided very much with air temperatures. It was assumed the measurement were taken too close to the surface to be relevant as cooling water offshore is usually taken at a certain depth to provide colder and more stable cooling water throughout the year. To be conservative a constant cooling water temperature of 10 °C was used. It is believed if data of cooling water were included it would not have a significant impact on the results because the condensation pressure were set so low that if it were any lower the steam quality, *X*, would become too low.

5.2 Heat and power requirements

To have heat and power demand restraints for a basis for the simulations, it was decided that all the models had to be able to deliver a maximum of 60 MW power and 22 MW heat. To deliver unforeseen extra power loads during the simulations it was also a requirement that the power cycles had to be able to deliver a minimum of 5 MW power at a short notice. In that regard the simple and combined cycle always had to have 5 MW available on one of the gas turbines, including allowance of 10 % over base load of the gas turbines for a short time period. Table 5.2 shows a summary of the simulated platform's heat and power demands.

Table 5.2 Chosen heat carrier and power and heat requirements.

Maximum power required [MW]	60
High-response spare power [MW]	5
Maximum process heat [MW]	22
Heat medium	Liquid water at 20 bar
Process heat temperature supply [°C]	170
Process heat temperature return [°C]	120
Transmission losses (electrification) [%]	10

The life time power load profile was taken from Pöyry's electrification study and it is their reported power profile over Edvard Grieg and Ivar Aasens at the Utsira High formation. [11] Table A.25 in the appendix shows a tabulated overview of the power profile. Most studies simplify the heat demand with a constant heat load for the platforms lifetime. But due to the rise of energy intensity and decrease in power production, an alternating heat load profile was designed to try to increase the realism of the simulations. The use of a constant or varying heat

load has very little impact on the results when extracting already available heat from the flue gas but affect the extraction steam cycles to a much larger degree. The power and heat load used for all of the simulations can be seen in Figure 5.2 and should be akin to the combination of Figure 2.4 and Figure 2.5.

It should be noted that a real power curve is likely to vary a lot daily, hourly and even every minute, depending on what activities are being done, like drilling. But due to the difficulties of predicting a high frequency of power change as well the extensive amount of simulation runtime needed to perform detailed simulations, the power curve used in this thesis is an average of a years' total spent energy and only changes yearly. However, it would be interesting to see how a detailed quasi-dynamic lifetime simulation would perform with collaboration with the industry for decision-making and power operation.

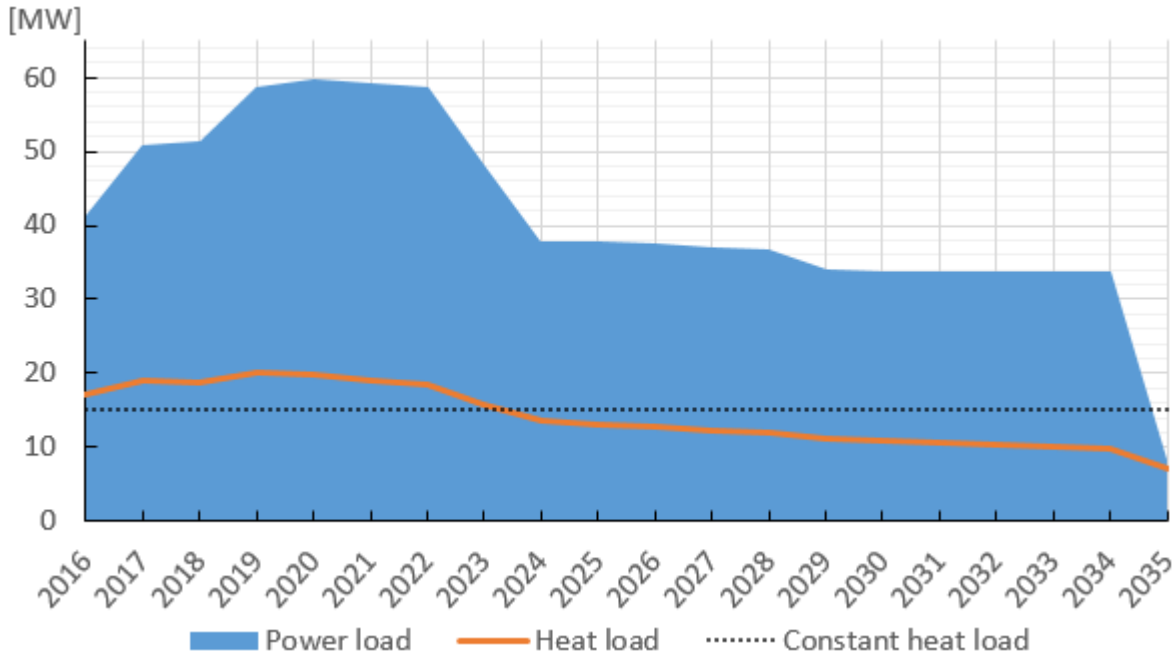

Figure 5.2 Power and heat loads used for the quasi-dynamic simulations. Varying heat load estimated while power load from Pöyry's study. [11]

The pumping power for the process heat water, though small but not insignificant over 20 years, was considered a part of the platform's total power consumption and not included as auxiliary losses.

5.3 Emissions and losses related to electricity from onshore

Due to the relative rigid and well developed hydro power generation it is assumed for the first simulations that the marginal power needed for electrification offshore will come from a European power mixture, as already discussed in chapter 2.3.

Transmission losses and the extra energy needed for export compression of the unused gas was set to an even 10 % of power load, as seen in Table 5.2. Even if one assumes that the power demand comes from Europe, it is not likely an equal power is transmitted the whole way from central Europe. The more likely case is that less power is exported from Norway and then the transmission losses would decrease. But the subsea cables from shore, transformer losses and gas export losses are definite. By also considering the average distribution losses in Norway is around 5 %, a total 10 % offshore distribution losses seemed conservative. [11] The increase in platform power demand due to export of the unused gas was not directly included, but it can be seen as a part of the 10 % transmission losses due to the proportionality of power consumption and unused gas.

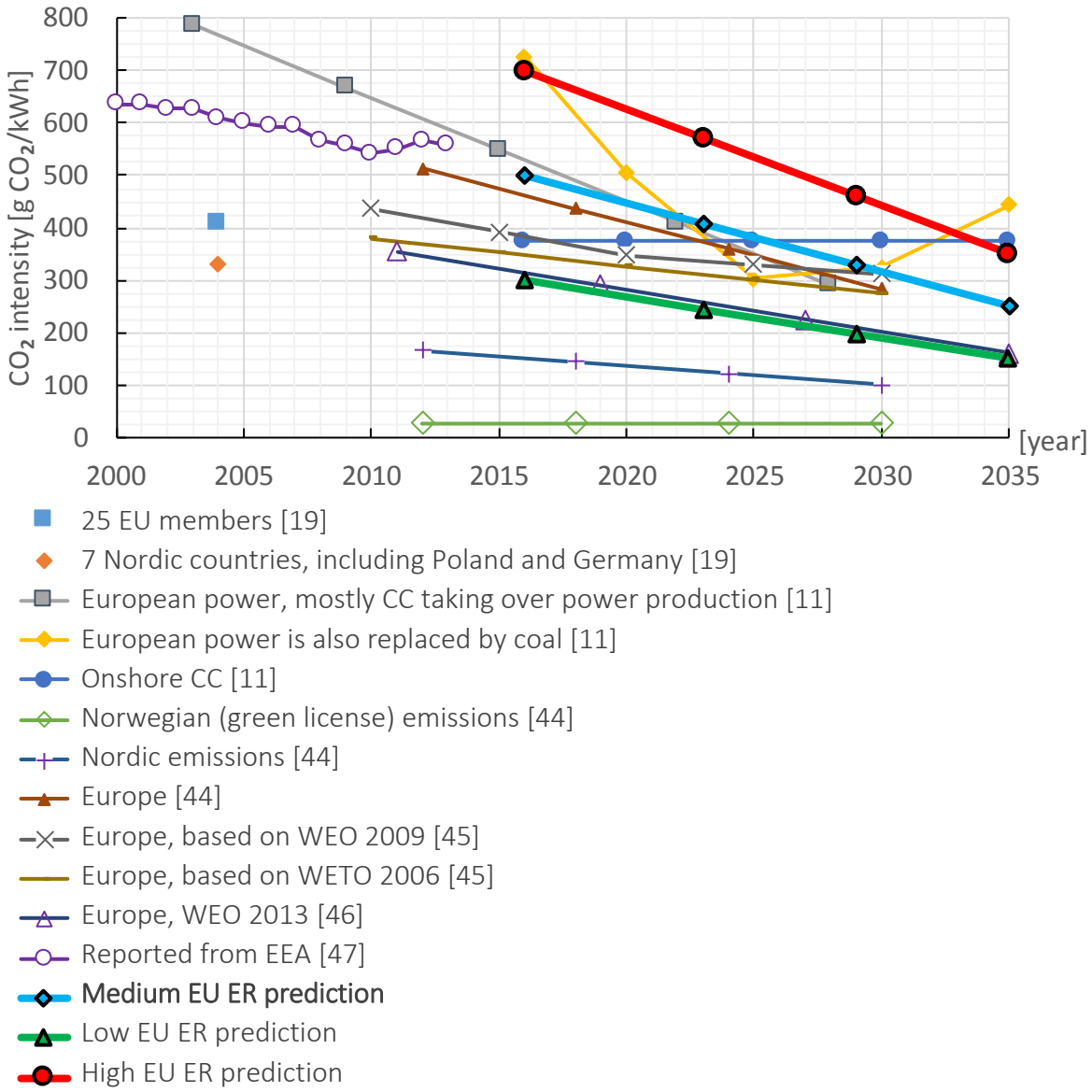

Figure 5.3 Collection of different ER estimates, predictions and reports. Then own medium, high and low linear estimates were made to use in the simulations. The medium EU ER prediction, set in bold, were used for the main electrification simulation.

A large number of ER predictions and reports were gathered to be able to make a better prediction of a future ER, as seen in Figure 5.3. Most weight were put upon what was reported through EEA [47] due to it being factual numbers reported based on total emissions from the power industry and power consumption. Many of the ER assumptions were considerably lower than reported and it was assumed that is because that the emissions included in those emission ratings were mostly based on power production, only fuel efficiencies and power make-up. The medium EU ER prediction, set in bold in the chart's legend, was used as the base ER for the simulations while the low and high prediction, as well as Nordic and Norwegian [44] emission ratings were included in the sensitivity analysis.

5.4 Runtime optimization and GT selection

To choose the most efficient and beneficial power turbines for each case, a selection of GE's aeroderivative turbines were simulated from 10 to 100 % part load with. As seen in Figure 5.4, even if a turbine, like the LM6000, has a rated efficiency above 40 %, a smaller turbine like the LM2500 will have lower emissions at power loads around 9 MW. The dips in efficiencies as the power increases is believed to be caused of adjusting the variable inlet guide vanes and TIT controlling, which gives an overall higher part load efficiency. Dependent on different power needs and cycle designed, the LM2500+G4, LM2500 PJ, LM2500+ and the LM6000 PF Sprint25 was used in the simulations.

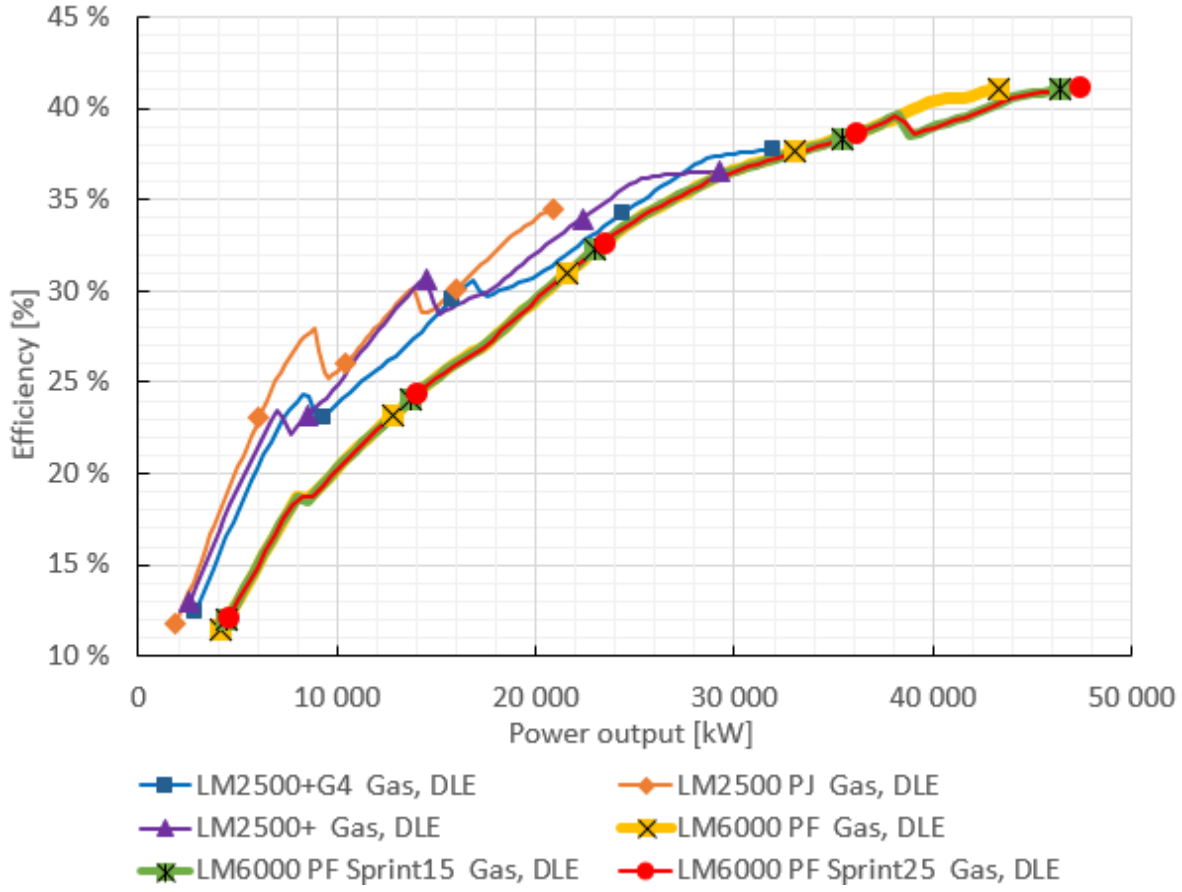

Figure 5.4 Efficiencies of different gas turbines at varying power load with0.99 bar at inlet, 1.04 bar at outlet, ambient temperature of 10 °C and RH of 82.8 %.

5.5 Parameters compared

To compare and screen out simulations in chapter 6, five different parameters were judged and compared: Total CO_2 emissions, weight, flexibility, responsiveness and redundancy.

5.5.1 CO_2 emissions

Only CO_2 emissions could be compared quantitatively from the simulations and it was the primary parameter the models were judged by. The life cycle analysis CO_2 instalment costs were assumed negligible and not considered in this study, with only 20 000 tonnes difference between electrification and simple cycle when one includes recycling at the end of the platforms lifetime. [11]

5.5.2 Weight

Weight estimations were simplified and approximated from similar studies or product manufacturers and scaled more or less linearly with heat transfer or power outputs. Turbine weights can generally be scaled with $\dot{m}_{gas/steam}^{3/2}$. [48] But the turbine weight is usually relatively small compared to total equipment weight so a linear scaling was deemed adequate due to limitations of weight consideration in the simulation software and the scope of this thesis. The weight estimations only give a rough approximation and can at least have inaccuracies up ±10 %.

5.5.3 Flexibility

Flexibility were judged by a power cycle's ability to run heat and power loads at large variations independent of each other without it affecting the efficiency to a large degree.

Flexibility were judged by a power cycle's ability to run heat and power loads at large variations without it affecting the efficiency to a large degree. For example, a steam extraction combined cycle, dependent upon design, may have to by-pass steam or reduce steam flows when running at full power loads and low process heat loads. Or might have to run the GT at higher power loads than needed to supply enough heat when heat demand is high and power demand is low.

5.5.4 Responsiveness

To achieve good comparison in responsiveness, dynamic studies must be concluded. In this thesis responsiveness were primarily judged by start-up time or time to achieve large changes in power load. If the platform operates at low activity, then goes to high activity, a large variation in steam flow might be needed or another gas turbine have to start up. Steam cycles can have start-up times between 10-30 minutes, depending on water temperature and designs. [27]

5.5.5 Redundancy

The redundancy parameter was dependent upon how well the power and heat cycles could operate with some parts shut off for maintenance or failure. Inherent low redundancy might

mean that two GTs have to be installed as back-up instead of one, if a combined cycle cannot give 50 % power load with one GT out of operation. Or if a steam extraction cycle goes out of

5.6 Ebsilon Professional

For the model simulations EBSILONProfessional version 11.04.01 was used [5]. Most of the internal software calculations were done by large industry fluid tables and component-specific characteristic lines and input specification values. Pressures and temperatures are inserted at key points in the simulations to define input and desired output of different components. If invalid values are entered or calculated energy balances does not add up, the program throws an error and cancels calculations.

Following tables were used within the software to provide liquid and gas properties at different states:

- Water/steam: IAPWS-IF97.
- Air/flue gas: LibHuGas (real gas).
- Saltwater: Lib-SeaWa (2009)

The built-in optimization calculator was used for finding optimal mass flows at design point for the steam cycles. Steam mass flow was optimized by maximising $\dot{W}_{ST}$, using $\dot{m}_{steam}$ and $\dot{W}_{GT}$ as variables and using the pinch point in the OTSG, maximum temperature out of the OTSG and the required total power as restrictions. For the lifetime analysis Ebsilon's built in programming tool was used, EbsScript. It is based the PASCAL syntax and Free Pascal but does not support classes and multidimensional array amongst other things. It features a large built in Help library and a large variation in components. [5]

To give accurate gas turbine performances VTU-Energy's Ebsilon Professional gas turbine library. [6] The library uses original equipment manufacturer performance data in according with ISO 2314 and ASME PTC 22 and correction curves for off-design performance. That makes the need for validation of the gas turbine not needed as it is assumed that that the results provided by the VTU library is in accordance with live data. Because the whole gas turbine being a single component and the limited data the component gives, no cycle diagrams or data could be extracted from the gas turbine component.

6 Process description and selection

After defining restrictions, conditions and requirements of power generation offshore, different cycles were simulated to compare, and the most suited alternatives were selected to modify and optimize. Due to time limitations simple and combined cycles and variations thereof, as well as electrification, were considered. More 'exotic' power cycles, like the Kalina cycle, the organic Rankine cycle, STIG cycle or the supercritical CO_2 cycle would be interesting to compare in a lifetime analysis but electrification, simple and combined cycle is still the most promising power technology offshore and were therefore prioritized.

Table 6.1 gives an overview of the chosen cycles chosen to be simulated. It gives a short defining description and gas turbines used. Cases 1a and 1b were two different variants of power provided directly by gas turbines and WHRU used for process heat. Cases starting with the number 2 are different variants of the combined cycle, while case 3 is power from shore with gas providing heating.

Table 6.1 Overview of the simulated cases with case number,

Case	Short description	Gas turbines used
1a	Simple cycle with WHRU	2x LM2500+G4
1b	Simple cycle with WHRU, different GTs.	1x LM2500+G4 1x LM6000PF S25
2a	Combine cycle with steam extraction	1x LM2500+G4 1x LM2500PJ
2b	Combined cycle with steam extraction and separated GT with WHRU	2x LM2500+G4
2c	Combined cycle with backpressure	1x LM2500+G4 1x LM2500+
2d	Combined cycle with a gas boiler	1x LM6000PF S25
3	Electrification from onshore with a gas boiler	-

A detailed overview of the design of all the major components can be found in the appendix chapter A.1. The variables kept constant in all the different cases is shown in Table 6.2. Pressure losses and minimum pinch point temperature were based on similar studies and the relation between area surface discussed in chapter 4.2.4. [27, 33, 49-51] Isentropic, generator and mechanical efficiencies were based on Thermal power generation by Olav Bolland. [18] The pressure drop at the inlet and in the stack was chosen conservatively as 10 mbar, to simulate filters and duct losses, as well as keeping a high enough overpressure out the stack to allow the flue gas to exit the stack.

5 °C were used as the ambient temperature for setting the design point for all the cases. It made it able to deliver enough heat through the WHRU at the same gas turbine load during the varying temperatures set in chapter 5.1. Minimum part load was set to 15 % for all gas turbines to always be within range of the VTU library load characteristics, which allowed for part loads down to 10 %.

Table 6.2 Overview of design requirements for all the major equipment used in the different models.

Ambient pressure [bar]	1.00
Relative Humidity [%]	82.8
Air filter Δp [bar]	0.010
Stack Δp [bar]	0.010
$p_{GT,in}$ [bar]	0.99
$p_{GT,out,WHRU}$ / $p_{GT,out,\ OSTG}$ [bar]	1.022 / 1.040
Flue gas Δp_{WHRU} / Δp_{OSTG} [bar]	0.012 / 0.03
Minimum pinch point $\Delta T_{pinch,OSTG}$ [K]	35
Generator efficiencies η_{gen} [-]	0.985
Mechanical efficiencies η_{mech} [-]	0.998
Pump isentropic efficiencies $\eta_{s,pump}$ [-]	0.7
HP steam turbine efficiency $\eta_{s,HP,ST}$ [-]	0.92
LP steam turbine efficiency $\eta_{s,LP,ST}$ [-]	0.88
Minimum steam quality, X [-]	0.87

Fouling, maintenance, back-up generators testing and other emissions were not included in the analysis. Degeneration of equipment will lead to higher lifetime emissions but unknown new efficiency-increasing technology might also reduce total emissions.

6.1 Simple cycle

Both simple cycle cases are quite similar; the only differences are exchanging one of the GTs and slightly variation of the design of the corresponding WHRU. Figure 6.2 of case 1a and Figure 6.3 of case 1b show that fact where they are both providing 50 MW power and 15 MW heat at off-design.

After filtering the air, the air goes inn at the front of the gas turbine into the compressor, labelled the air intake in the figures. Then gas is injected and burned at a mass rate of 2.7-2.8 kg/s, as shown in the figures, in the combustion chamber at the middle of the gas turbine component, before the exhaust gas goes through the turbine and comes out at around 500 °C. Each turbine drives the compressor of the gas turbine and a generator, which in Figure 6.2 both yield 25 MW power each. Then the flue gas either goes through a WHRU, or some or all of it is bypassed

directly to the stack. Which WHRU that is used depends on the load of the gas turbines, the turbine at highest load is used for providing process heat. The amount of flue gas bypassed the WHRU regulates the supply process heat temperature, while the water mass flow in the heat cycle regulates how much process heat that is provided. For simplifications the heat consumer component extracts all the heat available until the water temperature is at 120 °C.

The simple cycles were validated by checking the results and looking for any inconsistencies, like negative (backward) mass and heat flows, energy and mass balance violations and GT loads above base load. Manual calculations accord to equation (3.25), (3.26) and (3.27) were done to verify WHRU calculations. The gas turbine component is based on live industry data and was assumed to give good correct results within the ambient conditions and power loads used.

6.1.1 Case 1a – base case

Case 1a was made to simulate how most standard offshore platforms are powered. It is based upon a dual LM2500+G4 setup with a WHRU each which gives great redundancy and flexibility in operation. Both GT skids weigh around 150 tonnes and both WHRU estimated to around 70 tonnes each gives a total estimated weight of 440 tonnes, which made it the cycle with the higher power to weight ratio, except for electrification. [31, 32] As anticipated it was also the cycle with highest lifetime GGE, with a total of 4 mega tonnes CO_2 emitted.

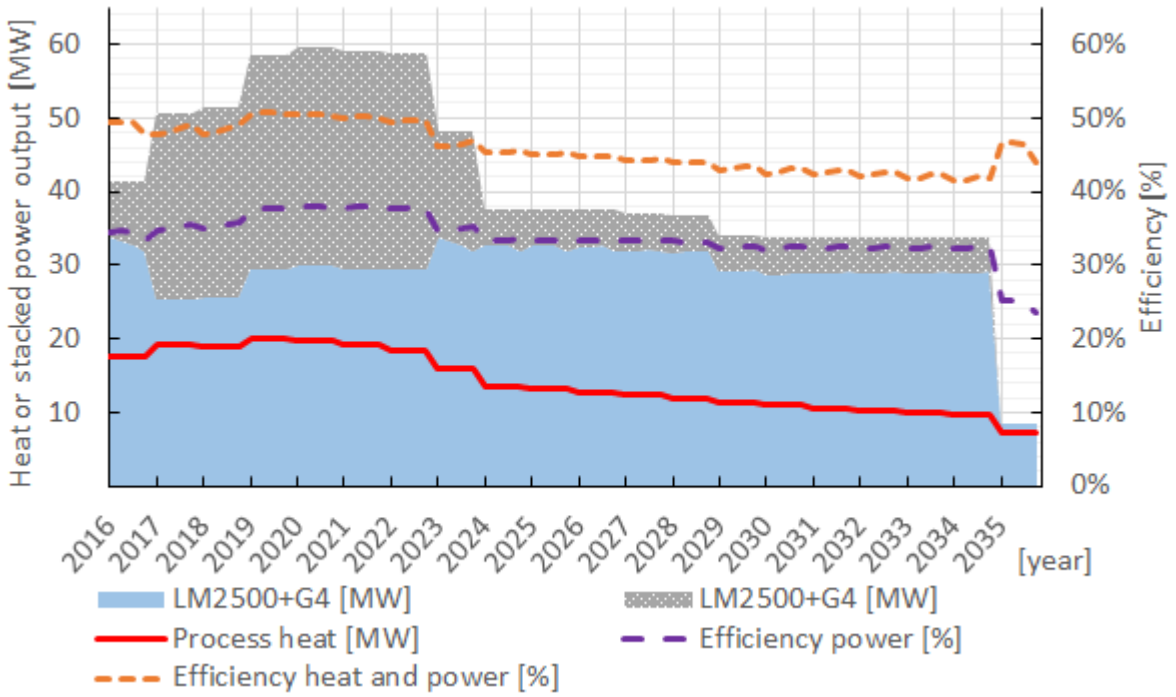

Figure 6.1 Power loads, heat loads and efficiencies throughout 20 year lifetime. The area power loads are stacked on top of each other and have almost a 60 MW load at peak while it runs around 30-40 MW load for a majority of the time.

Figure 6.1 shows the performance and the load of each turbine throughout the 20 years simulated operation time, with the power and heat loads from Table A.25. It has a decent electrical efficiency around 40 % at highest load and activity but runs at a relatively low efficiency of around 33 % for a majority of the lifespan. The total heat and power efficiency barely reaches 50 % at its best and ranges between 40-50 %. The load division were found, by mapping out the efficiencies at different load combinations, to be good when maximizing the load of one GT and minimizing the load of the other below 50 MW total power load, and dividing the power load equally above 50 MW total power load. Figure 6.1 also shows that most of the load is primarily given by one turbine for simplifying the graph. In real life the load sharing would vary more due to fouling and maintenance reasons.

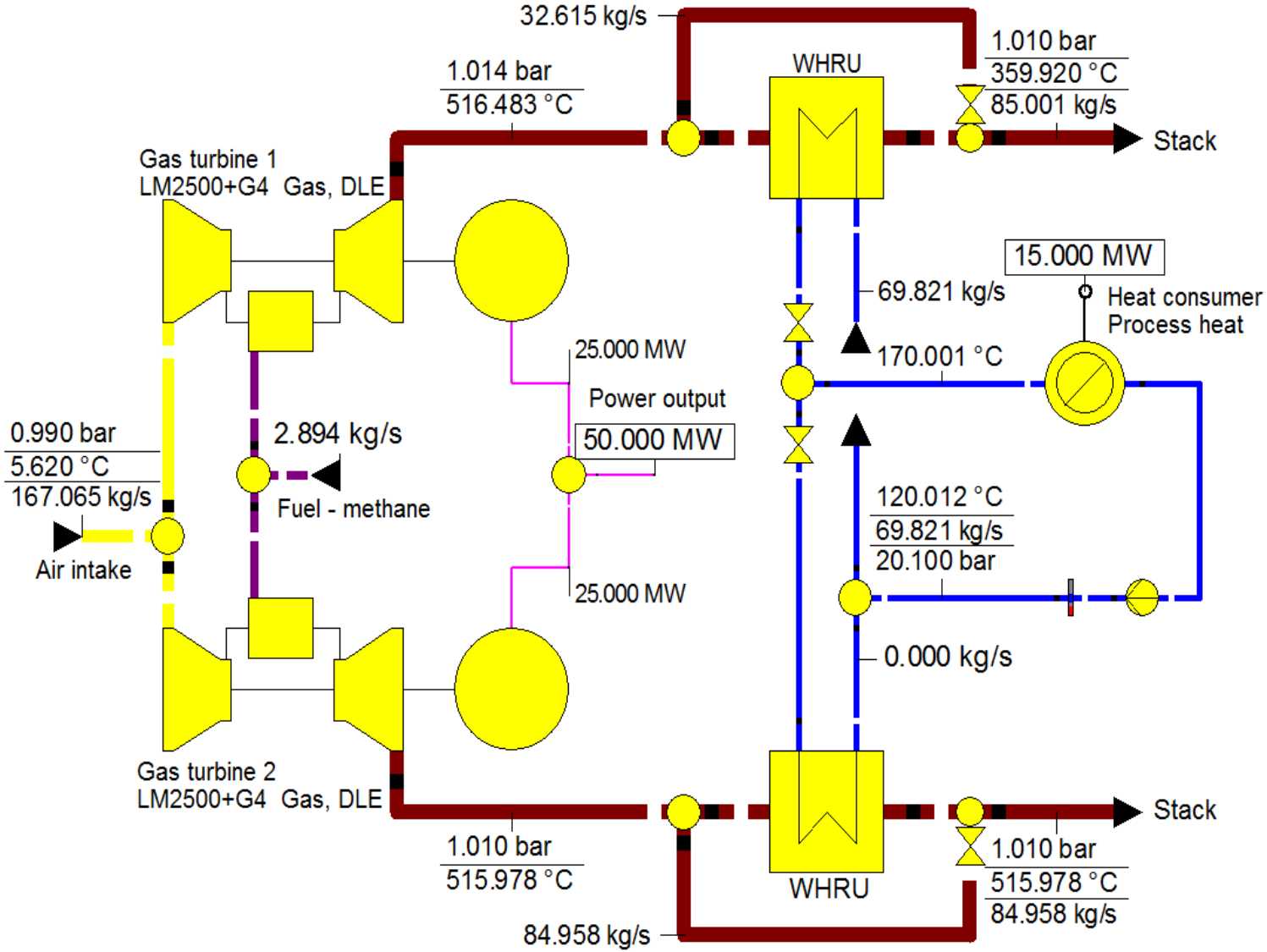

Figure 6.2 Overview of case 1a, simple cycle with 2x LM2500G4+ and a WHRU for each GT, in Ebsilon Professional at off-design delivering 50 MW power and 15 MW heat.

6.1.2 Case 1b – simple cycle with a LM6000

The LM6000 gas turbine from GE is relatively larger than the LM2500+G4 used in case 1b. Its total skid weight was assumed about 200 tonnes, conservatively approximated from LM6000 unit data sheet, LM2500G4+ unit data sheet and the weight of 150 tonnes of the LM2500G4+ complete offshore skid. [30, 31, 52] Both WHRU were assumed to weigh the same as in case 1a, which gave a total weight of 490 tonnes. [32] But the LM6000 also have a higher power rating of 47 MW and a higher efficiency for a longer power load range than the G4, as seen in Figure 5.4. Figure 6.4 shows how having one larger and one smaller GT allows for a larger flexibility and room for better optimization of power load sharing between the GTs, by having a smaller fuel consumption at 50 MW than case 1a.

Figure 6.3 shows the power sharing of the GTs and the efficiencies during the platforms lifetime. By having a larger GT that can run closer to optimal load for a longer period of the lifetime of the platform, while having a smaller GT that helps out during the extra high power needs, the lifetime power efficiency was in the 36-40 % range for almost the whole period and it lowered the total emissions to circa 3.7 mega tonnes CO_2. It still has the same flexibility and inherent redundancy as case 1a and it is assumed that the larger size of the main GT does not affect the responsiveness of the power cycle to a larger degree.

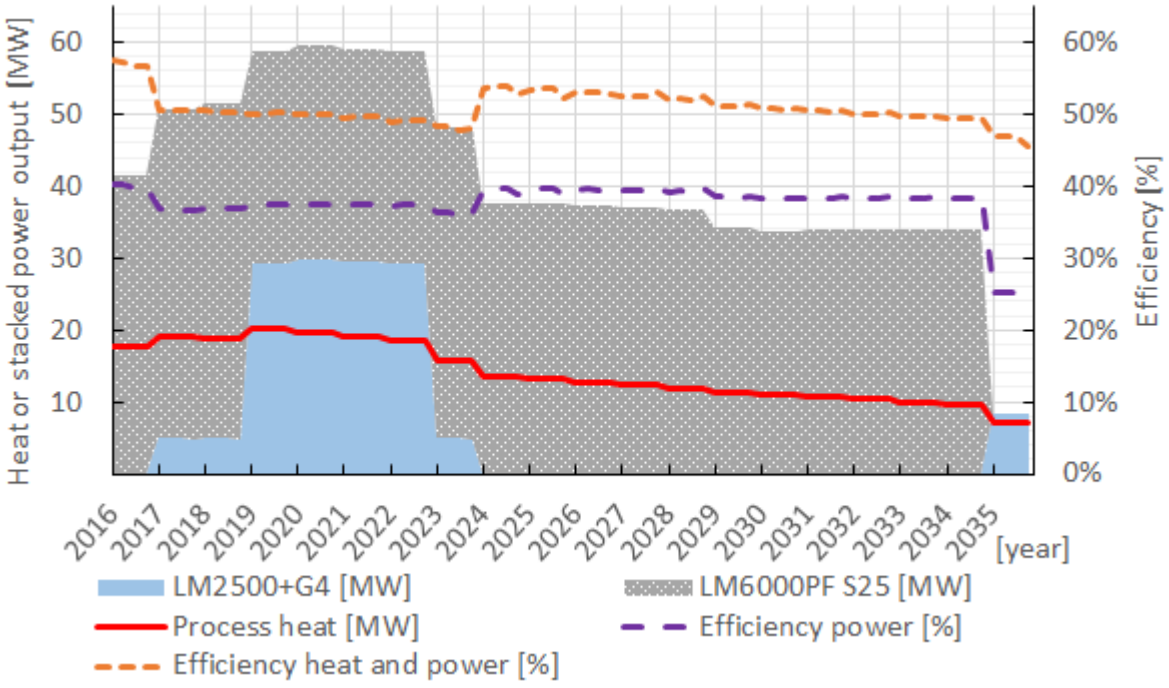

Figure 6.3 Case 1b showing lifetime heat and stacked power production with power and total efficiencies.

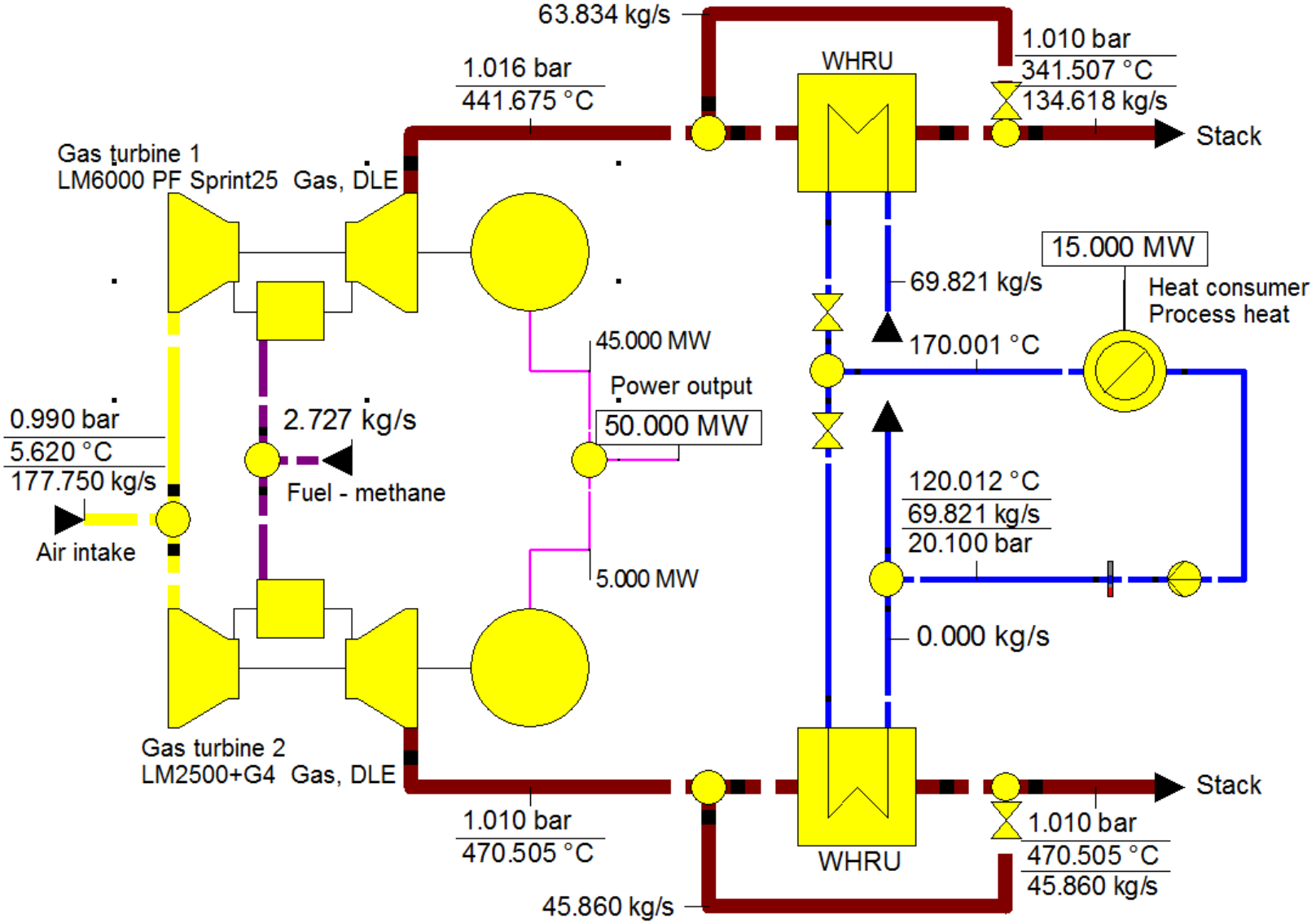

Figure 6.4 Overview of case 1b model in Ebsilon Professional; simple cycle with a LM2500G4+ and a LM6000 with a WHRU for each GT, at off-design delivering 50 MW power and 15 MW heat.

6.2 Combined cycle

Kloster's weight assumptions of 150-175 tonnes for a steam cycle skid in the 15-20 MW power range, including generator, turbine, condenser and auxiliary systems, were used and approximated linearly to the design steam turbine power of each combined cycle case studied. [53] Lars Nord and Olav Bolland calculated the weight of an OTSG around 100 tonnes when coupled with a single LM2500+G4. In that regard the weight of the OTSGs was scaled up linearly dependent on flue gas mass flows and temperatures. [33] An extra 50 tonnes were added as a precaution for water treatment and tanks, process heat equipment and because of the higher complexity steam extraction entails, as limited weight data was found of combined heat and power steam cycles. Table 6.4 gives an weight distribution overview of case 2b, the basic combined cycle.

To validate the steam cycle simulations, the combined cycle was run at no process heat supply at 15 °C ambient temperature, 1.013 bar ambient pressure and 60 % RH. The LM2500+G4 was set to base load while the other GT was off. By running the cycle at off-design and compare it to similar combined cycle studies with single pressure OTSG, the combined cycle simulations in Ebsilon Professional were validated. The simulation was compared to Nord, Emanuele and Bolland's weight and power optimization study [33] and Nord and Bolland's [36] Steam bottoming cycles offshore study. The results were positive with slightly better results which were expected, considering the larger OSTG designed to take a larger flue gas flow, than other study's simulations:

Table 6.3 Simulation with a single GT at full load, no heat consumption at off-design to validate the simulation. The HRSG in the Ebsilon simulation was designed for higher mass flows from 2 gas turbines rather than one like the other simulations and the results were a bit higher, as expected.

Full load and no heat comparison	Ebsilon Professional simulation	Nord, Emanuele and Bolland (GT PRO) [33]	Nord and Bolland (GT PRO) [36]
Net electrical output [MW]	44.1	43.5	42.9
Net electrical efficiency [%]	52.4	51.7	51.0
GT gross [MW]	32.2	31.9	32.1
ST gross [MW]	12.2	12.0	11.3

During each lifetime simulation, each model was run several hundred times and a part of validation the results was to ensure no error messages or warnings appeared. T-s graphs and Q-T diagrams were checked at different off-design points as well as mass and volume flows were controlled to not go beyond a components design characteristics.

The steam and condensation pressure of the steam cycle was chosen after Lars Nord studies [33] where it was shown by using OTSG and selecting relatively low pressures, the weight to power ratio of the cycle can be minimized with an improvement in overall efficiency. Therefore, a condensation pressure of 0.04 bar was chosen instead of the commonly higher condensation pressures offshore. After deciding the pressures, the superheat was minimized to 480 °C to reduce material costs and low OTSG exit pinch point, while still having more than 90 % steam quality at ST outlet. At off-design when the flue gas temperature was low, the steam high temperature were set to the minimum value of 480 °C or flue gas temperature - 35 K to avoid simulation errors and have a more efficient cycle with a high steam flow: $T_{steam}=MIN(480,T_{flue\ gas}-35)$. A lower temperature difference was tested, between $T_{steam}=MIN(480,T_{flue\ gas}-5)$ to $T_{steam}=MIN(480,T_{flue\ gas}-35)$. The best results were between $T_{steam}=MIN(480,T_{flue\ gas}-20)$ and $T_{steam}=MIN(480,T_{flue\ gas}-35)$. It was chosen in the end to stay at -35 to be conservative and have a higher steam flow.

The steam extraction pressure was chosen to have saturation temperature of 175 °C and the heat was extracted from the steam with a condenser and an economizer. Ideally de-superheating, condensing and sub-cooling of the steam extract would have been done with a single heat exchanger to save space. To reduce space even more offshore, water mist could have been injected into the extracted steam, cooling down the superheated steam and making use of the latent energy in the condenser and reducing sensible heat transfer.

6.2.1 Case 2a – combined cycle with two GTs and steam extraction

Figure 6.6 shows the combined cycle as it appears in Ebsilon Professional, with added labels for the main components. It delivers 50 MW net power, which is provided by the two GTs and the HP and LP steam turbine while the pressure and cooling water pump power is subtracted. The LM2500+G4 is run at base load while the steam turbines and the LM2500 PJ delivers the remaining power and heat into the steam cycle to get enough power. After the air and fuel goes into the gas turbines and power is extracted, flue gas goes out and into the OTSG unit, which consists of 3 separate components in the software. After a large portion of the heat in the flue gas is extracted to the steam cycle, the flue gas leaves the OTSG and enters the stack at 180 °C.

At design point, each OTSG component is designed as an economizer, evaporator and superheater. But the program allows sliding heating areas at off design and simulates the behaviour of a proper OTSG unit. In the figure, water enters the bottom of the OTSG at 72 °C and is heated at a constant pressure of 22 bar, and leaves the superheater at the top of the OTSG at 480 °C as steam. The steam enters the high pressure steam turbine (HP ST). A third of the mass flow exits at the steam extraction at around 9 bars and gives off heat to the process heat cycle. The steam extraction mass flow is controlled by the process heat cycle temperature, always ensuring 170 °C. The rest of the steam enters the low pressure steam turbine (LP ST) and is expanded down to 0.04 bar at a steam quality of 92.5 % in the figure. The steam is then condensed into water in the condenser, before being pumped, in two intervals, up to 22 bar again while being re-joined with the water from the extraction heat.

Figure 6.5 shows the T-s diagram, created in Ebsilon Professional, of the cycle operating at the same off-design point as shown in Figure 6.6, and it corresponds well with the theoretic cycle in Figure 4.9. It depicts how the different parts of the steam cycle affect the entropy and temperature of the steam. The OSTG heats the water, evaporates it and superheats the steam before expanding through the turbines with some entropy loss. The throttle between the two turbines is an isenthalpic process but gives entropy losses. The steam exits the turbines and is condensed at a constant temperature and pressure. The extraction steam also gives off superheat in the condenser to the process heat cycle and is economized before re-joining the rest of the steam.

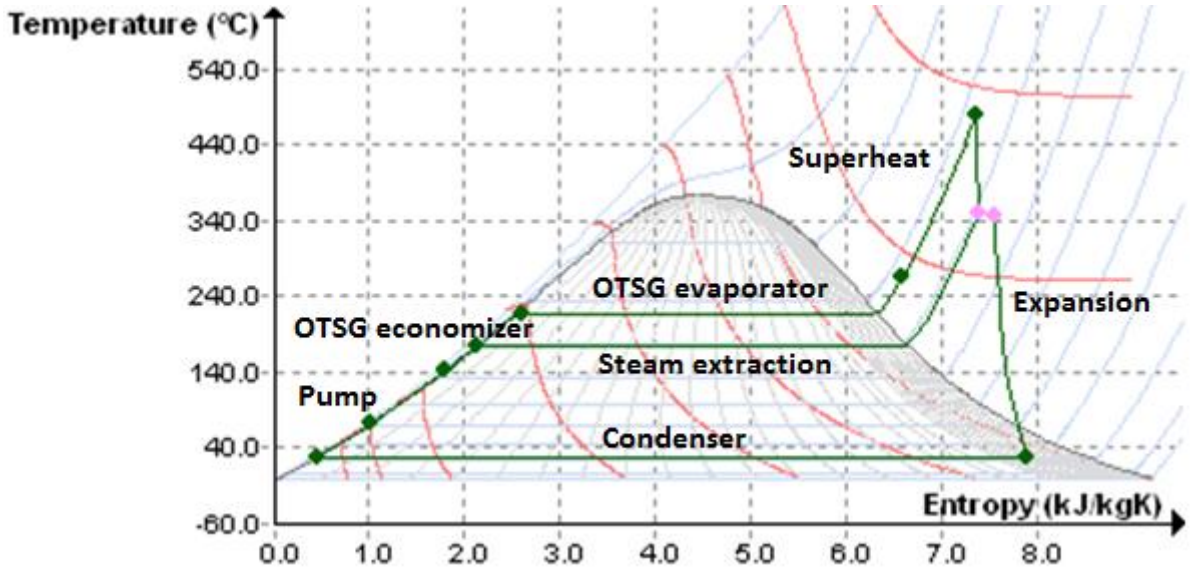

Figure 6.5 50 MW power and 15 MW heat with the key processes and components labelled.

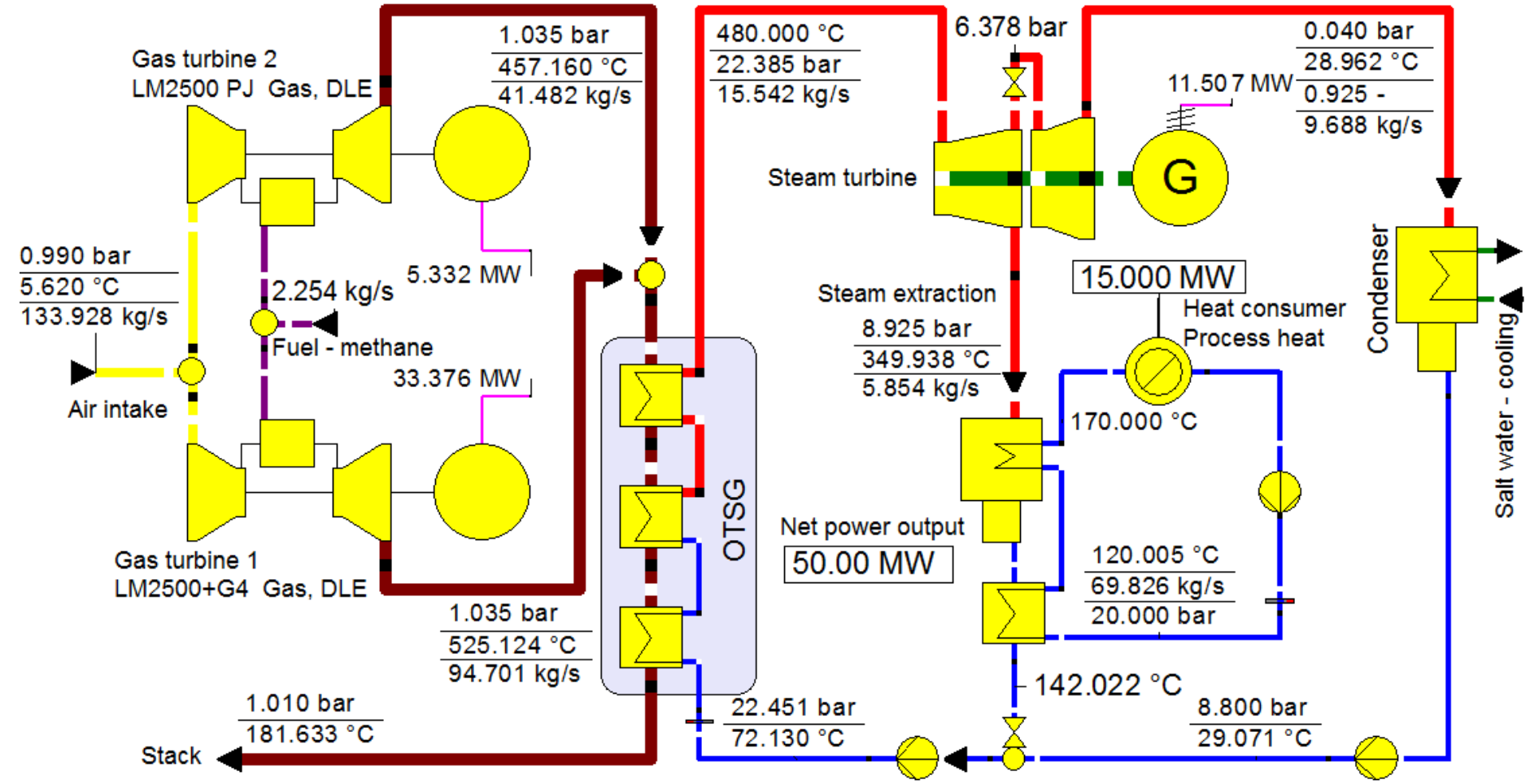

Figure 6.6 Model 2a in Ebsilon Professional. One LM2500+G4 and a LM2500 PJ combined with an extraction steam cycle delivering 50 MW net power and 15 MW process heat.

A Q-T diagram was also drawn of the heat transfer in the OTSG at design point, to control the minimum pinch point and compare it with the theory in Figure 4.14. The flue gas loses its heat as the top red line and goes from the top right corner of the diagram down to below 200 °C at the left. The blue bottom line shows the water being heated then evaporated at a constant temperature, before being superheated up to 480 °C. A Q-T diagram of the steam extraction was also made to check the pinch point and to validate it was behaving correctly. It can be found in Figure A.1 in the appendix.

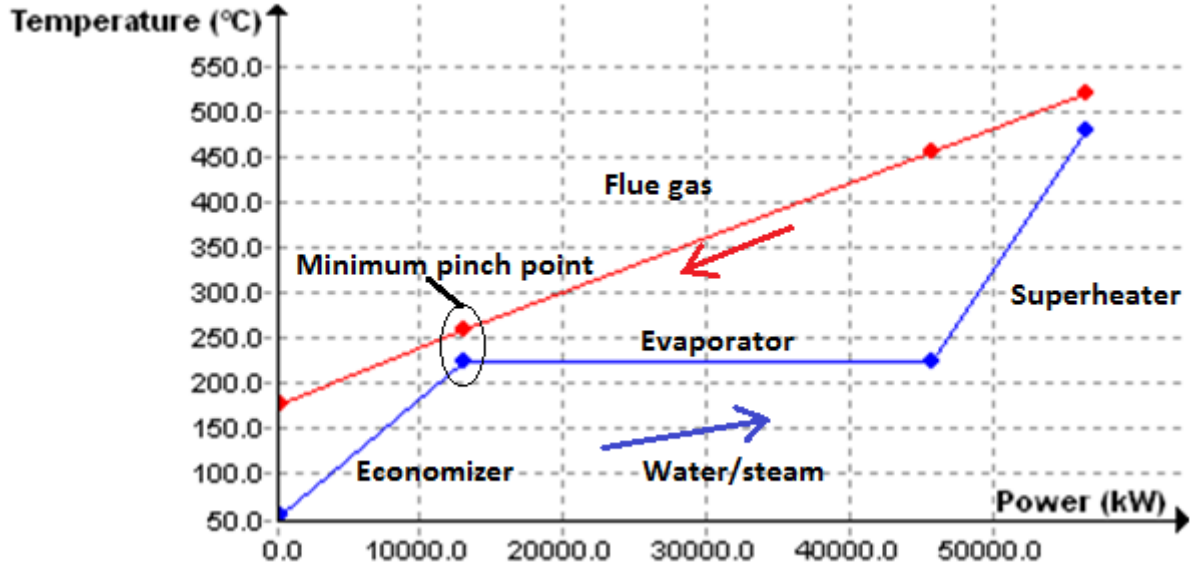

Figure 6.7 A Q-T diagram of the OTSG at design point. The minimum pinch point is identified between the economizer and evaporator area of the HRSG and it was verified it was not below a temperature difference of 35 K. The flue gas losses energy and temperature down to the left in the diagram while the water/steam energy and temperature increases up to the right.

Figure 6.8 shows the efficiency and loads of the combined cycle simulations. By adding a steam bottoming cycle, the power efficiency was increased to around 45 % for the platform's lifetime while total efficiency was around 60 %. The total CO_2 emissions totalled a bit above 3.1 mega tonnes CO_2, more than 20 % less CO_2 than the simple cycle case. But on the other hand it weighs almost 50 % more, is less flexible in operation and has a lower redundancy with only one system for providing process heat. The responsiveness of case 2a was judged as medium because it could provide 50 MW of the power from only GTs and were in that way not that much reliant on the less responsive steam cycle. The figure also shows how the ambient temperature can affect the efficiency to a large degree, by having to run with two GTs during the warm season from year 2024 to 2029 while a single GT is sufficient, while still having 5 MW spare power capacity, during the cold seasons.

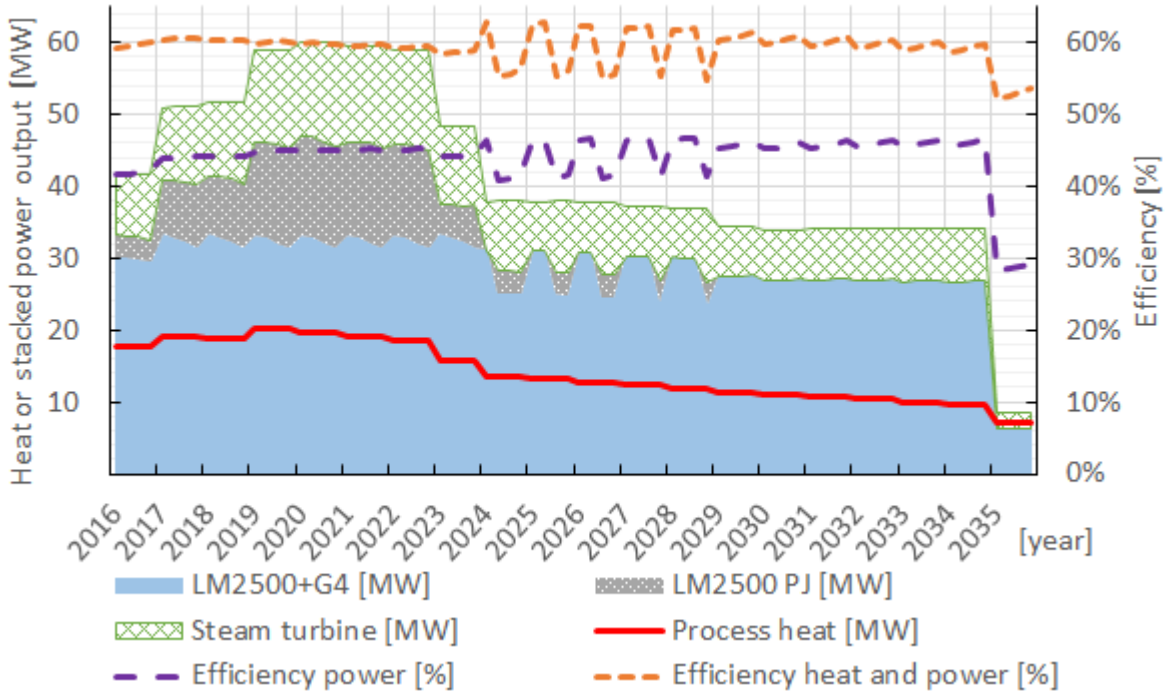

Figure 6.8 Case 2a showing the heat load, power load sharing between the two GTs and the ST. Electric and total efficiency is shown in dashed lines.

Table 6.4 show the weight estimation of the combined cycle in case 2a. It is not very accurate but should give a fair idea of the weight expectancy of installing the power technology offshore. A LM2500 PJ were used instead of two LM2500+G4 due to higher efficiencies in the power range needed as well as its smaller size. It comes at the cost of lower redundancy and less flexibility in how the two GTs are operated. The LM2500 PJ skid were approximated by its engine weight, the LM2500+G4 engine weight and its total skid weight. The OSTG were scaled up from Nord's study with higher heat flows while the steam turbine skid was judged after Kloster's study. 50 tonnes were added for steam extraction and extra water equipment. [30, 31, 33, 53, 54]

Appendix chapter A.2 explains and shows the core of the script used to manage a correct power and heat load output of case 2a. Variants of it were used for the other combine cycle cases. In a real combined cycle, the GT load would increase when a power demand is increased. As the steam generation increases, the GT load partially decrease and let the steam generator handle a part of the increased power load.

Table 6.4 Rough estimates of case 2a's power equipment. An extra 50 tonnes were added additionally to sized-up estimations from sources, for steam extraction equipment, water tanks and treatment.

Equipment	Estimated weight [tonnes]
LM2500+G4 skid [31]	150
LM2500 PJ skid [31, 54]	125
Steam turbine skid [53]	150
OSTG [33]	150
Extra water tanks and water treatment	30
Steam extraction	20
Total	625

6.2.2 Case 2b – combined cycle with extraction and separate WHRU

To increase the redundancy of the combined cycle in case 2a, having a combined cycle with a single GT and a separated GT with its own WHRU was tested. That way, a smaller OTSG can be used and a slightly lighter steam cycle equipment, while still having high efficiencies for a large portion of the platform's end operation time. With 2 LM2500+G4 skids, a WHRU at 70 tonnes, a smaller OTSG of 100 tonnes and a smaller steam cycle skid of 90 tonnes, the total weight was estimated to 610 tonnes. [31-33, 53] Having two G4s also makes the platform completely independent on the steam cycle and gives high redundancy and flexibility.

The WHRU was only considered as a reserve process heat source and was not utilized during the first simulations done in this chapter. In Figure 6.9 the WHRU is not connected to the process heat cycle to provide less clutter in the figure. The only other differences between case 2b and 2a, except separating a GT from the steam cycle, is the resulting smaller steam flows due to the smaller flue gas flow going through the OTSG. In Figure 6.10 it can also be seen that the steam cycle is more optimized to run with a single GT and the other GT has to be used less during the warm seasons after the year 2024. The performance is significantly worse during the first part of the platform's lifetime when the heat and power loads are high and the steam cycle runs at lower efficiency. The results gave total lifetime emissions of 3.3 mega tonnes CO_2.

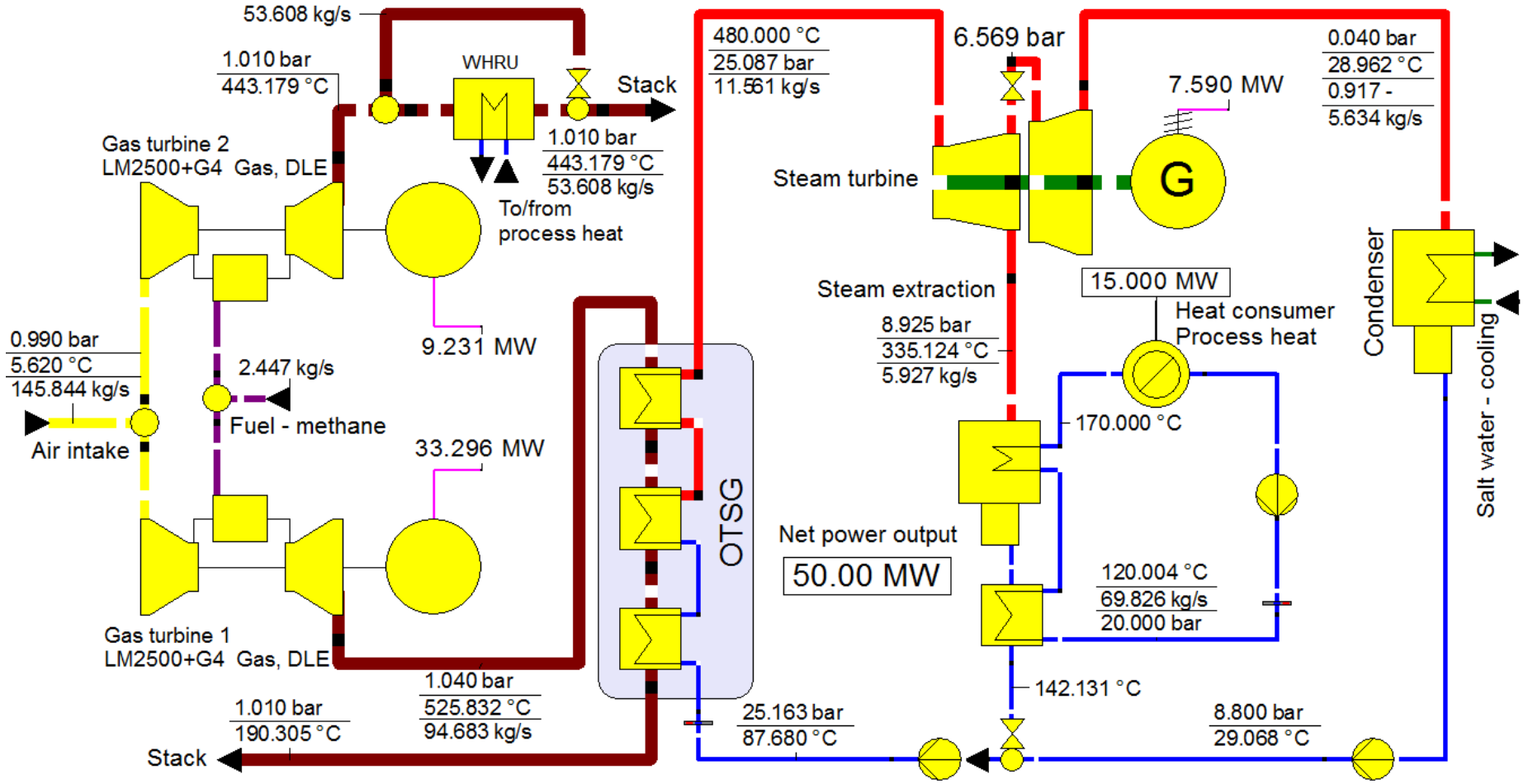

Figure 6.9 Case 2b shown. One gas turbine, LM2500+G4, delivers power and flue gas heat to an extraction steam cycle. Another LM2500+G4 has a separated WHRU in reserve to deliver heat if the steam cycle is offline. WHRU connections simplified as it was only for back-up and it did not deliver any heat during the simulations.

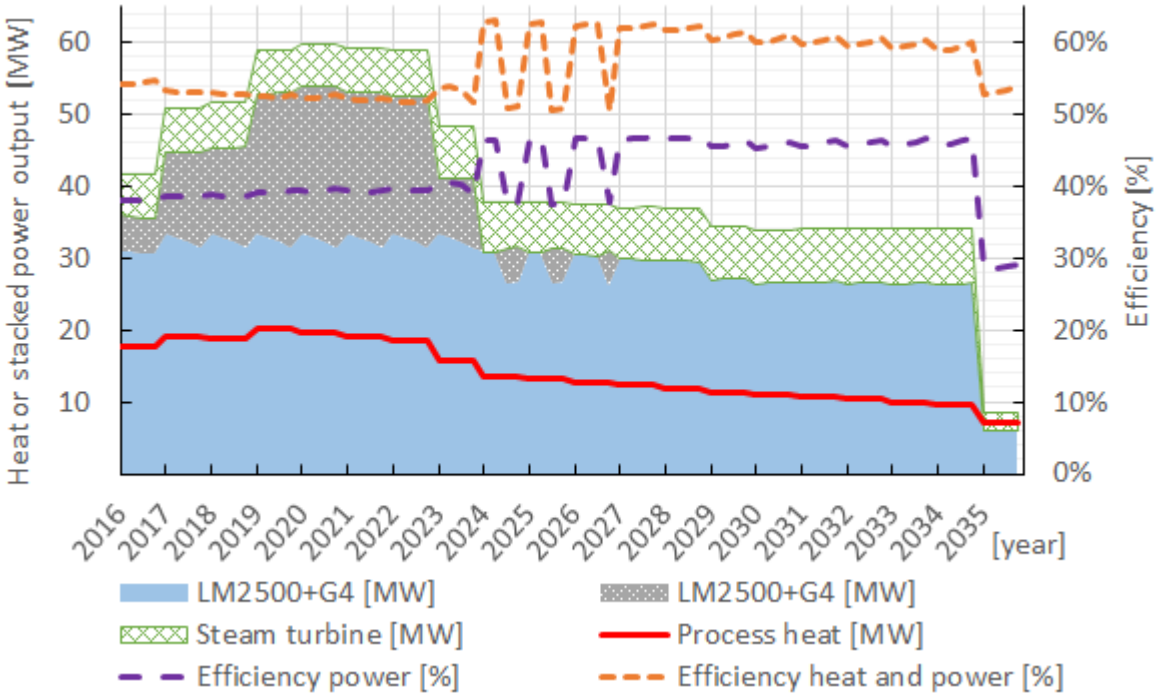

Figure 6.10 Case 2b's combined cycle and simple cycle power profile with higher redundancy and responsiveness.

6.2.3 Case 2c – combined cycle with backpressure process heat

The use of a backpressure combined cycle were also tested, mostly to confirm how that it is ill suited when providing process heat at 170 °C. It emitted 3.8 mega tonnes CO_2 during the lifetime simulations. A version at a lower backpressure, providing process heat at 120 °C, was also tested and resulted in 3.5 mega tonnes CO_2 emitted. Both backpressure models performed worse than any of the other combined cycle simulations. A backpressure combined cycle would only be able to perform better than an extraction cycle with lower process heat temperatures and/or higher process heat load requirements. Any break-even points, when a backpressure combined cycle is better than an extraction combined cycle, were not found, but would have been interesting to find out as a large amount of process heat is needed at lower temperatures, as seen in chapter 2.2.

The process heat condenser and the main condenser were run in parallel, as seen in Figure 6.11. A lower backpressure could have been used if they were run in series and more of the steam superheat was utilized to provide process heat. But due to design difficulties and the initial bad results, even at 120 °C, no further improvements were tested.

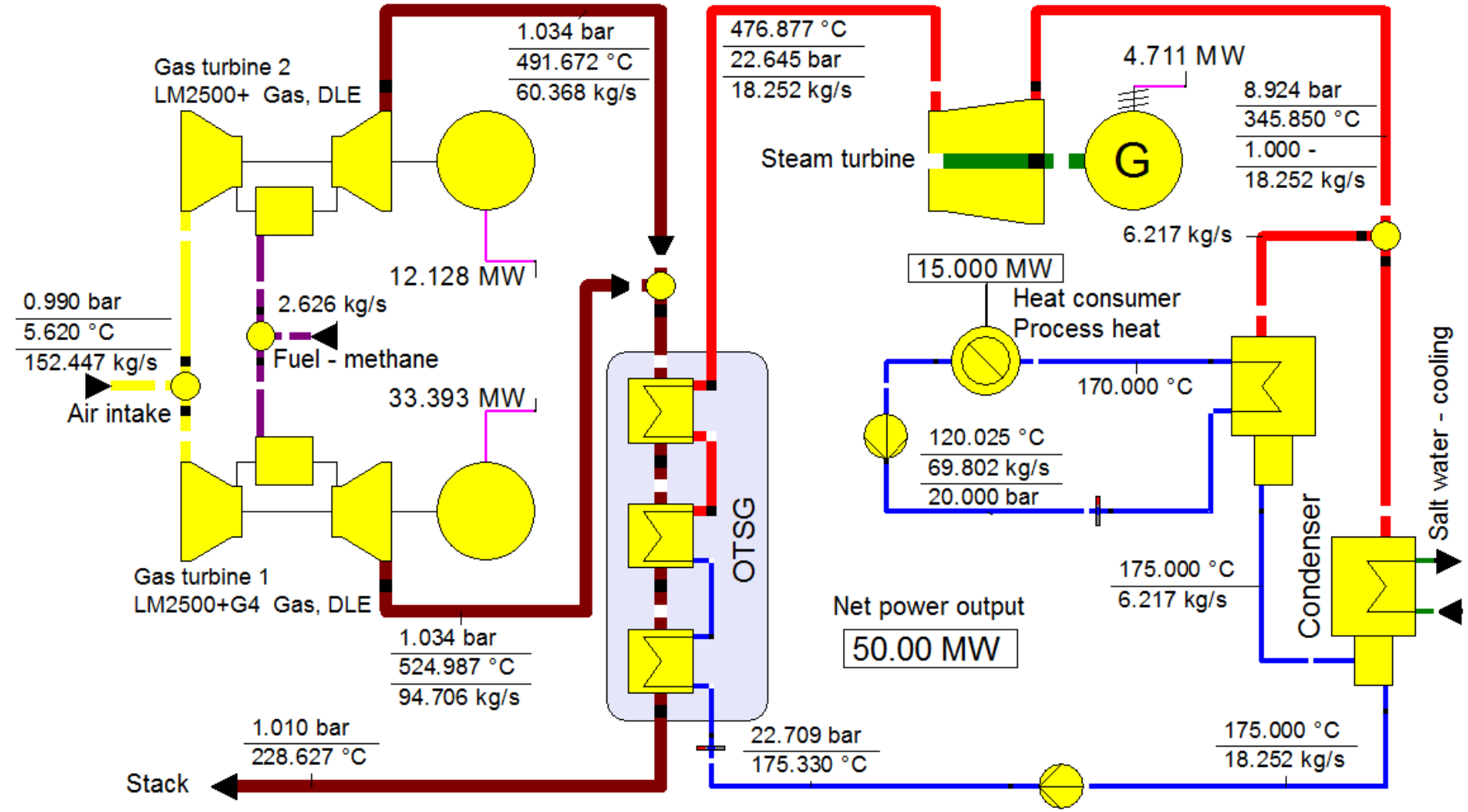

Figure 6.11 Backpressure combined cycle case 2c, providing process heat at a high temperature of 170 °C and a high backpressure of 8.9 bars.

Other than having a higher backpressure and no steam extraction, the power cycle function the same way as case 2a. Because of lower power efficiency, a LM2500+ had to be used instead of a smaller LM2500 PJ. One of the positives of the backpressure cycle was how it always had enough process heat, as long the steam cycle was in operation, and could be adjusted independently to power demand. By having two gas turbines being able to deliver 60 MW by their own, the cycle has an high flexibility and responsiveness. But the redundancy is low, with only one process heat source.

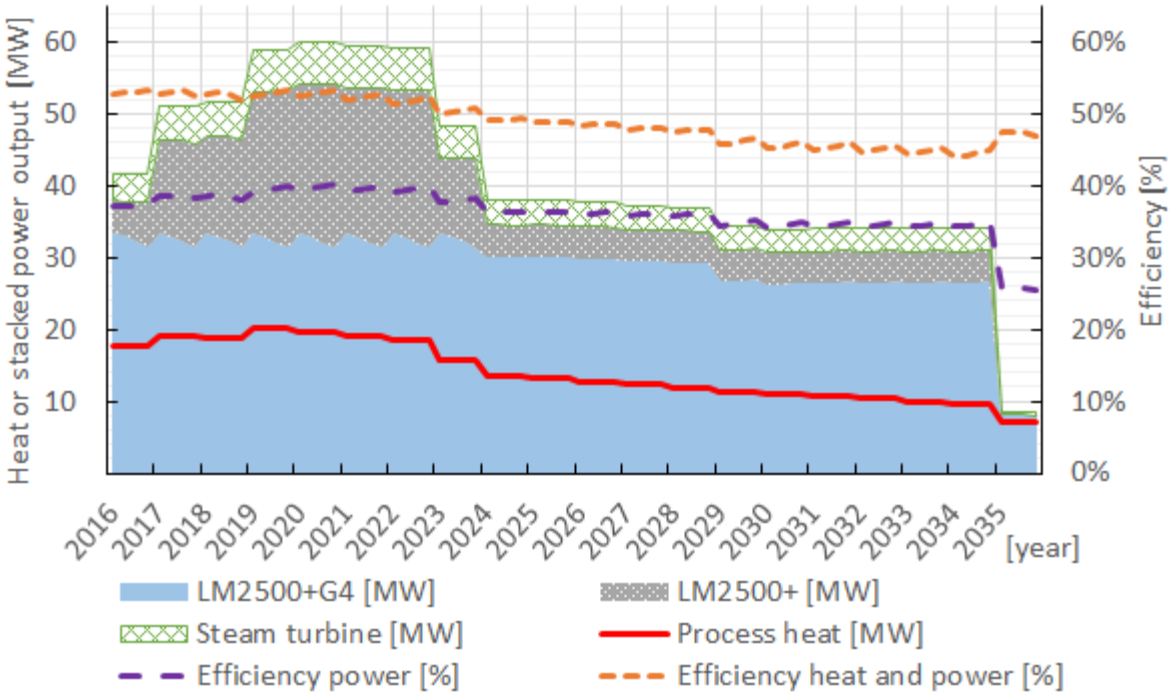

Figure 6.12 Case 2c at 170 °C process heat. Lower power efficiency requires the cycle to use two GTs at all times.

Figure 6.12 show the smaller power output the steam cycle gives with a backpressure process heat system, compared to case 2a, which requires both GTs to run at all times and significantly hampers the reduction of GGE.

The back-pressure process heat equipment was assumed to weigh the same as the steam extraction case. The LM2500+ skid was estimated at 150 tonnes, OTSG at 180 tonnes and steam skid at 60 tonnes. Which gave a total of 580 tonnes. The back-pressure process heat cycle at 120 °C were estimated to weigh 595 tonnes with a slightly smaller OSTG but a larger steam cycle skid. [31-33, 53, 55]

6.2.4 Case 2d – combined cycle with a LM6000 and a gas boiler for heat

In case 2d the combined cycle was tried to optimize for power while using a gas burner as a process heat source. Figure 6.13 shows the more simple, pure power combined cycle at 50 MW power. By using the LM6000, 60 MW max power is reached with only the single gas turbine slightly above base load and the steam cycle, which would not be possible with steam extraction. The LM6000 has a lower flue gas temperature, which gives a steam temperature of 420 °C. The condensing pressure has to be raised to 0.07 bar to obtain a steam quality above 0.9 at the turbine exit.

A gas boiler was used to provide heat, as seen in Figure 6.15. The next sub-chapter, with the electrification case, will go through its description. Figure 6.13 shows the relative high power delivered by the steam cycle and the high power efficiency close to and below 50 % for the whole lifetime. But by using a gas boiler separately to provide heat, the total lifetime CO_2 emissions were still higher than case 2a, with 3.4 mega tonnes CO_2. It also has a very low redundancy with only one GT and a steam cycle to provide all the power, and only one source of heat. The need for the steam cycle to run for a majority of the lifetime also gives it low flexibility and responsiveness.

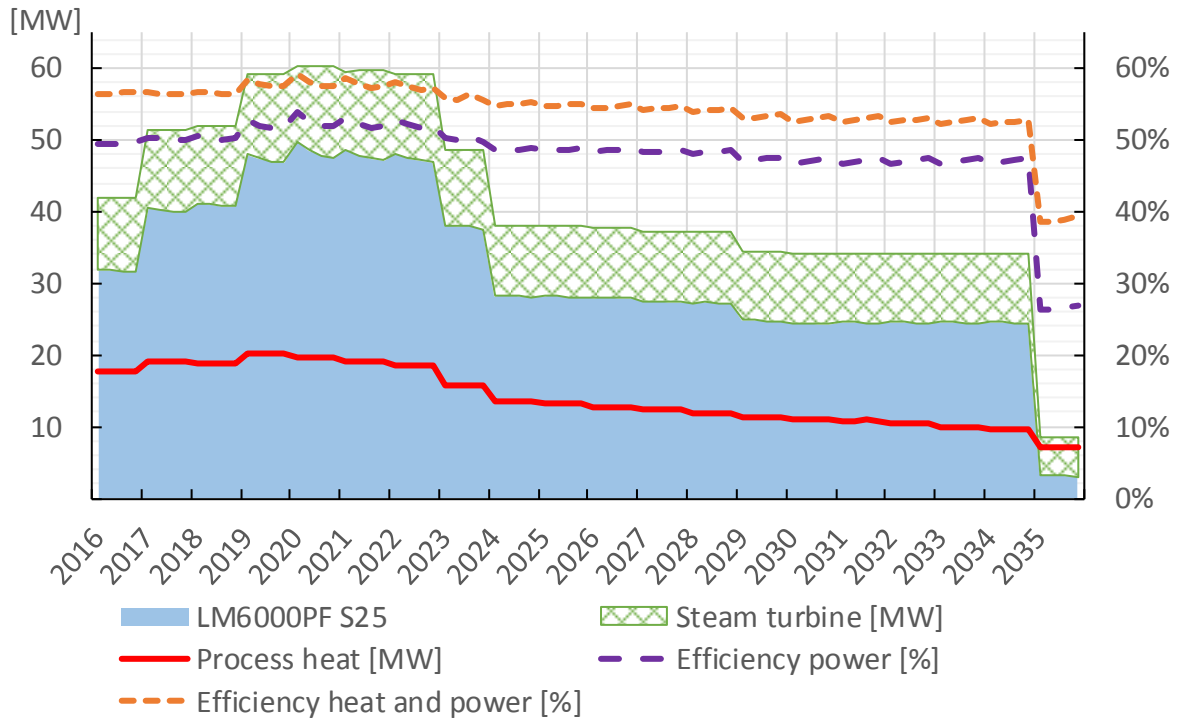

Figure 6.13 Optimized CC with a single GT and an own external gas boiler providing heat.

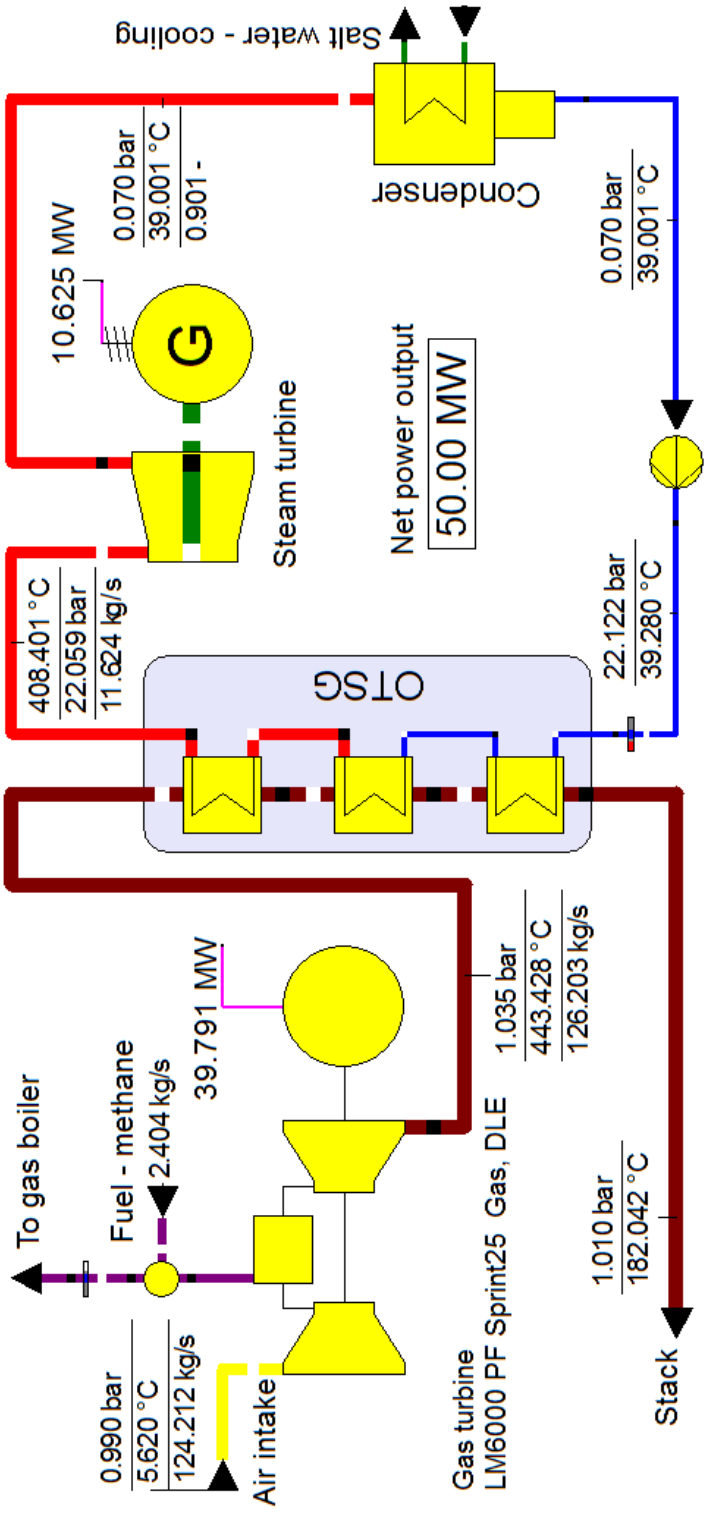

Figure 6.14 The combined cycle with a single LM6000 provides 50 MW power. By focusing on power production, a higher power efficiency is obtained. Figure 4.15 shows the gas boiler providing the process heat.

The OSTG was estimated to weigh about 125 tonnes in case 2d and the steam cycle was estimated at 110 tonnes. With 30 tonnes for the water treatment and accessories, 200 tonnes for the LM6000 skid and 70 tonnes for the gas boiler, ending with a total weight of 535 tonnes. [30, 31, 33, 42, 52, 53]

6.3 Case 3 – electrification

In the electrification case, it was assumed no bottlenecks in the power grid. The inherent ER of the electric power used were calculated/predicted onshore, and the power arriving at offshore therefore had a higher ER because of 10 % transmission losses. The ER used was the medium EU prediction in Figure 5.3 (500-250 kg CO_2/kWh), and equation (3.50) shows how the CO_2 emissions from onshore power was calculated.

The calculation of onshore power production can be seen in equation (3.44). The emissions were calculated by setting up a custom stream which delivered both power and CO_2 emissions. More detailed information about the custom power and CO_2 stream can be seen in chapter A.1.7 in the appendix.

The gas boiler used to provide heat can be seen in Figure 6.15. Due to little information regarding gas boilers offshore were found, a conservative efficiency of 85 % were used because of size and weight limiting factors offshore. An industrial gas boiler can have efficiencies up to 92 %. An industrial gas boiler from Hoval weighed 73 tonnes at 20 MW heat capacity. A gas boiler with a lower efficiency and wet weight of 70 tonnes were assumed in this thesis, being able to deliver 22 MW heat at design point. [42]

The weight of the transformer needed in case of electrification is dependent on type (wet/dry) voltages and size. By using 1.2 tonnes per MVA [56] and assuming a power factor of 0.9, the transformer weight was estimated to about 100 tonnes and the total electrification around 120 tonnes with necessary switchgear, cable risers and control equipment. That give a total estimated weight of 190 tonnes to deliver heat and power during electrification. Of course, if the electrification is retrofitted, only a part of the already installed power cycle have to be removed to fit the electrification equipment while the remaining equipment can be kept as a redundancy. [11]

The efficiency at design point were controlled by limiting the combustion chamber outlet temperature to 730 °C, by the use of cooling air, as seen in Figure 6.15. The process heat is extracted from the flue gas before some of the remaining heat is used to pre-heat the air used in the combustion chamber, at a stoichiometric ratio of 1.2. The combustion chamber was assumed to have a pressure loss of 15 mbar and a fan was used to push the air and flue gas through the system. The fuel gas input was controlled by the process heat water temperature and the water mass flow in the heat cycle were controlled by desired heat demand, as in the other cases.

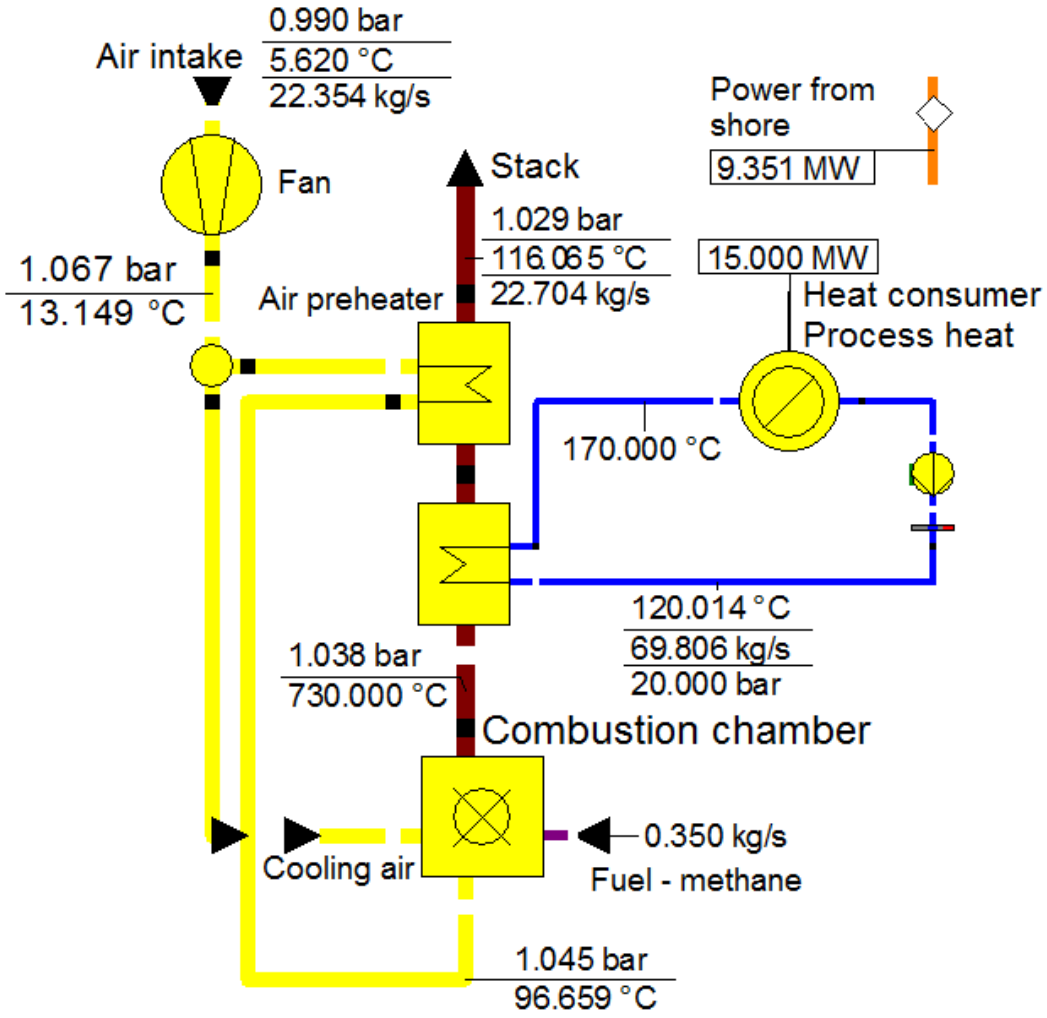

Figure 6.15 An overview of the gas burner and the custom stream providing CO_2 emissions and power from shore.

Figure 6.16 shows the power and heat load during electrification, as well as gas boiler efficiency. The green dashed line shows the produced onshore power used to calculate the CO_2 emissions. The results, with an electric emission rating from 500 to 250 kg CO_2/kWh, gave a total of 3.6 mega tonnes CO_2 emitted during the platform's lifetime.

It was also calculated that as long the estimated lifetime average onshore power ER is below 213 kg CO_2/kWh, it is better using electrical direct heating than using a gas boiler at ~85 % efficiency, which had an ER of 235 kg CO_2/kWh.

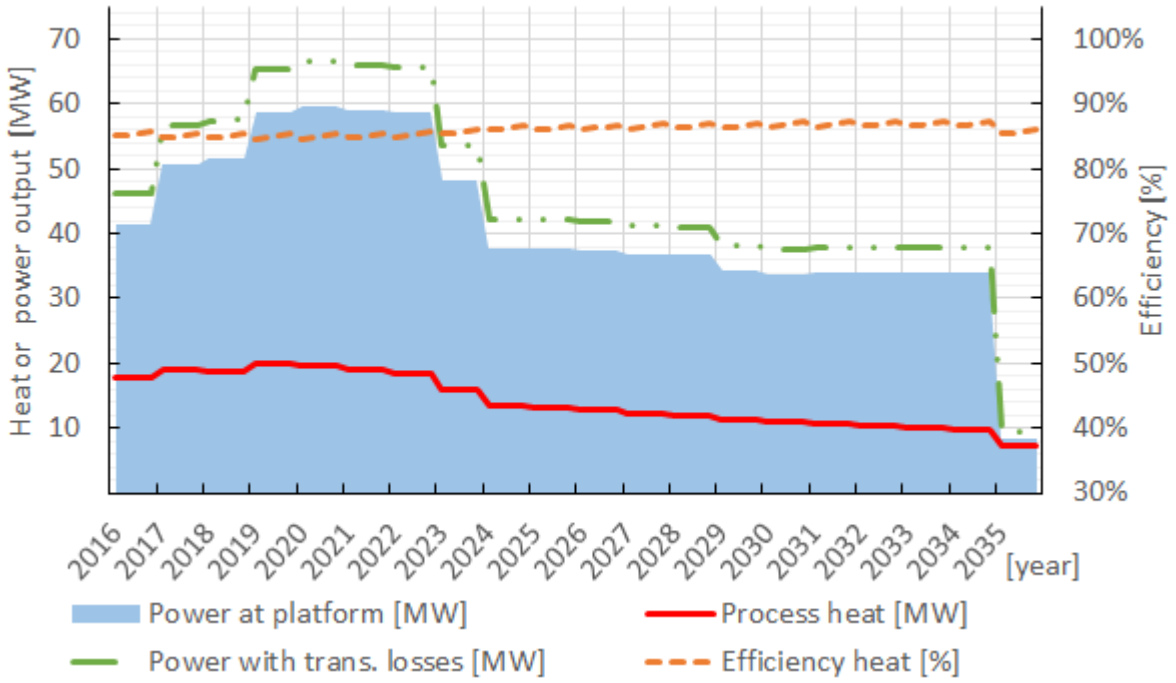

Figure 6.16 Electrification case showing heat and power loads as well as produced power onshore including the transmission losses and extra auxiliary power used by the fan.

6.4 Summary and screening

Table 6.5 gives a summary of the emission results and qualitatively judged properties of the different cycles. Cases 2c and 2d were screened out for further testing in chapter 7 and 8 because of the relatively high weight and CO_2 emissions and low redundancy and flexibility, and low responsiveness of case 2d. Case 1a was kept for further testing because it is the most used cycle offshore and as such a good alternative to compare the other results to. Case 1b was kept for its relatively small weight increase of 11 % compared to case 1a and its rather large reduction of CO_2 emissions. The combined cycle case 2a, was kept only due to its low emissions while case 2b was kept since it seemed a good trade-off between a combined cycle and a simple cycle. Electrification, case 3, was kept due to its high dependency on chosen ER, which will be explored more in the sensitivity analysis in chapter 8, and because the importance it will have in the future as the European emission ratings lowers.

Table 6.5 Summary table

Case	1a	1b	2a	2b	2c	2c120	2d	3
CO_2 [10^9 kg]	4.015	3.662	3.138	3.348	3.772	3.464	3.402	3.600
Weight [10^3 kg]	440	490	625	610	580	595	535	190
Redundancy	+	+	÷	+	÷	÷	÷	÷
Flexibility	+	+	÷	+	+	+	÷	+
Responsive	+	+		+	+	+	÷	+

Figure 6.17 show yearly emissions for all the different cases. It shows that with the predicted ER, electrification is the worst alternative the first years, but after the years 2023 to 2027, electrification becomes a better alternative, emissions-wise, than the other options. For example, 5 years with case 1a simple cycle, then retrofitting onshore power and using it for 15 years with case 3 would give a total CO_2 emission of 3.46 mega tonnes, which is lower than either one of them. It is also interesting to point out that the longer a platform is operated or the later it is built; the more relevant electrification will be to reduce GGE.

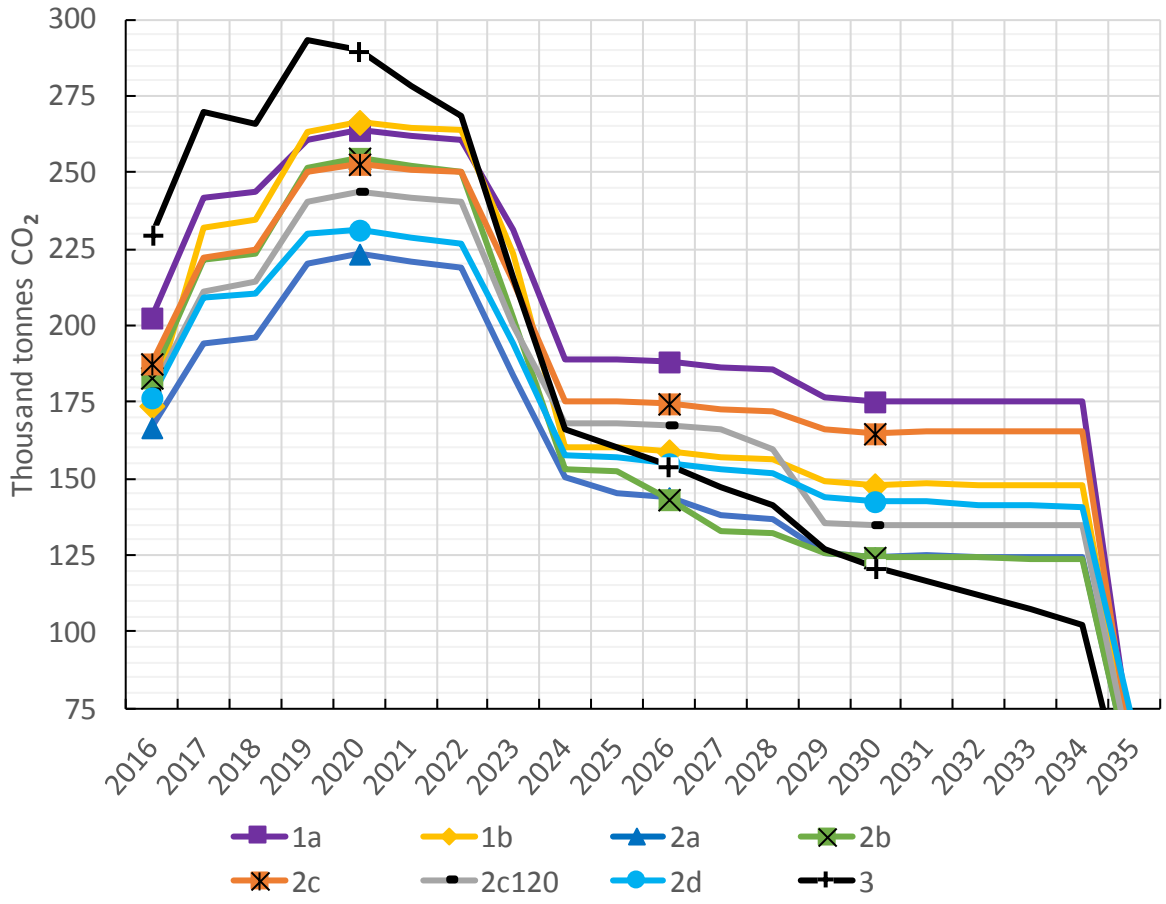

Figure 6.17 Yearly CO_2 emissions from the simulated cases. A backpressure case with the unfair advantage of 120 °C process heat is also included, for curiosity's sake.

Figure 6.18 shows a graphical representation of the total CO_2 emissions of each case. The simple cycle of case 1a had the worst and highest emissions with more than 4 Mt CO_2, while the combined cycle of case 2a had the best performance with 22 % less GGE at 3.3 Mt CO_2. The backpressure cycle could not compete with steam extraction for heating, even with 50 K lower process heat temperature, at the same heat loads. Electrification had relatively high CO_2 emissions, with 3.6 Mt because of the high emission rating chosen for the onshore power. In the sensitivity analysis other ER will be explored.

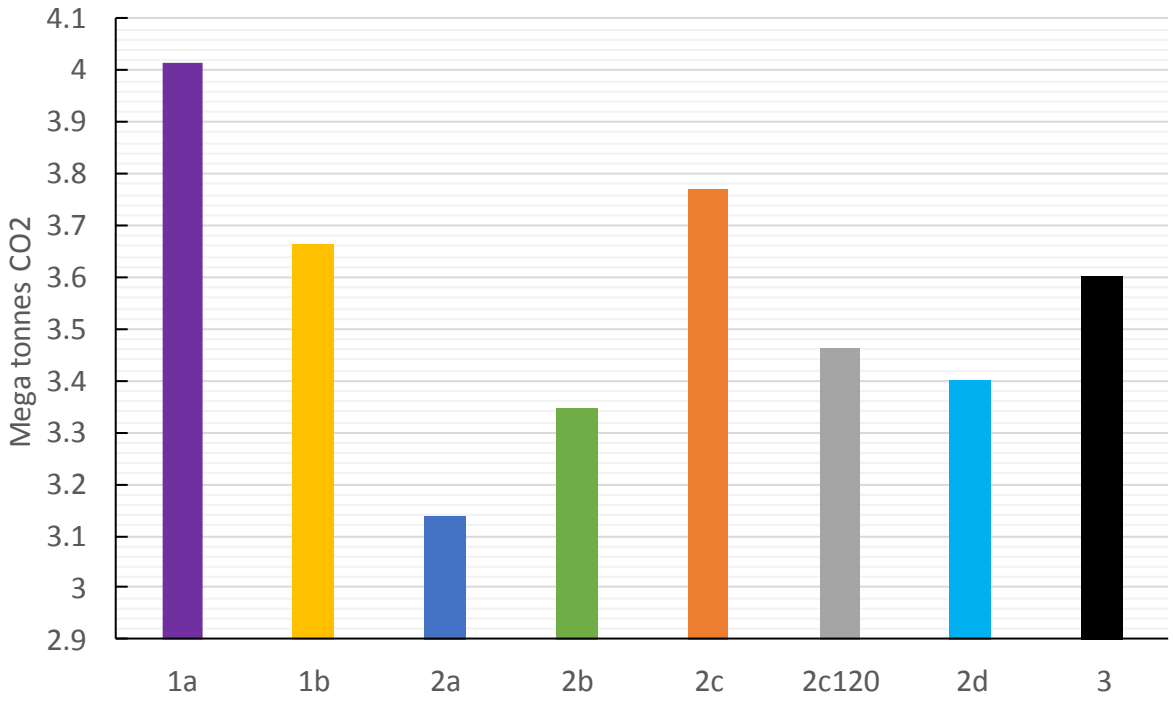

Figure 6.18 Total CO_2 emitted after 20 years. Notice the scaling of the y-axis and that the best case only had 22 % less CO_2 emissions than the worst case.

7 Modifications and optimization of selected designs

Table 7.1 gives an overview of the designs chosen to be modified and optimized in this chapter and for further sensitivity analysis and discussion in chapter 8.

Table 7.1 Overview of the cases chosen to be kept for further analysis.

Case	Short description	Gas turbines used
1a	Simple cycle with WHRU	2x LM2500G4+
1b	Simple cycle with WHRU and a larger GT	1x LM2500G4+ 1x LM6000PF S25
2a	Combine cycle with steam extraction	1x LM2500G4+ 1x LM2500PJ
2b	Combined cycle with steam extraction and simple cycle with WHRU	2x LM2500G4+
3	Electrification from onshore with a gas boiler	-

To optimize the cases in terms of flexibility and CO_2 emissions (efficiencies), primarily 3 things were considered:

1. Change of design points of the components used in the software.
2. Minor modifications of the designs.
3. Optimizing the scripts that ran the lifetime simulations; more specifically to increase the efficiencies at given power and heat demands.

The weight increase of modifying design points was also considered qualitatively, i.e. higher pressure levels or higher *UA* values generally meant a weight increase. Flexibility was measured in the cycles' ability to give a good efficiency at different power and heat loads and their ability to provide heat and power unrelated to the other to a larger degree.

7.1 Simple cycle optimization – case 1a and 1b

As the number of components used in the simple cycle cases were limited, there were not any beneficial modifications of the designs that were found without increasing the weight. The only main component that could be altered in the simple cycle was the WHRU. A larger and heavier WHRU can give the process heat needed with less pressure drop. A smaller WHRU will give a

larger pressure drop or less heat extraction from the exhaust gas which saves weight at the expense of operation flexibility. To verify, a size increase was imitated by lowering the pressure drop from 12 mbar to 8 mbar in case 1a. That would give a higher efficiency of the GTs because of a lower backpressure. The results were a 0.03 % reduction in CO_2 emissions from the original simulations in chapter 6. Since no quantitative weight considerations were done in the thesis, it was decided to be conservative regarding weight and keep the WHRU pressure drop at the original level.

Then it was tried to optimize the runtime operation of the GTs by modifying the scripts used in Ebsilon Professional. It was done by implementing a numerical function that checked the efficiency of 50 steps – by maximising the load of one GT to sharing the load evenly between both GTs, then selecting the load share which gave the best efficiency. That gave a 0.57 % GGE reduction in case 1a, with 3.992 mega tonnes CO_2 emitted. Figure 7.1 shows the results of the optimized load sharing between the two LM2500+G4 gas turbines and can be compared to the load sharing in Figure 6.1 by having smaller variation in one of the GTs.

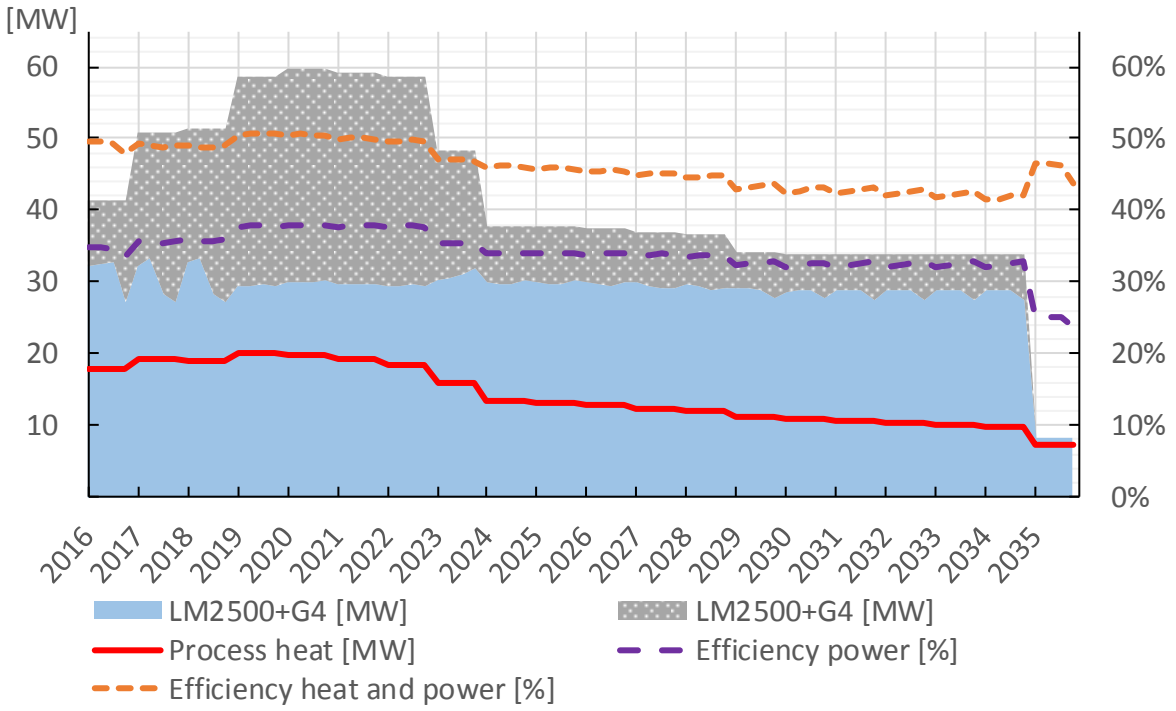

Figure 7.1 Case 1a power load and efficiency profile with optimized load sharing between the two gas turbines.

Case 1b were also optimized similarly but had a smaller improvement, mostly due to not sharing power loads by letting the LM6000 run alone for a majority of the lifetime. The results were 3.658 mega tonnes CO_2, which were a 0.11 % reduction from the simulations in chapter 6.

7.2 Case 2a – combined cycle modifications and optimization

In the modification of design point of case 2a, a variation of steam pressure levels and temperatures were first tested to verify the decisions done in chapter 6. The best pressure and temperature was found to be 25.77 bar and 484 °C, while still having a minimum pinch point of 35 K, which confirmed the decisions taken from Olav Nord's study of weight and power optimization. [33] By increasing the temperature however, the OSTG size and weight increases and it was decided to keep the same temperature and pressure levels.

Then it was decided to try to optimize the design point of the LP ST while avoiding a higher inlet pressure than the extraction pressure, decided by Stodola's law. The design mass flow in the LP ST was decreased from 13.7 kg/s to 11.3 kg/s. That gave the best results, with an emission reduction of 0.40 %. But it also directly reduces the flexibility of the cycle without by-passing some steam around the LP ST when the power demand is high and little process heat is needed.

The flexibility and overall efficiency could have been increased the same way with higher flexibility, by using a throttle at the LP ST inlet, which would open at higher pressure and allow for a higher backpressure of the HP ST while also having a throttle at the steam extraction cycle which would stay open except when the LP ST inlet pressure was above the saturation pressure of 175 °C. But due to limitations of controlling the throttle valves or inexperience in use of the software; no good solution for the design was found.

It was also tried to reduce emissions by designing the heat and power loads used for the longest time during the platform's lifetime. The results from the tries for 40 MW power design is shown in Table 7.2 along a selection of the other modifications. It was found that by designing for lower power loads directly reduces the OTSG and efficiency at higher power loads, which diminishes the effect. Another down-side was at lower steam flow design points, the turbine inlet pressure levels was as high as 35 bar at 60 MW power, if the max steam flow were not restricted. Such high pressures would likely require heavier and thicker walls in the OSTG, pipes and high pressure steam turbine.

Designing for lower optimized power loads and limiting steam flows at higher gas turbine loads do reduce the size and weight of the combined cycle, however resulting with more than 3 % more CO_2 emissions.

Table 7.2 Showing a large variation of modifcation to the design and design points of the combined cycle case 2a. A percentage lifetime emisisons reduction is shown compared to the results in chapter 6 of 3.138 mega tonnes CO_2.

Description of modification of design and design point from the original in chapter 6	Change in emissions
P_{HP}=20 bar and $T_{HP,steam}$=450 °C.	+0.49 %
P_{HP}=30 bar, $T_{HP,steam}$=480 °C, P_{cond}=0.06 bar.	+0.56 %
P_{HP}=25.77 bar and $T_{HP,steam}$=484 °C.	÷0.23 %
Higher design mass flow in the lower pressure steam turbine.	÷0.38 %
Optimizing STs for 40 MW net power and higher design mass flow in LP ST.	÷0.21 %
Optimizing STs for 40 MW net power and higher design mass flow in LP ST and limiting steam flows to avoid pressures much higher than 25 bar.	+3.76 %
Optimizing STs for 40 MW net power and allowing the LP ST inlet pressure to glide up to 12 bar, from 8.9 by extracting steam at 12 bar and throttling it.	+1.74 %

Due to the small total efficiency increases with the cost of lower flexibility or heavier equipment for all the different modifications, it was decided to keep the design point used in chapter 6. Options for optimizing the runtime scripts to increase load sharing between the turbines were also considered in the combined cycle cases. But due to the simulations of the combined cases already ranged between 10-30 minutes (to obtain the correct power and heat loads for different ambient temperatures and loads, for more explanation see chapter A.2) for a single lifetime simulation, adding another numerical optimization on top, and multiplying the simulation time, was not deemed feasible with the current hardware and time restrictions.

7.3 Case 2b – combination of simple and combined cycle

Due to the similarities to case 2a, not many design point modifications were tested in case 2b. The combined cycle was already optimized well with regards to flexibility and design point. However, by modifying the process heat cycle and utilizing the WHRU as well as steam extraction, whenever the second GT was operating, the total efficiency was increased significantly.

The modifications of case 2b are shown in Figure 7.3. The pressurized process heat water is first heated by the economizer in the stream extraction cycle, before any available heat is taken from the WHRU, until it reaches desired temperature. If it does not reach 170 °C, the water is heated by steam extraction from the steam turbine. The steam extraction mass flow is controlled in such a manner that a temperature of 170 °C is always reached. The process heat water mass flow is controlled by the heat load.

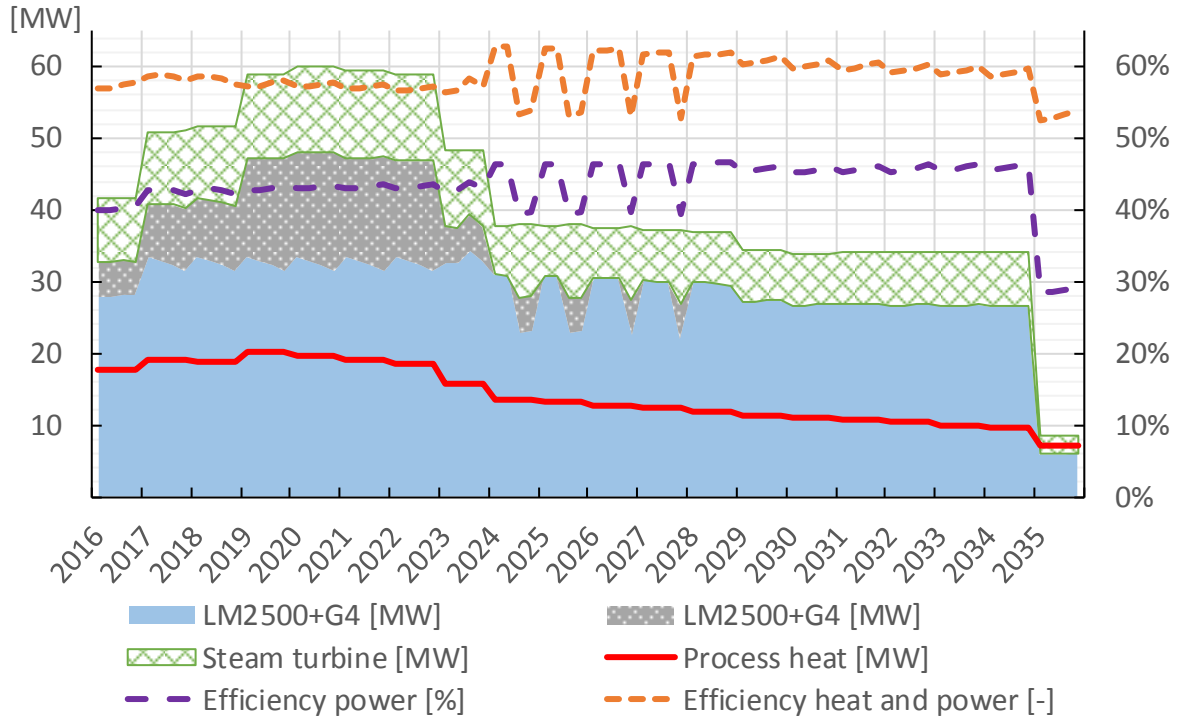

Figure 7.2 A higher efficiency of case 2b is whenever both GTs are in operation, compared to the results in Figure 6.10.

Figure 7.2 shows that by utilizing the WHRU whenever both gas turbines are in operating increases the efficiency at the higher power demands, compared to the simulations done in chapter 6 and Figure 6.10. Valves can easily be fitted to be able to use the two different process heat options independently of each other to retain the case's original flexibility and redundancy, or together to increase efficiency, as shown in Figure 7.3. This modification reduced the GGE by 4.46 % without much weight increase, and gave a final result of 3.2 mega tonnes CO_2 emitted during the platform's lifetime.

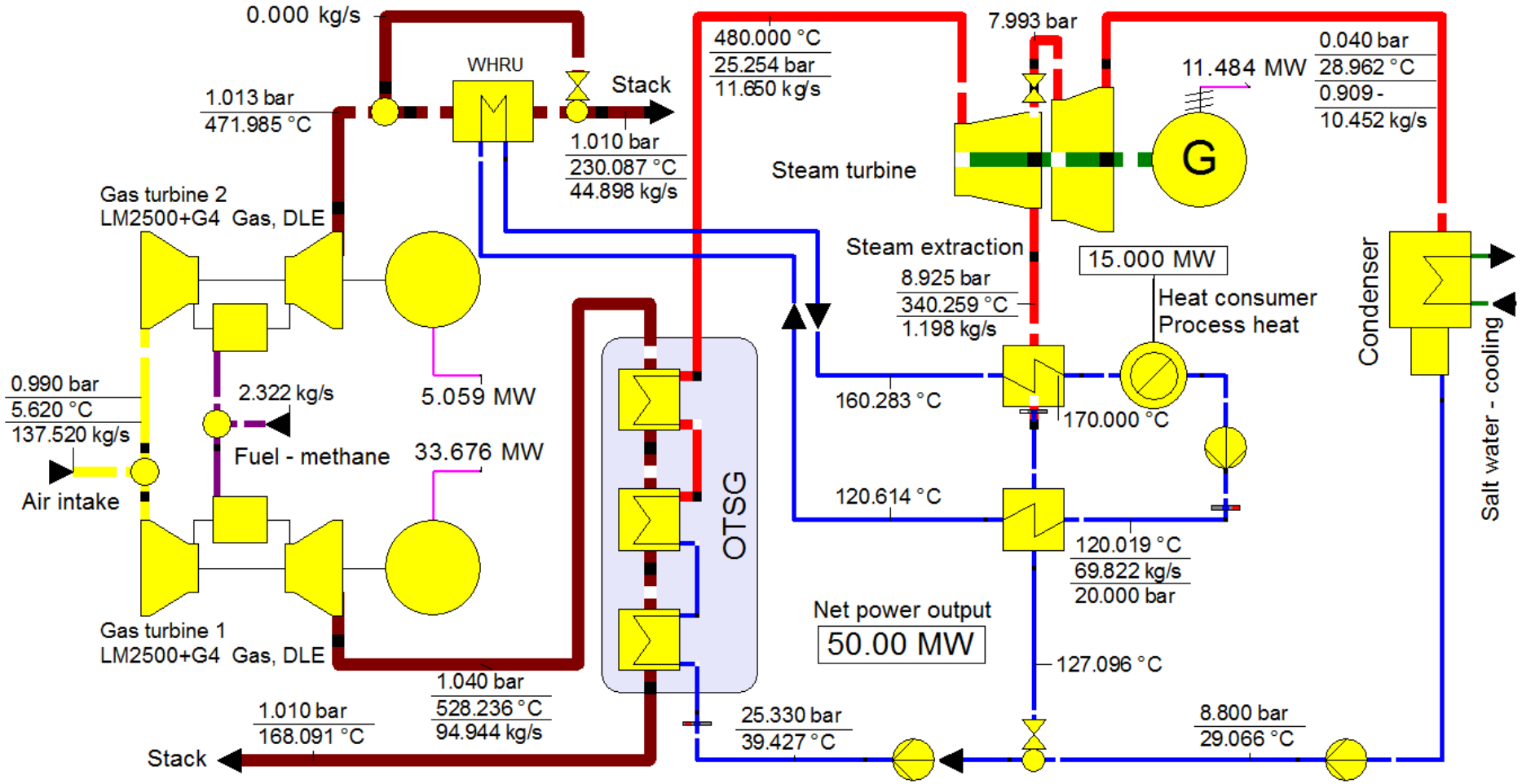

Figure 7.3 Shows how the modified process heat cycle of case 2b looks, and how it operates by taking available heat from HRSG, when available and thereby increasing the combined cycle efficiency. The remaining heat needed to achieve 170 °C is taken from steam extraction, if the WHRU does not provide enough heat.

7.4 Case 3a – variants of the electrification case

No modifications of the design were found in the electrification case, as the gas boiler was designed to achieve a certain efficiency and because of restrictions in modifying the onshore power. Other design variants were tested, however. The use of an industrial burner with an efficiency of 90 % reduced to total GGE to 3.56 mega tonnes CO_2. The re-use of an WHRU from case 1a was also tested. Maximum temperature entering the WHRU was then limited to 550 °C and it resulted in an efficiency of below 50 % at 22 MW heat load, and a lifetime result of 4 Mt total CO_2 emissions.

7.5 Flexibility

Further flexibility analysis was conducted on the optimized offshore power cycles. For each case the heat load was maximized, up to 22 MW, at power loads from 5 MW up to 60 MW. The average ambient temperature of 9.37 °C was used, with the same ambient pressure and RH conditions of 1.00 bar and 82.8 %.

Figure 7.4 show the results of maximizing the heat output. Both combined cycle cases reached 22 MW heat output at around 15 MW power load. The simple cycles were able to reach above 21 MW heat load at 23 MW power but not full 22 MW heat load before 30 MW power load of a single GT. Because of the optimizing script, the heat load varies between 21 and 22 MW after 30 MW power. If full 22 MW heat was needed after 30 MW power load, it would take little effort and loss of efficiency by adjusting the power loads slightly to obtain it. Being able to reach more than 21 MW power at 23 MW heat load was deemed satisfactory. It would be an rare operation case if that more heat would be needed at so low platform activity.

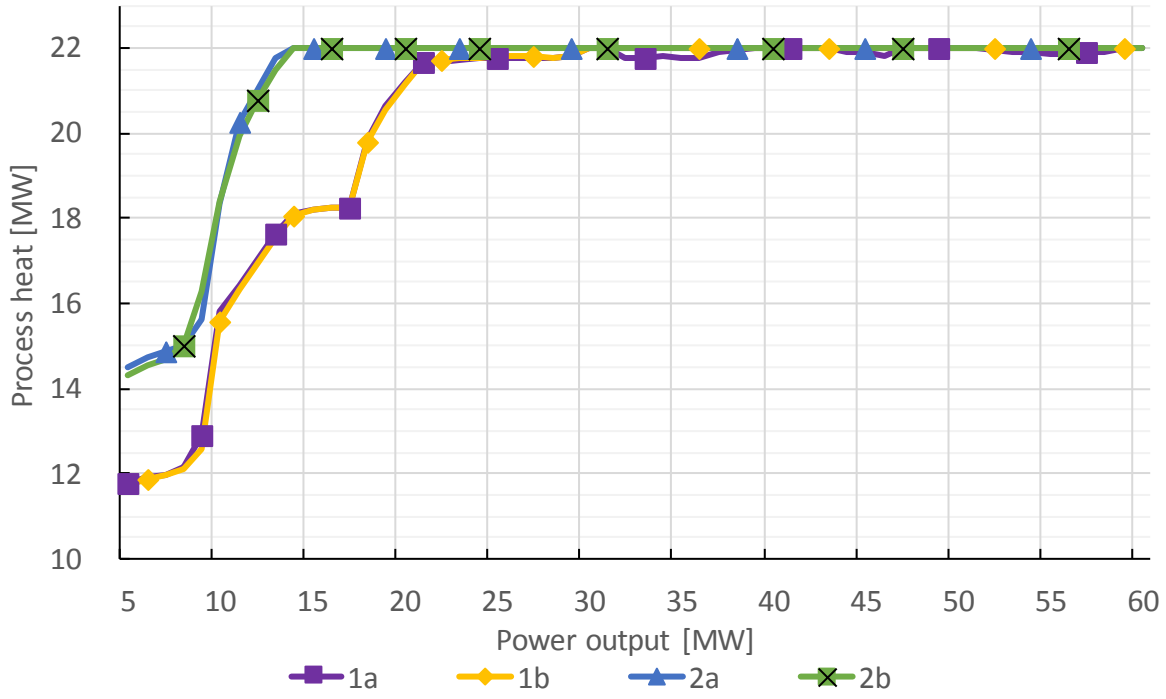

Figure 7.4 Maximized heat load, up to 22 MW, of each power cycle of power loads from 5 MW to 60 MW.

Figure 7.5 shows the total efficiencies while maximizing heat load up to 22 MW. It shows that case 2b, the combined cycle optimized for a single GT performs best as long it can run on that single GT. When more than one GT must be operated, case 2a gives a better total efficiency. Case 1b performs relatively well in the 35-45 MW power range, until the second GT must be operated.

Tests regarding minimum heat load flexibility was not conducted. It would not affect the performance of the simple cycles, but it is important to note that zero heat load in the combined cases would require steam flow restriction or by-pass of the LP ST due to the designs current swallowing capacity restrictions. If not a control system were installed that allows for a gliding middle pressure higher than the extraction pressure, bypassing steam would lower the power efficiency compared to running at minimum heat loads without by-passing any steam. If steam were bypassed and all the steam were cooled at condensing pressure, the OTSG water inlet temperature would be at below 30 °C and less steam could be generated which reduces the power produced by the HP ST.

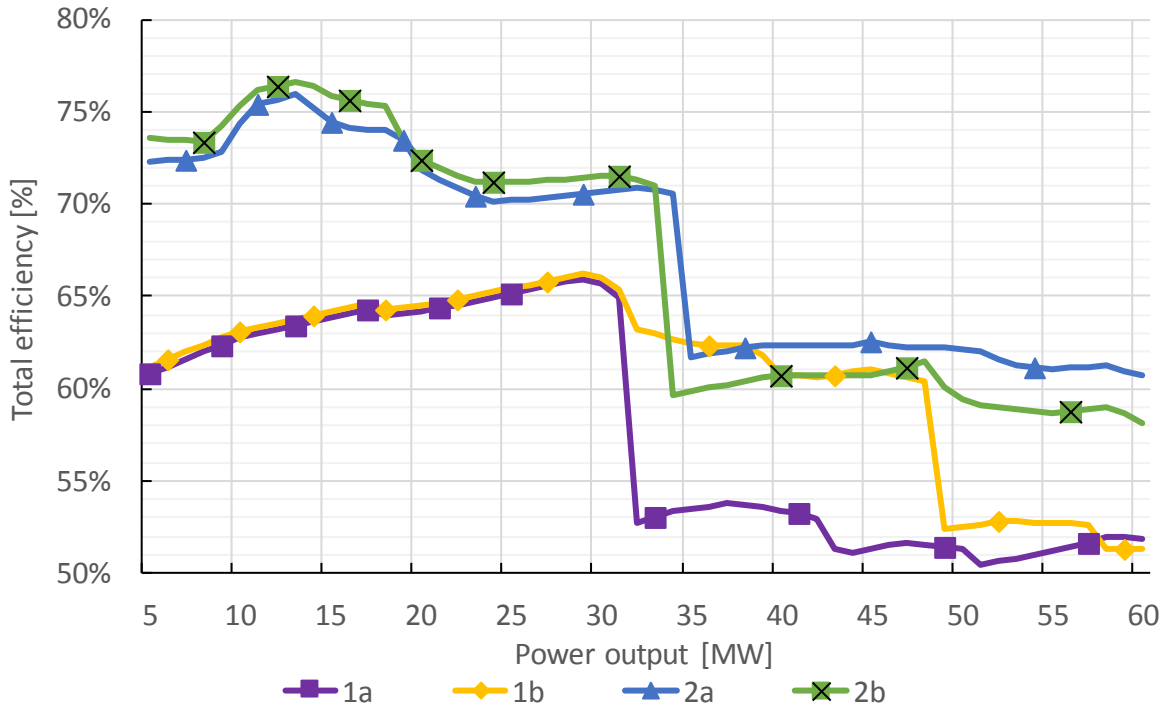

Figure 7.5 Total efficiencies when heat load is maximized up to 22 MW heat. Even though the heat load affects the steam cycle power efficiency directly, cases 2a and 2b show a better efficiency than the simple cycle cases.

7.6 Process heat temperature

Modifications of all the designs were also conducted to test how the change in process heat temperature affects the performance of each cycle. The design points were altered by ±50 K, providing process heat at 120 °C and 220 °C and having return temperatures of 70 °C and 170 °C. The simple cycle cases were hardly affected at all, while case 2b was most affected by increasing the lifetime CO_2 emissions by 9.79 %. Case 2b was more affected due to the lower steam flows it could withdraw extraction steam from. Having larger steam flow means that a smaller fraction of the steam will be extracted and it will have a smaller impact. The results suggest that WHRU or gas boilers are better at higher process temperatures while combined cycles are better the lower process heat temperature is required, as shown in Figure 7.6.

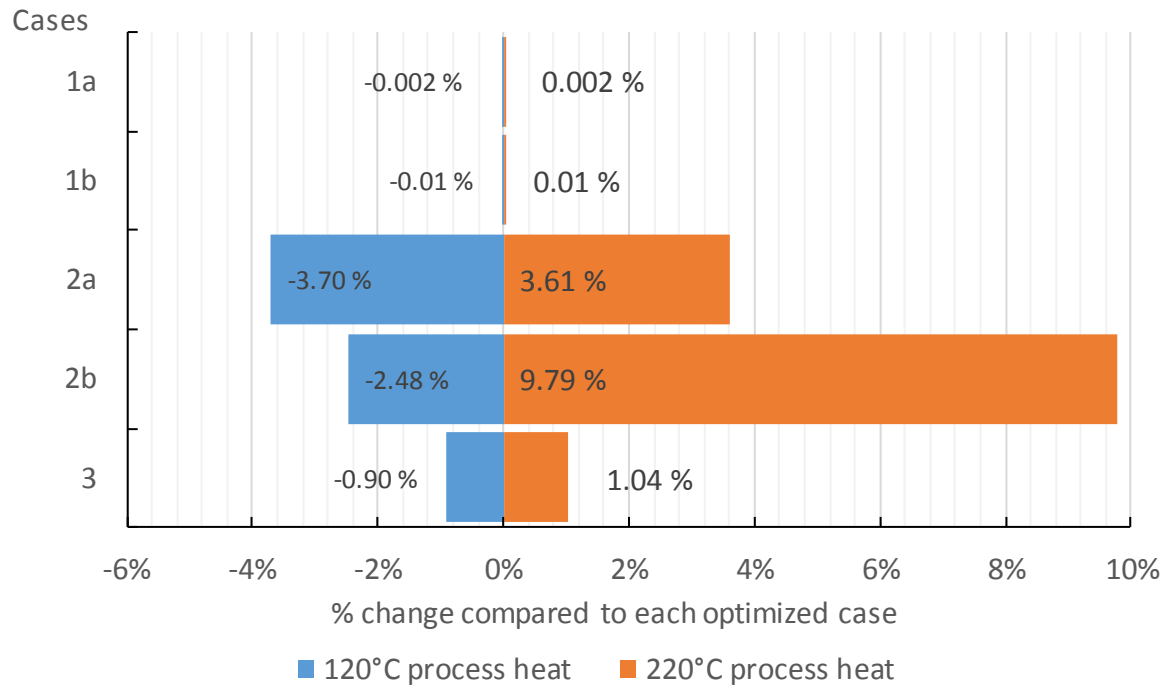

Figure 7.6 Alterations in designs to provide process heat at ±50 K.

At 220 °C the saturation pressure of the steam was above 23 bar, which made the HP ST provide very little power. At such high temperatures it would be more practical to extract steam directly from the OTSG before any steam turbine or use an own WHRU.

8 Sensitivity analysis and discussion

In this chapter sensitivity analysis was performed and a final discussion and summary of the results made in this chapter, and chapter 6 and 7. Due to still having five cases the author deemed relevant for providing power and heat offshore, the sensitivity analysis had to be somewhat simplified.

8.1 Sensitivity analysis

Sensitivity analysis was done by increasing and decreasing the variables that was judged to affect the results the most by one step, namely the power load, heat load and ambient temperatures. Lifetime period would also affect the results to a large degree but the yearly emissions shown in Figure 6.17 gives a good indication how the different cases would perform with varying operation times. At longer lifetimes electrification will be more and more favourable as green electric energy becomes, hopefully, more and more prevalent in Europe and rest of the world.

The sensitivity to power loads were tested by increasing and decreasing the power load with 4 MW at all times. A ±4 MW power change is equal to ±9.4 % change in total power spent over 20 years and a ±7.2 % total heat and energy spent. If the total efficiency would change little with power loads, the total GGE should change with 7.2 % as well. The value of 4 MW was used because of the maximum limit of power some of the cycles could produce.

The same way the heat load was changed by a constant ±2 MW heat, based upon the maximum limit of heat production at the chosen designs. A 2 MW change in heat load gives 14.1 % larger heating energy spent for process heating and a 3.6 % change in total energy spent. At last, the ambient temperature was changed with a constant ±5 °C. +5 °C is equal to a platform considerably further south with average winter temperatures around 10 °C. ÷5 °C has average winter temperatures around 0 °C and summer temperatures around 10 °C, and can have weather similarities to the Baltic sea. The RH and ambient pressure was kept constant as in the previous simulations.

As a measurement, the change in lifetime CO_2 emissions were used and compared to the optimized cases chosen in chapter 7, which also gives an indication in efficiency change.

8.1.1 Simple cycle sensitivity analysis – case 1a and 1b

In the simple cycle of case 1a the change in heat load had a very minor significance on total emissions, as expected. As can be seen in Figure 8.1, at higher power load the emissions increased with almost 7.2 % and were equal the extra energy expenditure. But because the simple cycle's emissions are almost independent of heat load, an expected 9.4 % larger GGE should be expected if the efficiency was unchanged. As expected, the increase of 7.2 % in GGE shows that the power efficiency of case 1a was increased when it could be run at more optimal part loads.

With less power the emissions were reduced significantly. The reason is because it allowed the platform to run on a single GT for the last 10 years of the platforms lifetime, thereby increasing the power efficiently significantly.

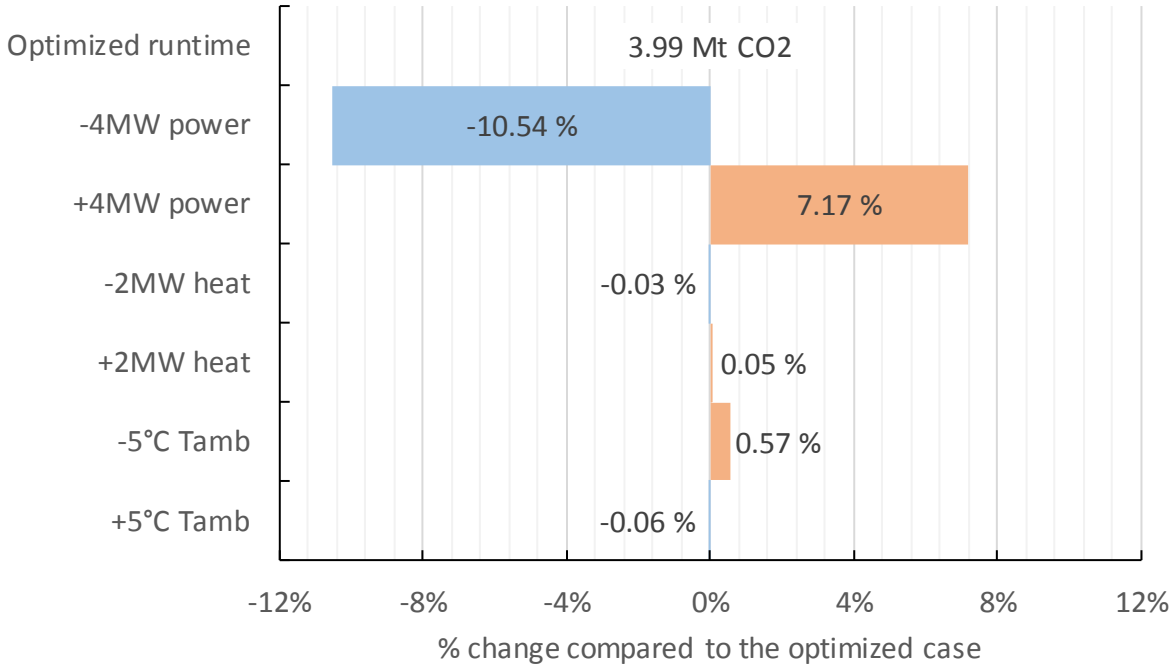

Figure 8.1 Sensitivity analysis of case 1a. Unexpected results with worse performance at higher ambient temperatures. Better performance at both higher and lower power loads, compared to total lifetime power spent.

Due to the characteristics of the GT in the VTU library, the emission change when changing the ambient temperature was opposite to what was expected. It is believed caused by that the GTs are run at a constant power load, instead of a constant part load, which combined with the efficiency dips seen in Figure 5.4 (due to VIGV and TIT controlling) gives a rare case of worse

performance with lower ambient temperatures. In a real case, the operation of the GT could probably be improved so that it gave a better performance at lower ambient temperatures.

Case 1b gave the same expected results of being primarily unaffected by heat load, having a better efficiency at lower ambient temperatures and a slightly worse total CO_2 emissions at +5 °C higher ambient temperatures, as seen in Figure 8.2.

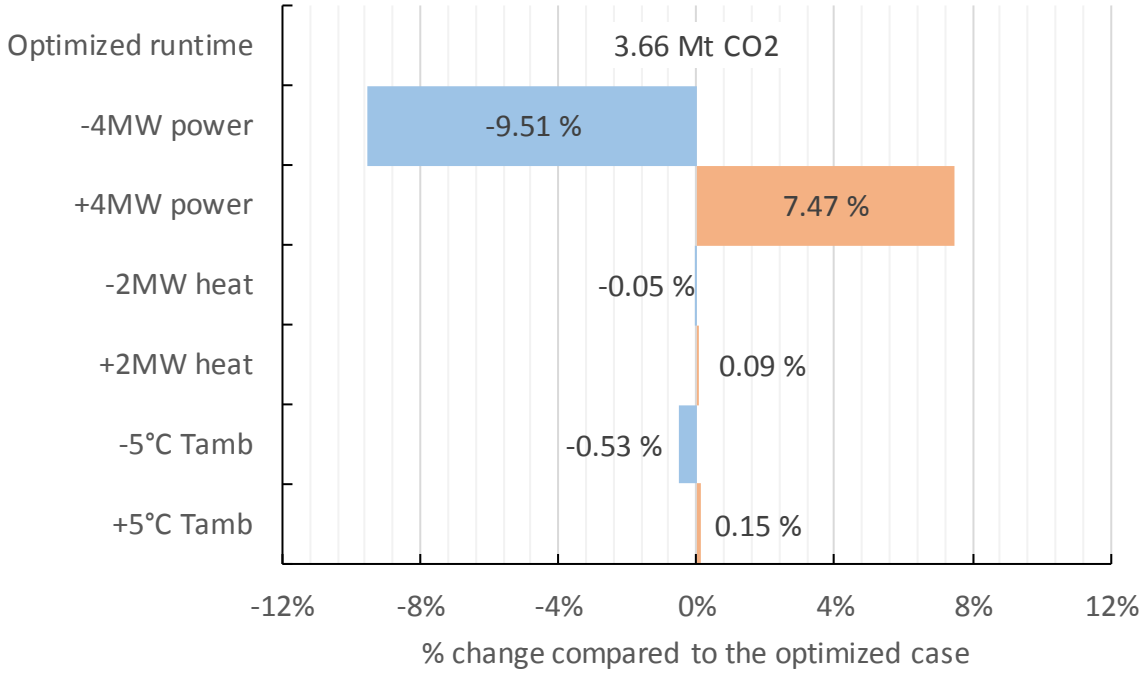

Figure 8.2 Sensitivity analysis of case 1b. Results as expected when changing heat load and ambient temperature. Better performance at both higher and lower power loads, compared to total lifetime power spent.

Both the increase and decrease also increased the power efficiency of case 1b. Figure 8.3 shows how the optimized load share is during the platform's lifetime when the power load is decreased by 4 MW. At later stages of the platform's lifetime the use of the smaller GT becomes more efficient and reduces the total emissions related to power usage. By running at +4 MW power loads the power efficiency also becomes higher as in case 1a, with the turbines running at higher part loads, and the total emissions are only increased by 7.47 %.

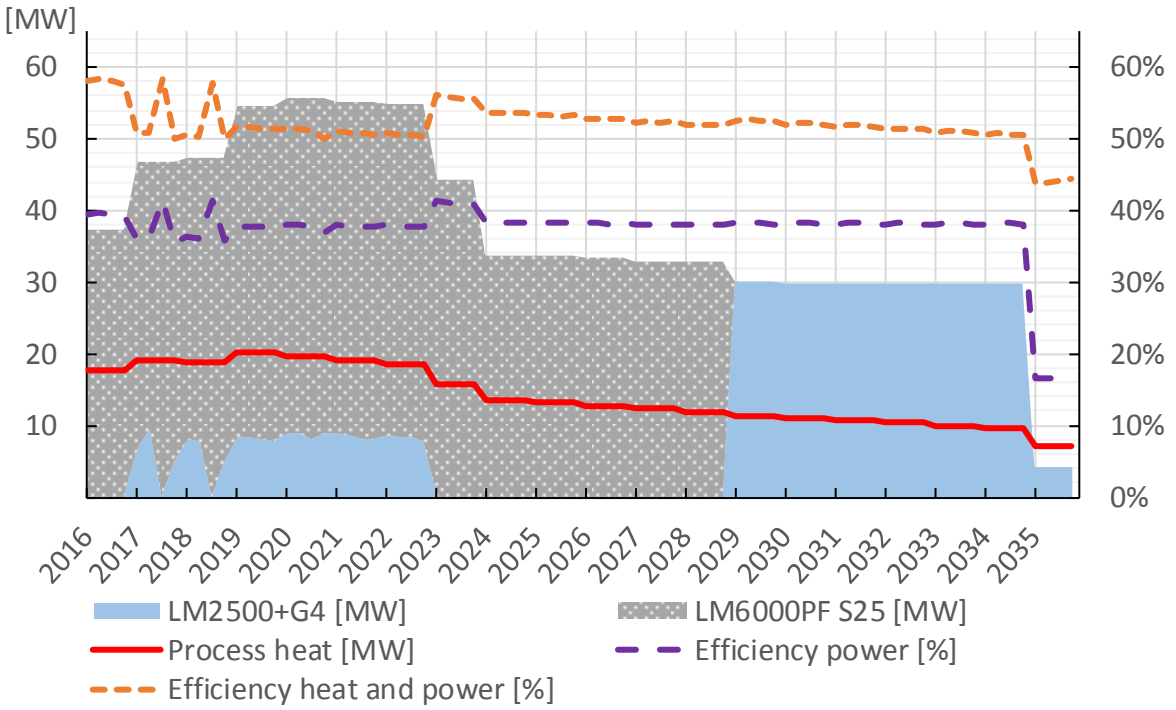

Figure 8.3 Optimized load share between the GTs at ÷4 MW power loads. At low power demands it is more efficient to use the LM2500+G4.

8.1.2 Combined cycle sensitivity analysis – case 2a and 2b

Because of the choices of design points for the steam cycles, both case 2a and 2b responded negatively to changes in power. That can be seen in Figure 8.4 and Figure 8.5, by having about the same reduction in emissions as the reduction in energy expenditure at 7.2 %. At higher power loads the lifetime emissions increases more than the total increase in heat and power usage.

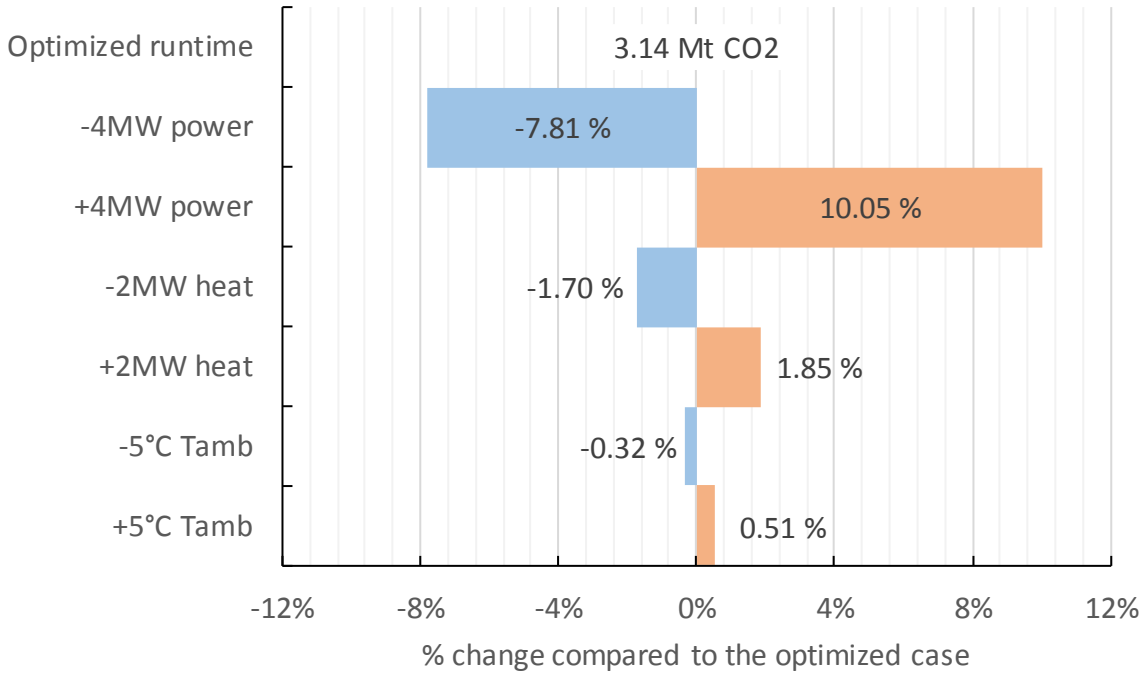

Figure 8.4 Sensitivity analysis results for case 2a. The combined cycles were more sensitive to ambient temperature and heat load change, and responded worse to power load change than the simple cycles.

Case 2b had a higher sensitivity to the increase in temperature than the other cases. The reason was that when the temperature increased it forced the power cycle to run on two GTs more often at the platforms later lifetime. As expected, the combined cycles were more sensitive to heat load changes, due to how it affects the steam cycle efficiency directly by changing the steam flow in the LP ST. But the change in emissions were still about half the change in energy usage, which was ± 3.6 % with ±2 MW heat load change.

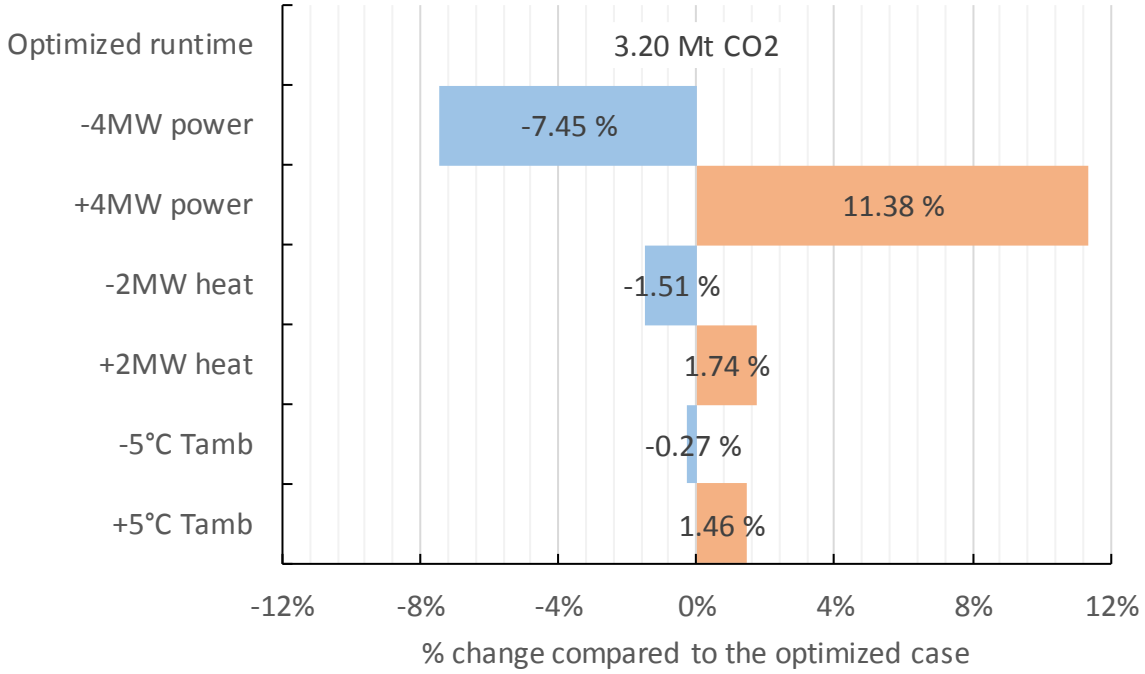

Figure 8.5 Sensitivity analysis results for case 2b. The combined cycles were more sensitive to ambient temperature and heat load change, and responded worse to power load change than the simple cycles.

8.1.3 Electrification sensitivity analysis – case 3

The same sensitivity analysis were done in the case of electrification as well, to confirm that the change in power changes emissions directly and that the gas boiler were only slightly affected by change in ambient temperatures and heat loads, as seen in Figure 8.6. The 7.79 % emission change seen in the figure is higher than the 7.2 % energy change because of transmission losses and auxiliary power needed to run the fan.

Different emission ratings were also tried as a sensitivity analysis in case of electrification. As expected, the calculated CO_2 emissions changed dramatically with chosen emissions the onshore power is assumed to have. Figure 8.7 in the summary shows the results. Following emission ratings were tested, taken from the data gathered in Figure 5.3:

- Low EU ER prediction (300-150 kg CO_2/kWh)
- High EU ER prediction (700-350 kg CO_2/kWh)
- Onshore CC (344 kg CO_2/kWh) [11]
- Nordic emissions (166-100 kg CO_2/kWh) [44]
- Norwegian (green license) emissions (kg CO_2/kWh) [44]

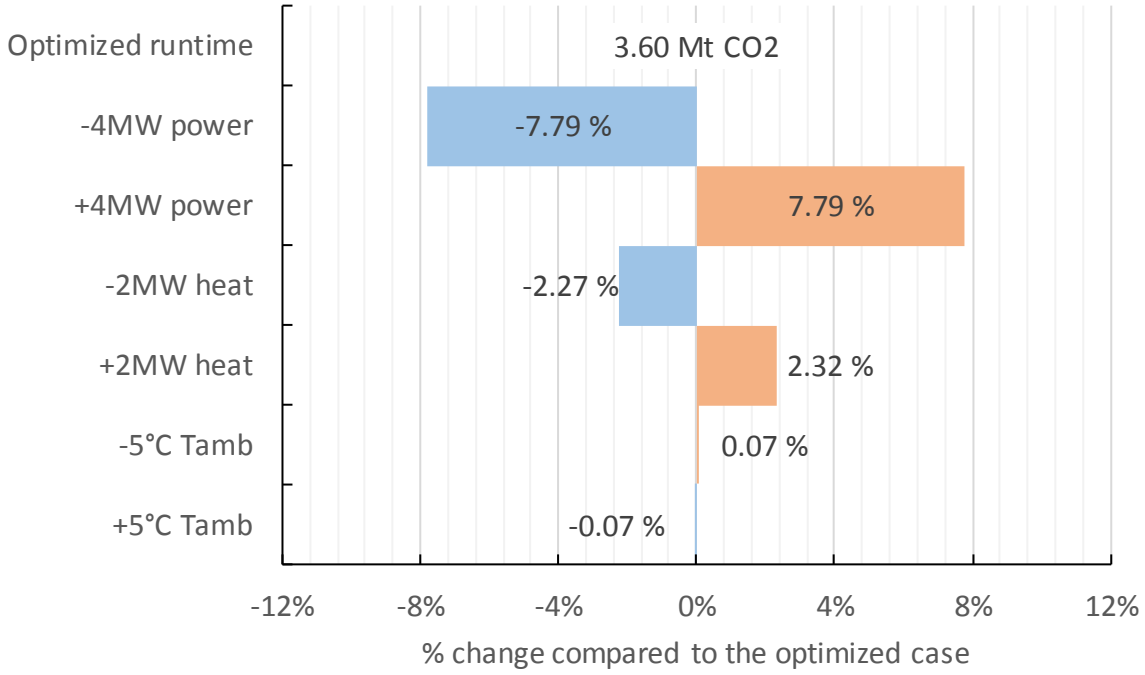

Figure 8.6 Electrification and gas boiler case remained largely unaffected of changes in loads and ambient temperature.

8.2 Summary

Here a summary of the most important findings will try to be discussed. Table 8.1 gives an overview of the emissions from the optimized power cycles and their lifetime total efficiencies, calculated by equation (3.43). It shows the assumed minimum price of the emitted CO_2 during the platform's lifetime. It was calculated with a price of 500 NOK per tonne CO_2 and no inflation. In the future, the CO_2 price is predicted to rise much more rapidly than inflation. [1] By using a combined cycle instead of a simple cycle, the CO_2 costs can be reduced by a minimum of 400 million NOK, according to the findings in this study. At a cost of a power cycle's installed weight above 600 tonnes instead of around 440 tonnes and a more complex power cycle.

A combination of a simple cycle and a combined cycle, case 2b, seemed especially beneficial for the chosen operating conditions in this thesis, after modifying the model and allowing for both GTs to provide process heat. It had only slightly higher CO_2 emissions than the pure combined cycle, lower weight, higher flexibility and redundancy than case 2a.

If the platform area is very limited or the instalment costs are extra high, the use of a variation of gas turbines might improve the overall performance while increasing the weight by a smaller degree. Case 1b, with 50 tonnes higher instalment weight, reduced the lifetime emissions, compared to case 1a, by 334 thousand tonnes CO_2.

Table 8.1 An overview of the final results of the offshore power cycles. Electrification is not included due to CO_2 taxation of inherent ER is not clear and efficiencies are not comparable.

	Case 1a	Case 1b	Case 2a	Case 2b
Lifetime total efficiency [%]	46.6	50.9	59.5	58.3
CO_2 emissions [10^9 kg]	3.992	3.658	3.138	3.198
CO_2 costs [10^6 NOK]	1996	1829	1569	1599

The optimization of the simulation runtime, in chapter 7.1, also showed the importance of having good operating software offshore. By small costs the operation can be optimized and CO_2 emissions lowered. The sensitivity analysis showed that choosing a good design point is important for the combined cycles, but it also showed that by being more selective in platform activity, the efficiency can be increased. Depending on operation costs and oil prices, it can be beneficial to reduce activity levels and power demands during the summers, as seen in Figure 6.8 for example. By reducing the power demand or requiring less spare GT power during the summers between the years 2024 and 2029, all the power demand can be provided by a single GT and the large dips in efficiency can be avoided.

Figure 8.7 gives a graphical overview of the emissions of the different cases, including different ER ratings associated with the onshore power. It shows the importance of making good CO_2 ER predictions is essential in comparing electrification with other power cycles. It is also believed that more thorough studies of emission ratings associated with electrification is needed in the growing complexity of the electric power market, to make more meaningful comparisons and research regarding electrification of the NCS. But no matter what ER as used, as long the onshore power becomes cleaner and no revolution of offshore power cycles appears, electrification will become the cleanest alternative in the future.

Even if electrification is the cleanest offshore power alternative, it still might not be the best option to reduce the global CO_2 emissions due to the high abatement costs. Resources could be better spent in Europe or in Norway on more cost-effective options to reduce emissions, or research regarding reducing emissions. Wind power or other green energy sources can also be

built ‘guarantee’ clean electricity offshore in case of electrification. But as already argued in chapter 2.3, if it is cost effective to build more green energy, it is unlikely that not electrifying the NCS would change that fact.

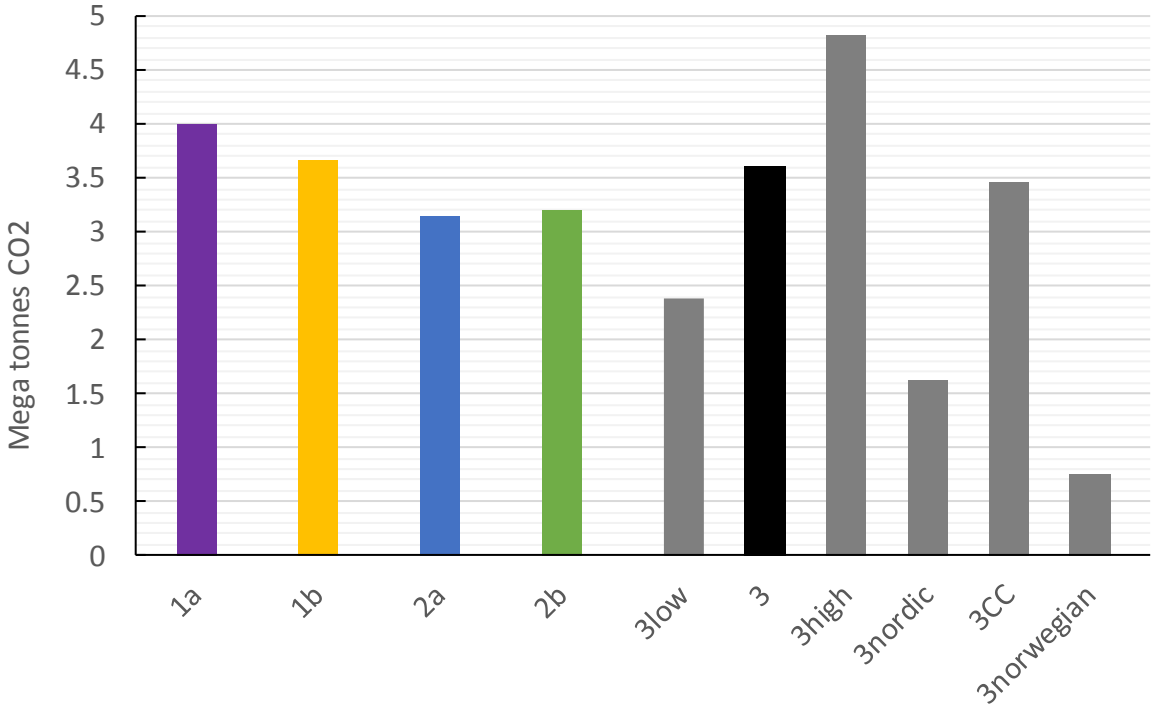

Figure 8.7 The final CO_2 emissions results, including results from different emission ratings of onshore power.

9 Conclusion

In this thesis the question, "*What are good options for heat and power generation offshore and how do they perform in a lifetime analysis?*", tried to be answered. First a literature study was conducted to find heat and power requirements offshore, and good heat and power supply cases. Then a power and heat requirement model of an offshore platform, with load profiles, were created and the most suited alternatives were simulated in Ebsilon Professional, supplying the modelled platform during a lifetime of 20 years. Emission rates for onshore power were also assumed and predictions were made 20 years into the future. It was found that backpressure combined cycles were unsuitable for process temperatures above 120 °C. Five remaining options were kept for further analysis: two simple cycle cases with WHRU, a combined cycle, a combination of a combined and simple cycle and electrification from shore.

The optimized simple cycle with two GE LM2500+G4 gas turbines and WHRUs, case 1a, were found to have a lifetime emission of 3.99 mega tonnes CO_2. A modified simple cycle case with a LM2500+G4, a LM6000PF and WHRUs had 3.66 mega tonnes CO_2 with only 50 tonnes extra power cycle weight. The combined cycle with two gas turbines, case 2a, gave the lowest emissions, with 3.14 mega tonnes CO_2. It also had the highest weight and lowest flexibility.

Case 2b, the combination of a GT with a bottoming steam extraction cycle and another LM2500+G4 with a WHRU, was judged the best alternative for the modelled platform. It had high flexibility, lower weight than a normal combined cycle but on-par emissions and a lifetime total efficiency of 58.3 %.

It was found in the case of electrifying the NCS, it is important to find the true emission rating cost of electric power to be able to compare it directly with offshore power cycles. In the primarily assumption of marginal power from EU and a predicted emission rating from 500 to 250 kg CO_2/kWh, electrifying the modelled platform would emit 3.6 mega tonnes CO_2, providing power for 20 years while a gas boiler provided heat. It was also found that if the electric emission ratings are below 213 kg CO_2/kWh, it could be argued that direct electric heating is more environmental-friendly than burning natural gas.

As the CO_2 emission goals become stricter and the CO_2 prices increases, the emission rating of electric power will decrease. The later an offshore platform is built or the longer it is operated; the more favourable electrification will be.

9.1 Further work

To be able to better compare electrification with onshore power cycles, it is essential that more research is conducted and the emission ratings of power from shore is better determined. Analysis of the electric power make-up for a platform would help ratifying emission rating emissions and future predictions. Research in spending resources for reducing CO_2 emissions elsewhere instead of electrifying the NCS is also highly relevant, considering the high abatement costs of electrification.

In closer regards to offshore power cycles and a step further in taking more use of combined cycles offshore, dynamic testing and modelling would be an important step to validate if steam bottoming cycles are a step in the right direction for supplying flexible and reliable high efficiency heat and power offshore. Cooperation and further testing with one of the three already built steam cycles on the NCS would also be a large step towards finding out if combined cycles are a good option for the future.

Performing flexibility and lifetime analysis of more innovative cycles like the Kalina cycle, the organic Rankine cycle, STIG cycle or a supercritical CO_2 cycle for optimising cogeneration offshore would also be interesting. Additionally, in the case of electrification, weight and process analysis of using heat pumps and sea water to provide process heat could provide a better alternative than using a gas boiler or direct electric heating.

References

1. Inernational Energy Agency and F. Birol, *World energy outlook 2015.* International Energy Agency, 2015. **1**.
2. Norwegian Petroleum Directorate. *Emissions to air*. 2016 [cited 2016 31.05.2016]; Available from: http://www.norskpetroleum.no/en/environment-and-techology/emissions-to-air/.
3. Norwegian Petroleum Directorate. *Production*. [Website] 2015 [cited 2015 15/12/2015]; Available from: http://www.norskpetroleum.no/en/production/production-of-oil-and-gas/.
4. Norwegian Petroleum Directorate. *Climate and the environment*. [Website] 2015 [cited 2015 15/12/2015]; Available from: http://www.norskpetroleum.no/en/framework/climate-and-environment/.
5. STEAG. *EBSILON Professional 11.04*. 2015; Available from: https://www.steag-systemtechnologies.com/ebsilon_professional+M52087573ab0.html.
6. VTU-Energy. *Gas Turbine Library for EBSILONProfessional*. 2015; Available from: http://www.vtu-energy.com/Gas-Turbine-Library/en/1746.
7. Norwegian Petroleum Directorate. *Norway's petroleum activity*. [Website] 2015 [cited 2015 15/12/2015]; Available from: http://www.norskpetroleum.no/en/framework/norways-petroleum-history/.
8. Norwegian Petroleum Directorate. *Recent activity*. [Website] 2016 [cited 2016 31.05.2016]; Available from: http://www.norskpetroleum.no/en/developments-and-operations/recent-activity/.
9. Det norske oljeselskap ASA, Statoil, and Baryerngas norge, *Plan for utbygging og drift av Ivar Aasen*, in *Lisensene PL001B, PL028B og PL242*. 2012.
10. Ministry of Petroleum and Energy. *Emissions to air from the petroleum sector*. 2008 31.05.2016]; Available from: www.regjering.no.
11. Pöyry, *CO2-emissions effect of electrification.* Econ Report no. R-2011-041, 2011.
12. Vanner, R., *Energy use in offshore oil and gas production: trends and drivers for efficiency from 1975 to 2025.* Policy Studies Institute (PSI) Working Paper, September, 2005.
13. Bedwell, I., S. Das, and E. McCall. *Extending the Life of Mature Facilities*. 2015; Available from: http://www.spe.org/news/article/extending-the-life-of-mature-facilities.
14. Bothamley, M. *Offshore processing options for oil platforms*. in *SPE Annual Technical Conference and Exhibition*. 2004. Society of Petroleum Engineers.
15. Nguyen, T.-V., et al., *Life performance of oil and gas platforms: Site integration and thermodynamic evaluation.* Energy, 2014. **73**: p. 282-301.
16. Badeer, G.H., *GE's LM2500+ G4 Aeroderivative Gas Turbine for Marine and Industrial Applications.* GE Energy, Paper No. GER-4250, 2005.
17. Saravanamuttoo, H.I.H., et al., *Gas turbine theory*. 6th ed. ed. 2009, Harlow: Prentice Hall.
18. Bolland, O., *Thermal power generation*. 2014: Department of Energy and Process Engineering - NTNU.
19. OD, et al., *Kraft fra land til norsk sokkel.* 2008.
20. Fossland, E.A. and R.S. Hauge, *Power from shore to Utsira High: evaluation of the project's cost efficiency and its effect on Norwegian and European emissions.* 2013.
21. LUNDBERG, S. and K.E. KASKI, *Strøm fra land til olje-og gassplattformer*. 2011, ZERO.
22. NVE - Norges vassdrags- og energitilsyn. *Varedeklarasjon 2014*. 2015 [cited 2016 30.05.2016]; Available from: https://www.nve.no/elmarkedstilsynet-marked-og-monopol/varedeklarasjon/varedeklarasjon-2014/.
23. Moran, M., *Principles of engineering thermodynamics*. 7th ed., SI version. ed. 2012, Hoboken, N.J: Wiley.
24. Bakken, L.E., *Thermodynamics Compression and Expansion Processes*.
25. Schultz, J.M., *The polytropic analysis of centrifugal compressors.* Journal of Engineering for Gas Turbines and Power, 1962. **84**(1): p. 69-82.

26. Incropera, F.P., D.P. DeWitt, and T.L. Bergman, *Principles of heat and mass transfer*. 7th ed. ed. 2013, Singapore: Wiley.
27. Kehlhofer, R., et al., *Combined-cycle gas and steam turbine power plants, third edition*. 3rd ed ed. 2009: PennWell Corporation.
28. Oljedirektoratet, *Utslipp av NOx fra petroleumsvirksomheten på norsk sokkel.* 2013.
29. General Electric. *LM2500*. [cited 2015 17/11/2015]; Available from: https://powergen.gepower.com/products/aeroderivative-gas-turbines/lm2500-gas-turbine-family.html.
30. General Electric, *LM2500+G4 Marine Gas Turbine datasheet*. 2016.
31. General Electric Oil and Gas, *SeaSmart Offshore Package™ for power generation or mechanical drive*. 2016.
32. Halvorsen group. *Waste heat recovery units*. 2016 03.06.2016]; Available from: http://www.halvorsen.no/product/waste-heat-recovery-units.
33. Nord, L.O., E. Martelli, and O. Bolland, *Weight and power optimization of steam bottoming cycle for offshore oil and gas installations.* Energy, 2014. **76**: p. 891-898.
34. Paffel, K., *Best practices for steam turbine maintenance and operation.* Plant Engineering, 2011.
35. !!! INVALID CITATION !!! [23, 35].
36. Nord, L.O. and O. Bolland, *Steam bottoming cycles offshore - Challenges and possibilities.* Journal of Power Technologies, 2012. **92**(3): p. 201.
37. Leonardo, P., et al., *WASTE HEAT RECOVERY FOR OFFSHORE APPLICATIONS*. 2012, Unpublished.
38. Hamid, E., P. Pilidis, and M. Newby, *The performance modelling of a single and dual pressure unfired once through steam generator*. 2011. p. 181-191.
39. Shin Nippon Machinery CO. LTD, *Internal Extraction Pressure Control Steam Turbine.* 2009.
40. Akhtar, S.Z., Power Eengineering, and Bechtel Power Corporation, *Proper Steam Bypass System Design Avoids Steam Turbine Overheating.* 2003.
41. Statoil, *Utsira high electrification sketch*. 2012.
42. Hoval. *THW-I HTE Industrial Gas Boiler*. 2015 [cited 2015 08.12.2015]; Available from: http://www.hoval.co.uk/products/thw-i-hte/?mobile=true.
43. Norwegian Metrological Institute. *Weather data from station no. 76926, Sleipner A.* 2016 [cited 2016 12.04.2016]; Available from: eklima.met.no.
44. Torvanger, A. and T. Ericson, *Fører elektrifisering av plattformer på norsk sokkel til reduserte CO2-utslepp?* CICERO Report, 2013.
45. Asplan Viak and Jernbaneverket, *Environmental analysis Climate - Norwegian High Speed Railway Project Phase 3.* 2012.
46. Inernational Energy Agency and F. Birol, *World energy outlook 2013.* International Energy Agency, 2013. **1**.
47. European Environment Agency, *Overview of electricity production and use in Europe*. 2016.
48. Rivera-Alvarez, A., M.J. Coleman, and J.C. Ordonez, *Ship weight reduction and efficiency enhancement through combined power cycles.* Energy, 2015. **93**: p. 521-533.
49. Flatebø, Ø., *Off-design simulations of offshore combined cycles*, in *Department of Energy and Process Engineering*. 2012, Norwegian University of Science and Technology, NTNU: NTNU.
50. Følgesvold, E.R., *Combined heat and power plant on offshore oil and gas installations*, in *Faculty of Engineering Science and Technology*. 2015, Norwegian Univeristy of Science and Technology: NTNU.
51. Nord, L.O. and O. Bolland, *Design and off-design simulations of combined cycles for offshore oil and gas installations.* Applied Thermal Engineering, 2013. **54**(1): p. 85.
52. General Electric, *LM6000 Marine Gas Turbine datasheet*. 2016.
53. Kloster, P., *Energy Optimization on Offshore Installations with Emphasis on offshore Combined Cycle Plants*, in *Offshore Europe Conference*, S.o.P.E. Inc, Editor. 1999.
54. General Electric, *LM2500 Marine Gas Turbine datasheet*. 2016.

55. General Electric, *LM2500+ Marine Gas Turbine datasheet*. 2016.
56. ABB, *Environmental Product Declaration Power Transformers 40/50 MVA (ONAN/ONAF)* 2003.

A Appendix

A.1 Detailed design information

Here all the detailed design point values and information for the major components are presented for each case to allow for verification and reproduction of the results.

A.1.1 Case 1a

Table A.1 Specifications of the gas turbines used in case 1a.

Both gas turbines	
Model types	2x LM2500G4+ Gas, DLE
Frequency [Hz]	50
Power rating [MW]	32.006
Exhaust flow rating [kg/s]	89.906
Exhaust temperature rating [°C]	529.51
Cooling duty [MW]	0
GT fuel	Methane
Fuel LHV [kJ/kg]	50,047
GT inlet Δp [bar]	0.010
Stack Δp [bar]	0.010
Gas turbine generator efficiency [%]	98.5

Table A.2 Specifications of the WHRUs used in case 1a.

Both WHRUs	
Ebsilon component number	26
UA [kW/K]	93.102
$\dot{Q}$ [kW]	21,967
$\dot{m}_{flue\ gas}$ [kg/s]	91.260
$T_{flue\ gas\ in}$ [°C]	498.593
$T_{flue\ gas\ out}$ [°C]	282.651
$p_{flue\ gas\ in}$ [bar]	1.022
$p_{flue\ gas\ out}$ [bar]	1.010
$\dot{m}_{water}$ [kg/s]	102.345
$T_{water\ in}$ [°C]	120
$T_{water\ out}$ [°C]	170
Flue gas Δp [bar]	0.012
ΔT_{lm} [k]	235.95
Direction of flow	Counter current

A.1.2 Case 1b

Table A.3 Specifications of the gas turbines used in case 1b.

Gas turbine 1	
Model type	LM6000 PF Sprint25 Gas, DLE
Frequency [Hz]	50
Power rating [MW]	47.132
Exhaust flow rating [kg/s]	131.689
Exhaust temperature rating [°C]	453.54
Cooling duty [MW]	0
GT fuel	Methane
Fuel LHV [kJ/kg]	50,047
GT inlet Δp [bar]	0.010
Stack Δp [bar]	0.010
Gas turbine generator efficiency [%]	98.5
Gas turbine 2	
Model type	LM2500G4+ Gas, DLE
Frequency [Hz]	50
Power rating [MW]	32.006
Exhaust flow rating [kg/s]	89.906
Exhaust temperature rating [°C]	529.51
Cooling duty [MW]	0
GT fuel	Methane
Fuel LHV [kJ/kg]	50,047
GT inlet Δp [bar]	0.010
Stack Δp [bar]	0.010
Gas turbine generator efficiency [%]	98.5

Table A.4 Specifications of the WHRUs used in case 1b.

WHRU for GT1	
Ebsilon component number	26
UA [kW/K]	97.363
$\dot{Q}$ [kW]	21,967
$\dot{m}_{flue\ gas}$ [kg/s]	100.445
$T_{flue\ gas\ in}$ [°C]	477.229
$T_{flue\ gas\ out}$ [°C]	279.974
$p_{flue\ gas\ in}$ [bar]	1.022
$p_{flue\ gas\ out}$ [bar]	1.010
$\dot{m}_{water}$ [kg/s]	102.345
$T_{water\ in}$ [°C]	120
$T_{water\ out}$ [°C]	170
Flue gas Δp [bar]	0.012
ΔT_{lm} [k]	225.624
Direction of flow	Counter current
WHRU for GT2	
Ebsilon component number	26
UA [kW/K]	93.387
$\dot{Q}$ [kW]	21,967
$\dot{m}_{flue\ gas}$ [kg/s]	90.589
$T_{flue\ gas\ in}$ [°C]	498.885
$T_{flue\ gas\ out}$ [°C]	281.346
$p_{flue\ gas\ in}$ [bar]	1.022
$p_{flue\ gas\ out}$ [bar]	1.010
$\dot{m}_{water}$ [kg/s]	102.345
$T_{water\ in}$ [°C]	120
$T_{water\ out}$ [°C]	170
Flue gas Δp [bar]	0.012
ΔT_{lm} [k]	235.23
Direction of flow	Counter current

A.1.3 Case 2a

Table A.5 Specifications of the gas turbines used in case 2a.

Gas turbine 1	
Model type	LM2500G4+ Gas, DLE
Frequency [Hz]	50
Power rating [MW]	32.006
Exhaust flow rating [kg/s]	89.906
Exhaust temperature rating [°C]	529.51
Cooling duty [MW]	0
GT fuel	Methane
Fuel LHV [kJ/kg]	50,047
GT inlet Δp [bar]	0.010
Stack Δp [bar]	0.010
Gas turbine generator efficiency [%]	98.5
Gas turbine 2	
Model type	LM2500 PJ Gas, DLE
Frequency [Hz]	50
Power rating [MW]	21.265
Exhaust flow rating [kg/s]	67.886
Exhaust temperature rating [°C]	538.9
Cooling duty [MW]	0
GT fuel	Methane
Fuel LHV [kJ/kg]	50,047
GT inlet Δp [bar]	0.010
Stack Δp [bar]	0.010
Gas turbine generator efficiency [%]	98.5

Table A.6 OTSG specification and values at design point of case 2a, with a break-down of the different heat transfer areas.

OSTG	
$\dot{Q}$, total heat transfer [kW]	56350
$\dot{m}_{flue\ gas}$ [kg/s]	149.632
$\dot{m}_{water/steam}$ [kg/s]	17.700
Minimum pinch point [°C]	35
Flue gas Δp [bar]	0.03
Water/steam Δp [bar]	0.075
Economizer	
Ebsilon component number	71
Specification	Give saturated water out
UA [kW/K]	183.596
$\dot{Q}$ [kW]	12885
$T_{flue\ gas\ in}$ [°C]	259.856
$T_{flue\ gas\ out}$ [°C]	178.789
$T_{water\ in}$ [°C]	55.517
$T_{water\ out}$ [°C]	224.063
ΔT_{lm} [k]	70.180
Evaporator	
Ebsilon component number	71
Specification	Give saturated steam out
UA [kW/K]	312.377
$\dot{Q}$ [kW]	32561
$T_{flue\ gas\ in}$ [°C]	455.964
$T_{flue\ gas\ out}$ [°C]	259.151
$T_{water\ in}$ [°C]	224.063
$T_{water\ out}$ [°C]	224.010
ΔT_{lm} [k]	104.235
Superheater	
Ebsilon component number	71
Specification	Give T_{steam} = 480 °C
UA [kW/K]	99.960
$\dot{Q}$ [kW]	10904
$T_{flue\ gas\ in}$ [°C]	519.868
$T_{flue\ gas\ out}$ [°C]	455.964
$T_{water\ in}$ [°C]	224.010
$T_{water\ out}$ [°C]	480.000
ΔT_{lm} [k]	109.080

Table A.7 Specification and values at design point of steam turbines in case 2a.

HP turbine	
Ebsilon component number	6
P_{in} [bar]	25
Pressure mode	Sliding pressure, Stodola's law
P_{out} [bar]	8.925
T_{in} [°C]	480
T_{out} [°C]	335.571
$\dot{m}_{steam}$ [kg/s]	17.700
η_{is} [-]	0.92
$\eta_{mech.}$ [-]	0.998
Off design characteristics	$(\dot{V}_{in} / \dot{V}_{out}) / (\dot{V}_{in,nominal} / \dot{V}_{out,nominal})$
Extraction	
$P_{extraction}$ [bar]	8.925
$T_{extraction}$ [°C]	335.571
$\dot{m}_{extraction}$ [kg/s]	3.969
LP turbine	
Ebsilon component number	6
P_{in} [bar]	8.925
Pressure mode	Sliding pressure, Stodola's law
P_{out} [bar]	0.04
T_{in} [°C]	335.571
T_{out} [°C]	28.962
$\dot{m}_{steam}$ [kg/s]	13.731
η_{is} [-]	0.88
$\eta_{mech.}$ [-]	0.998
Off design characteristics	$(\dot{V}_{in} / \dot{V}_{out}) / (\dot{V}_{in,nominal} / \dot{V}_{out,nominal})$
Generator	
Ebsilon component number	11
$\eta_{gen.}$ [-]	0.985
Power factor (cos(φ))	0.85

Table A.8 Condenser and steam extraction components in case 2a. Sizing of condenser in case of steam turbine by-pass was not considered. The cooling water mass flow was very high and a higher water outlet temperature could have been considered, but it does not impact the overall performance of the CCGT to a significant degree.

Condenser	
Ebsilon component number	7
Specification	Give $T_{CW,out}$ =18.962 °C
UA [kW/K]	2150.182
$\dot{Q}$ [kW]	30094.872
Condensing pressure [bar]	0.040
T_{steam} [°C]	28.962
$\dot{m}_{steam}$ [kg/s]	13.731
Cooling water medium	Salt water
$\dot{m}_{CW}$ [kg/s]	884.079
Cooling water lift head [bar]	3
$T_{CW,in}$ [°C]	10.023
$T_{CW,.out}$ [°C]	18.962
ΔT_{lm} [k]	13.996
Process heat de-superheater and condenser	
Ebsilon component number	7
Specification	Give $T_{water,out}$ =170.000 °C
UA [kW/K]	1033.997
$\dot{Q}$ [kW]	20853
Condensing pressure [bar]	8.925
$T_{steam,in}$ [°C]	332.768
$T_{water,out}$ [°C]	175.000
$\dot{m}_{steam}$ [kg/s]	8.752
Process heat medium	Pressurised water
$\dot{m}_{process\ water}$ [kg/s]	102.409
$T_{process\ water,in}$ [°C]	122.631
$T_{process\ water,out}$ [°C]	170.000
ΔT_{lm} [k]	20.167
Process heat economizer	
Ebsilon component number	26
Specification	Terminal temperature difference 25 K
UA [kW/K]	30.764
$\dot{Q}$ [kW]	1139
$T_{water,in}$ [°C]	175.000
$T_{water,out}$ [°C]	145.010
$\dot{m}_{water}$ [kg/s]	8.752
Process heat medium	Pressurised water
$\dot{m}_{process\ water}$ [kg/s]	102.409
$T_{process\ water,in}$ [°C]	120.010
$T_{process\ water,out}$ [°C]	122.631
ΔT_{lm} [k]	37.013

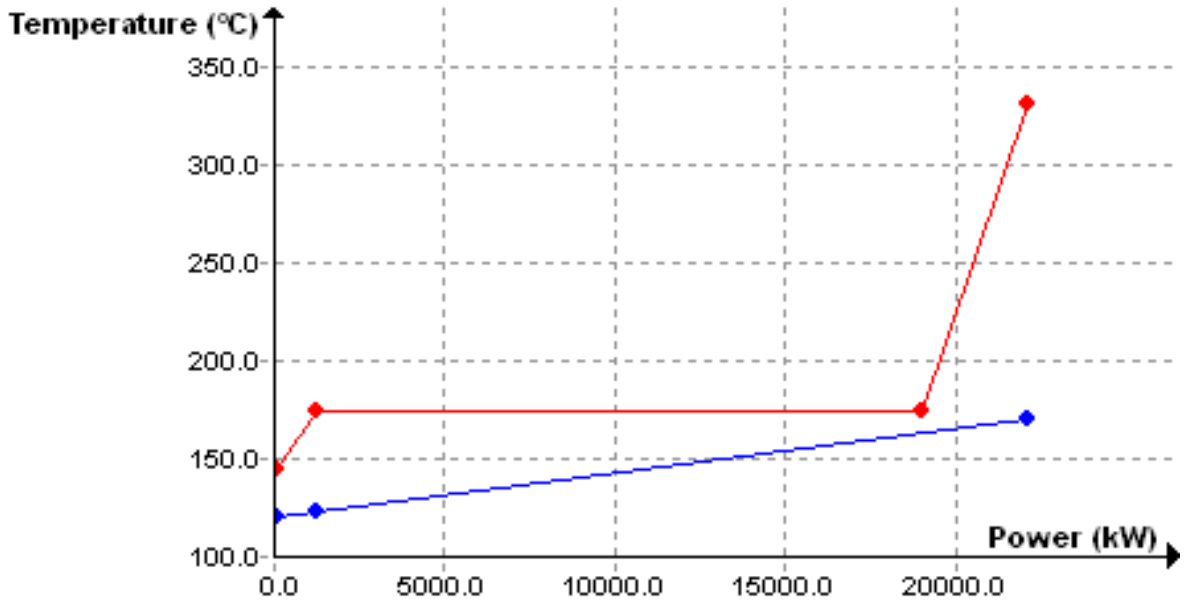

Figure A.1 A Q-T diagram of the process heat condenser and economizer in Ebsilon Professional, to verify that the minimum pinch point temperature was not too low. By zooming in it was found that it was at 12 K at design point of 22 MW process heat.

A.1.4 Case 2b

The design values shown here is after modifications were done in chapter 7. In the screening selection in chapter 6 the WHRU was not properly implemented and was only considered as a back-up.

Table A.9 Specifications of the gas turbines used in case 2b.

Both gas turbines	
Model types	2x LM2500G4+ Gas, DLE
Frequency [Hz]	50
Power rating [MW]	32.006
Exhaust flow rating [kg/s]	89.906
Exhaust temperature rating [°C]	529.51
Cooling duty [MW]	0
GT fuel	Methane
Fuel LHV [kJ/kg]	50,047
GT inlet Δp [bar]	0.010
Stack Δp [bar]	0.010
Gas turbine generator efficiency [%]	98.5

Table A.10 Specifications of the WHRU used in case 2b.

WHRU	
Ebsilon component number	26
UA [kW/K]	94.011
$\dot{Q}$ [kW]	21.937
$\dot{m}_{flue\ gas}$ [kg/s]	89.206
$T_{flue\ gas\ in}$ [°C]	498.885
$T_{flue\ gas\ out}$ [°C]	278.373
$p_{flue\ gas\ in}$ [bar]	1.022
$p_{flue\ gas\ out}$ [bar]	1.010
$\dot{m}_{water}$ [kg/s]	102.406
$T_{water\ in}$ [°C]	120.406
$T_{water\ out}$ [°C]	169.900
Flue gas Δp [bar]	0.012
ΔT_{lm} [k]	233.350
Direction of flow	Counter current

Table A.11 OTSG specification and values at design point of case 2b, with a break-down of the different heat transfer areas.

OSTG	
$\dot{Q}$, total heat transfer [kW]	37911
$\dot{m}_{flue\ gas}$ [kg/s]	95.016
$\dot{m}_{water/steam}$ [kg/s]	11.515
Minimum pinch point [°C]	35
Flue gas Δp [bar]	0.03
Water/steam Δp [bar]	0.075
Economizer	
Ebsilon component number	71
Specification	Give saturated water out
UA [kW/K]	129.997
$\dot{Q}$ [kW]	9635
$T_{flue\ gas\ in}$ [°C]	259.067
$T_{flue\ gas\ out}$ [°C]	173.048
$T_{water\ in}$ [°C]	29.462
$T_{water\ out}$ [°C]	224.063
ΔT_{lm} [k]	74.113
Evaporator	
Ebsilon component number	71
Specification	Give saturated steam out
UA [kW/K]	201.102
$\dot{Q}$ [kW]	21182
$T_{flue\ gas\ in}$ [°C]	460.042
$T_{flue\ gas\ out}$ [°C]	259.067
$T_{water\ in}$ [°C]	224.063
$T_{water\ out}$ [°C]	224.010
ΔT_{lm} [k]	105.333
Superheater	
Ebsilon component number	71
Specification	Give T_{steam} = 480 °C
UA [kW/K]	61.416
$\dot{Q}$ [kW]	7094
$T_{flue\ gas\ in}$ [°C]	525.248
$T_{flue\ gas\ out}$ [°C]	460.042
$T_{water\ in}$ [°C]	224.010
$T_{water\ out}$ [°C]	480.000
ΔT_{lm} [k]	115.500

Table A.12 Specification and values at design point of steam turbines in case 2b.

HP turbine	
Ebsilon component number	6
P_{in} [bar]	25
Pressure mode	Sliding pressure, Stodola's law
P_{out} [bar]	8.925
T_{in} [°C]	480
T_{out} [°C]	341.509
$\dot{m}_{steam}$ [kg/s]	11.515
η_{is} [-]	0.92
$\eta_{mech.}$ [-]	0.998
Off design characteristics	$(\dot{V}_{in} / \dot{V}_{out}) / (\dot{V}_{in,nominal} / \dot{V}_{out,nominal})$
Extraction	
$P_{extraction}$ [bar]	8.925
$T_{extraction}$ [°C]	341.509
$\dot{m}_{extraction}$ [kg/s]	0.019
LP turbine	
Ebsilon component number	6
P_{in} [bar]	8.800
Pressure mode	Sliding pressure, Stodola's law
P_{out} [bar]	0.04
T_{in} [°C]	341.509
T_{out} [°C]	28.962
$\dot{m}_{steam}$ [kg/s]	11.496
η_{is} [-]	0.88
$\eta_{mech.}$ [-]	0.998
Off design characteristics	$(\dot{V}_{in} / \dot{V}_{out}) / (\dot{V}_{in,nominal} / \dot{V}_{out,nominal})$
Generator	
Ebsilon component number	11
$\eta_{gen.}$ [-]	0.985
Power factor (cos(φ))	0.85

Table A.13 Condenser and steam extraction components in case 2b. Sizing of condenser in case of steam turbine by-pass was not considered. The cooling water mass flow was very high and a higher water outlet temperature could have been considered, but it does not impact the overall performance of the CCGT to a significant degree.

Condenser	
Ebsilon component number	7
Specification	Give $T_{CW,out}$ =18.962 °C
UA [kW/K]	1804.578
$\dot{Q}$ [kW]	25296
Condensing pressure [bar]	0.040
T_{steam} [°C]	28.962
$\dot{m}_{steam}$ [kg/s]	11.496
Cooling water medium	Salt water
$\dot{m}_{CW}$ [kg/s]	712.198
Cooling water lift head [bar]	3
$T_{CW,in}$ [°C]	10.023
$T_{CW,.out}$ [°C]	18.962
ΔT_{lm} [k]	14.018
Process heat de-superheater and condenser	
Ebsilon component number	124
Specification	Give $T_{water,out}$ =170.000 °C
UA [kW/K]	209.372
$\dot{Q}$ [kW]	20852
Condensing pressure [bar]	8.925
$T_{steam,in}$ [°C]	339.144
$T_{water,out}$ [°C]	175.000
$\dot{m}_{steam}$ [kg/s]	8.702
Process heat medium	Pressurised water
$\dot{m}_{process\ water}$ [kg/s]	102.403
$T_{process\ water,in}$ [°C]	122.640
$T_{process\ water,out}$ [°C]	170.000
ΔT_{lm} [k]	99.595
Process heat economizer	
Ebsilon component number	26
Specification	Terminal temperature difference 25 K
UA [kW/K]	30.581
$\dot{Q}$ [kW]	1139
$T_{water,in}$ [°C]	175.000
$T_{water,out}$ [°C]	145.019
$\dot{m}_{water}$ [kg/s]	8.702
Process heat medium	Pressurised water
$\dot{m}_{process\ water}$ [kg/s]	102.406
$T_{process\ water,in}$ [°C]	120.019
$T_{process\ water,out}$ [°C]	122.640
ΔT_{lm} [k]	37.017

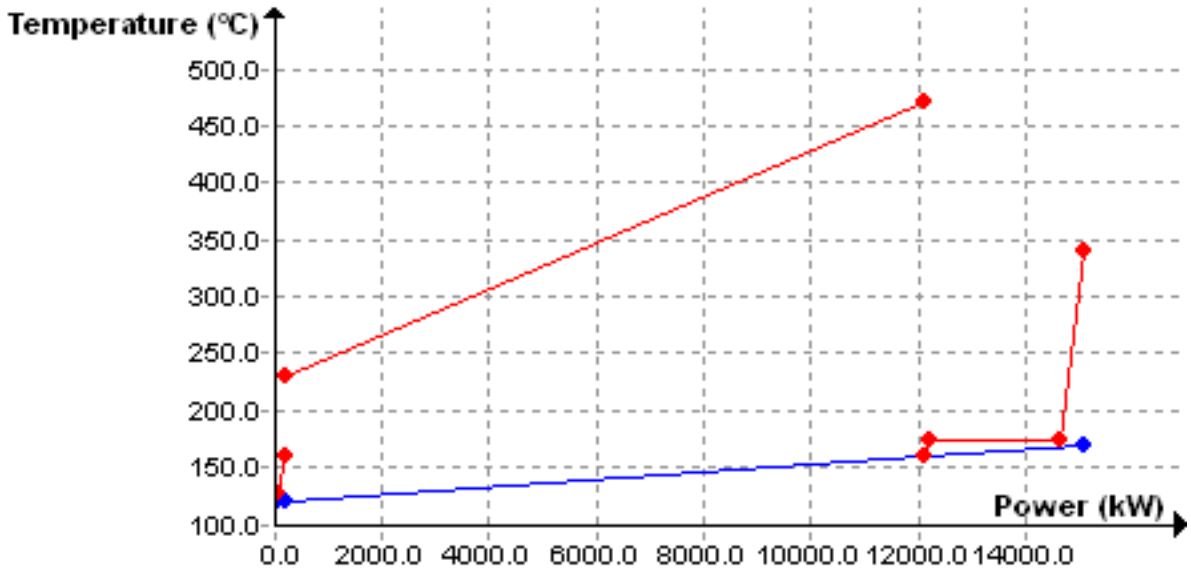

Figure A.2 A Q-T diagram of the process heat cycle in case 2b. The line that runs from 475 to 240 °C is the flue gas from the GT running at 5 MW load. Even at such low loads the flue gas can deliver the majority of the 15 MW process heat delivered in this case and increases the steam cycle efficiency by extracting less steam. The blue line is the process heat water going from 120 to 170 °C. Very low minimum pinch points are due to the low extraction steam mass flows.

A.1.5 Case 2c

Only the design points of the case with 170 °C process heat supply is shown here. The test of 120 °C process heat supply would only have been relevant in the screening selection if it could have performed equally to the extraction steam cycle.

Table A.14 Specifications of the gas turbines used in case 2c.

Gas turbine 1	
Model type	LM2500G4+ Gas, DLE
Frequency [Hz]	50
Power rating [MW]	32.006
Exhaust flow rating [kg/s]	89.906
Exhaust temperature rating [°C]	529.51
Cooling duty [MW]	0
GT fuel	Methane
Fuel LHV [kJ/kg]	50,047
GT inlet Δp [bar]	0.010
Stack Δp [bar]	0.010
Gas turbine generator efficiency [%]	98.5
Gas turbine 2	
Model type	LM2500+ Gas, DLE
Frequency [Hz]	50
Power rating [MW]	29.212
Exhaust flow rating [kg/s]	87.201
Exhaust temperature rating [°C]	530.83
Cooling duty [MW]	0
GT fuel	Methane
Fuel LHV [kJ/kg]	50,047
GT inlet Δp [bar]	0.010
Stack Δp [bar]	0.010
Gas turbine generator efficiency [%]	98.5

Table A.15 OTSG specification and values at design point of case 2c, with a break-down of the different heat transfer areas.

OSTG	
$\dot{Q}$, total heat transfer [kW]	54717
$\dot{m}_{flue\ gas}$ [kg/s]	173.497
$\dot{m}_{water/steam}$ [kg/s]	20.460
Minimum pinch point [°C]	35
Flue gas Δp [bar]	0.03
Water/steam Δp [bar]	0.075
Economizer	
Ebsilon component number	71
Specification	Give saturated water out
UA [kW/K]	96.603
$\dot{Q}$ [kW]	4475
$T_{flue\ gas\ in}$ [°C]	259.113
$T_{flue\ gas\ out}$ [°C]	235.196
$T_{water\ in}$ [°C]	175.396
$T_{water\ out}$ [°C]	224.063
ΔT_{lm} [k]	46.328
Evaporator	
Ebsilon component number	71
Specification	Give saturated steam out
UA [kW/K]	362.022
$\dot{Q}$ [kW]	37638
$T_{flue\ gas\ in}$ [°C]	455.177
$T_{flue\ gas\ out}$ [°C]	259.113
$T_{water\ in}$ [°C]	224.063
$T_{water\ out}$ [°C]	224.010
ΔT_{lm} [k]	103.965
Superheater	
Ebsilon component number	71
Specification	Give T_{steam} = 480 °C
UA [kW/K]	116.889
$\dot{Q}$ [kW]	12604
$T_{flue\ gas\ in}$ [°C]	518.843
$T_{flue\ gas\ out}$ [°C]	455.177
$T_{water\ in}$ [°C]	224.010
$T_{water\ out}$ [°C]	480.000
ΔT_{lm} [k]	107.828

Table A.16 Specification and values at design point of the back-pressure steam turbine and generator in case 2c.

HP turbine	
Ebsilon component number	6
P_{in} [bar]	25
Pressure mode	Sliding pressure, Stodola's law
P_{out} [bar]	8.924
T_{in} [°C]	480
T_{out} [°C]	335.570
$\dot{m}_{steam}$ [kg/s]	20.460
η_{is} [-]	0.92
$\eta_{mech.}$ [-]	0.998
Off design characteristics	$(\dot{V}_{in} / \dot{V}_{out}) / (\dot{V}_{in,nominal} / \dot{V}_{out,nominal})$
Generator	
Ebsilon component number	11
$\eta_{gen.}$ [-]	0.985
Power factor (cos(φ))	0.85

Table A.17 Main condenser and back-pressure condenser with de-superheating in case 2c. Sizing of the main condenser in case of steam turbine by-pass was not considered. The cooling water mass flow was very high and a higher water outlet temperature could have been considered, but it does not impact the overall performance of the CCGT to a significant degree.

Main condenser	
Ebsilon component number	7
Specification	Give $T_{CW,out}$ =20.000 °C
UA [kW/K]	243.158
$\dot{Q}$ [kW]	38889
Condensing pressure [bar]	8.924
$T_{steam,,in}$ [°C]	335.570
$T_{water,out}$ [°C]	175.000
$\dot{m}_{steam}$ [kg/s]	16.281
Cooling water medium	Salt water
$\dot{m}_{CW}$ [kg/s]	977.060
Cooling water lift head [bar]	3
$T_{CW,in}$ [°C]	10.023
$T_{CW,.out}$ [°C]	20.000
ΔT_{lm} [k]	159.937
Process heat condenser	
Ebsilon component number	7
Specification	Give $T_{water,out}$ =170.000 °C
UA [kW/K]	1053.841
$\dot{Q}$ [kW]	21961.278
Condensing pressure [bar]	8.924
$T_{steam,in}$ [°C]	335.562
$T_{water,out}$ [°C]	175.000
$\dot{m}_{steam}$ [kg/s]	9.194
Process heat medium	Pressurised water
$\dot{m}_{process\ water}$ [kg/s]	102.343
$T_{process\ water,in}$ [°C]	120.048
$T_{process\ water,out}$ [°C]	170.000
ΔT_{lm} [k]	20.839

A.1.6 Case 2d

Table A.18 Specifications of the gas turbine used in case 2d.

Gas turbine	
Model type	LM6000 PF Sprint25 Gas, DLE
Frequency [Hz]	50
Power rating [MW]	47.132
Exhaust flow rating [kg/s]	131.689
Exhaust temperature rating [°C]	453.54
Cooling duty [MW]	0
GT fuel	Methane
Fuel LHV [kJ/kg]	50,047
GT inlet Δp [bar]	0.010
Stack Δp [bar]	0.010
Gas turbine generator efficiency [%]	98.5

Table A.19 OTSG specification and values at design point in case 2d, with a break-down of the different heat transfer areas.

OSTG	
$\dot{Q}$, total heat transfer [kW]	40763
$\dot{m}_{flue\ gas}$ [kg/s]	138.501
$\dot{m}_{water/steam}$ [kg/s]	13.075
Minimum pinch point [°C]	35
Flue gas Δp [bar]	0.03
Water/steam Δp [bar]	0.075
Economizer	
Ebsilon component number	71
Specification	Give saturated water out
UA [kW/K]	131.621
$\dot{Q}$ [kW]	10401
$T_{flue\ gas\ in}$ [°C]	259.107
$T_{flue\ gas\ out}$ [°C]	189.222
$T_{water\ in}$ [°C]	39.331
$T_{water\ out}$ [°C]	224.063
ΔT_{lm} [k]	79.025
Evaporator	
Ebsilon component number	71
Specification	Give saturated steam out
UA [kW/K]	260.114
$\dot{Q}$ [kW]	24052
$T_{flue\ gas\ in}$ [°C]	416.632
$T_{flue\ gas\ out}$ [°C]	259.107
$T_{water\ in}$ [°C]	224.063
$T_{water\ out}$ [°C]	224.010
ΔT_{lm} [k]	92.469
Superheater	
Ebsilon component number	71
Specification	Give T_{steam} = 420 °C
UA [kW/K]	66.894
$\dot{Q}$ [kW]	6310
$T_{flue\ gas\ in}$ [°C]	456.995
$T_{flue\ gas\ out}$ [°C]	416.632
$T_{water\ in}$ [°C]	224.010
$T_{water\ out}$ [°C]	420.000
ΔT_{lm} [k]	94.323

Table A.20 Specification and values at design point of the back-pressure steam turbine and generator used in case 2d.

Steam turbine	
Ebsilon component number	6
P_{in} [bar]	25
Pressure mode	Sliding pressure, Stodola's law
P_{out} [bar]	0.070
T_{in} [°C]	480
T_{out} [°C]	335.570
$\dot{m}_{steam}$ [kg/s]	20.460
η_{is} [-]	0.88
$\eta_{mech.}$ [-]	0.998
Off design characteristics	$(\dot{V}_{in} / \dot{V}_{out}) / (\dot{V}_{in,nominal} / \dot{V}_{out,nominal})$
Generator	
Ebsilon component number	11
$\eta_{gen.}$ [-]	0.985
Power factor (cos(φ))	0.85

Table A.21 Main condenser and back-pressure condenser with de-superheating in case 2d. Sizing of the main condenser in case of steam turbine by-pass was not considered. The cooling water mass flow was very high and a higher water outlet temperature could have been considered, but it does not impact the overall performance of the CCGT to a significant degree.

Condenser	
Ebsilon component number	7
Specification	Give $T_{CW,out}$ =18.962 °C
UA [kW/K]	1168.827
$\dot{Q}$ [kW]	28326
Condensing pressure [bar]	0.070
$T_{steam,,in}$ [°C]	39.001
$T_{water,out}$ [°C]	39.001
$\dot{m}_{steam}$ [kg/s]	13.075
Cooling water medium	Salt water
$\dot{m}_{CW}$ [kg/s]	794.454
Cooling water lift head [bar]	3
$T_{CW,in}$ [°C]	10.023
$T_{CW,.out}$ [°C]	18.962
ΔT_{lm} [k]	24.234

Table A.22 The gas boiler were designed to have a conservative efficiency of 85 %, which was accomplished by adjusting the flue gas temperature out of the combustion chamber.

Gas boiler	
Efficiency [-]	0.85
ER [kg CO_2/MWh]	235
Combustion chamber	
Ebsilon component number	22
Specification	Give 730 °C flue gas
Combustion air stoichiometric ratio	1.2
$\eta_{combustion}$ [-]	0.995
$\dot{m}_{fuel}$ [kg/s]	0.517
Fuel	Methane
Fuel LHV [kJ/kg]	50,047
$T_{flue\ gas\ out}$ [°C]	730
$T_{combustion\ air.in}$ [°C]	105.030
$T_{cooling\ air.in}$ [°C]	24.878
$\dot{m}_{combustion\ air}$ [kg/s]	10.792
$\dot{m}_{cooling\ air}$ [kg/s]	22.571
Fuel LHV [kJ/kg]	50,047
Δp [bar]	0.015
Economizer	
Ebsilon component number	26
UA [kW/K]	116.038
$\dot{Q}$ [kW]	21972
$\dot{m}_{flue\ gas}$ [kg/s]	33.880
$T_{flue\ gas\ in}$ [°C]	730
$T_{flue\ gas\ out}$ [°C]	155.030
$p_{flue\ gas\ in}$ [bar]	1.030
$p_{flue\ gas\ out}$ [bar]	1.020
$\dot{m}_{water}$ [kg/s]	102.346
$T_{water\ in}$ [°C]	120.030
$T_{water\ out}$ [°C]	170.000
Flue gas Δp [bar]	0.01
Air preheater	
Ebsilon component number	25
Specification	50 K upper terminal temperature difference
UA [kW/K]	11.814
$\dot{Q}$ [kW]	878.578
$T_{flue\ gas\ in}$ [°C]	155.030
$T_{flue\ gas\ out}$ [°C]	130.481
$T_{air\ in}$ [°C]	24.878
$T_{air\ out}$ [°C]	105.030
ΔT_{lm} [k]	74.369

A.1.7 Case 3

The power from land was set up as a custom stream in Ebsilon Professional to be able to produce results through Ebsilon professional that were gathered in Excel. The mass flow was adjusted to adjust the onshore ER and power production to produce correct CO_2 emissions while the energy flow was used as power flow.

Table A.23 The set-up of the custom onshore power stream at 60 MW. Due to energy and mass flow limits within the software, an CO_2 fraction of 10 % were used.

Power stream	
Nitrogen mass fraction [-]	0.99
CO_2 mass fraction [-]	0.01
Mass flow	ER*Energy flow*100*3600/100
Energy flow	$(\dot{W}_{platform\ demand}+\dot{W}_{fan})$ / (1-TL)

Table A.24 The gas boiler were designed to have a conservative efficiency of 85 %, which was accomplished by adjusting the flue gas temperature out of the combustion chamber. A fan was used to provide air flows.

Gas boiler	
Efficiency [-]	0.85
ER [kg CO_2/MWh]	235
Combustion chamber	
Ebsilon component number	22
Specification	Give 730 °C flue gas
Combustion air stoichiometric ratio	1.2
$\eta_{combustion}$ [-]	0.995
$\dot{m}_{fuel}$ [kg/s]	0.517
Fuel	Methane
Fuel LHV [kJ/kg]	50,047
$T_{flue\ gas\ out}$ [°C]	730
$T_{combustion\ air.in}$ [°C]	105.030
$T_{cooling\ air.in}$ [°C]	24.878
$\dot{m}_{combustion\ air}$ [kg/s]	10.792
$\dot{m}_{cooling\ air}$ [kg/s]	22.571
Fuel LHV [kJ/kg]	50,047
Δp [bar]	0.015
Economizer	
Ebsilon component number	26
UA [kW/K]	116.038
$\dot{Q}$ [kW]	21972
$\dot{m}_{flue\ gas}$ [kg/s]	33.880
$T_{flue\ gas\ in}$ [°C]	730
$T_{flue\ gas\ out}$ [°C]	155.030
$p_{flue\ gas\ in}$ [bar]	1.030
$p_{flue\ gas\ out}$ [bar]	1.020
$\dot{m}_{water}$ [kg/s]	102.346
$T_{water\ in}$ [°C]	120.030
$T_{water\ out}$ [°C]	170.000
Flue gas Δp [bar]	0.01
Air preheater	
Ebsilon component number	25
Specification	50 K upper terminal temperature difference
UA [kW/K]	11.814
$\dot{Q}$ [kW]	878.578
$T_{flue\ gas\ in}$ [°C]	155.030
$T_{flue\ gas\ out}$ [°C]	130.481
$T_{air\ in}$ [°C]	24.878
$T_{air\ out}$ [°C]	105.030
ΔT_{lm} [k]	74.369

A.1.8 Tabled heat and power load profile

Table A.25 Tabled power and heat load profile used in the simulations.

Year	Power load [MW]	Heat load [MW]
2016	41.44	17.17
2017	50.76	19.14
2018	51.47	18.86
2019	58.66	20.07
2020	59.72	19.78
2021	59.10	19.11
2022	58.75	18.50
2023	48.19	15.89
2024	37.71	13.49
2025	37.71	13.15
2026	37.45	12.77
2027	36.92	12.34
2028	36.74	11.98
2029	34.16	11.29
2030	33.72	10.92
2031	33.90	10.64
2032	33.90	10.33
2033	33.90	10.03
2034	33.90	9.72
2035	8.34	7.14

A.2 Script used for running case 2a lifetime simulation

As the other scripts were similar with a few variations or less complex it was decided that it is enough to only include the lifetime simulation script for the combined cycle. Below is the core part of the script that was run to simulate a lifetime operation of a platform with a constant power and heat demand every year and 4 different ambient temperatures each year. After setting power, heat and temperatures, a for-loop is run 80 times (20 years, 4 times per year) and the results are written into string arrays before being written into an excel file when the script is finished. After the maximum power outputs at running 1 or 2 gas turbines are found a nested for-loop is used to iterate to the correct power output and breaks when the power error is below (power goal)/10000, which usually was found in 5-10 iterations. Initialization of variables, arrays, start values, excel formatting, writing of every string array to excel is and other non-essential code is removed.

```
//Heat and power profile
yearpower[0]  := 41.44;yearheat[0]  := 17.71;
yearpower[1]  := 50.76;yearheat[1]  := 19.14;
yearpower[2]  := 51.47;yearheat[2]  := 18.86;
yearpower[3]  := 58.66;yearheat[3]  := 20.07;
yearpower[4]  := 59.72;yearheat[4]  := 19.78;
yearpower[5]  := 59.10;yearheat[5]  := 19.11;
yearpower[6]  := 58.75;yearheat[6]  := 18.50;
yearpower[7]  := 48.19;yearheat[7]  := 15.89;
yearpower[8]  := 37.71;yearheat[8]  := 13.49;
yearpower[9]  := 37.71;yearheat[9]  := 13.15;
yearpower[10] := 37.45;yearheat[10] := 12.77;
yearpower[11] := 36.92;yearheat[11] := 12.34;
yearpower[12] := 36.74;yearheat[12] := 11.98;
yearpower[13] := 34.16;yearheat[13] := 11.29;
yearpower[14] := 33.72;yearheat[14] := 10.92;
yearpower[15] := 33.90;yearheat[15] := 10.64;
yearpower[16] := 33.90;yearheat[16] := 10.33;
yearpower[17] := 33.90;yearheat[17] := 10.03;
yearpower[18] := 33.90;yearheat[18] := 9.72;
yearpower[19] := 8.34; yearheat[19] := 7.14;

for i:=0 to years-1 do //set emission ratings
   begin
   yearER[i]:=500-i/19*250; //max at year 0, min at year 19
   //yearheat[i]:=15; //use to set a constant heat load
   if i>19 then
      yearpower[i]:=32.58;
   end;

//-------Weather profile----
//ambRH:=82.8
//ambP:=1.000
setlength(seasonT,4);
seasonT[0]:=5.62;
seasonT[1]:=7.40;
seasonT[2]:=10.50;
seasonT[3]:=13.97;

minpartload := 0.15;
sparepower := 5000;

//Lifetime simulation
for i:=0 to N-1 do
   begin
   getebsvar(heat, "cont_h.SCV");
   getebsvar(ambT, "val_air.T");
   powergoal := (yearpower[i/4 mod years]*1000);
   heat := yearheat[i/4 mod years]*1000;
   ambT := seasonT[i mod 4];
   println("Powergoal, heat & ambT:" + printtostring(powergoal) +
", " +printtostring(heat)+" & " +printtostring(ambT));

   getEbsvar(gt1, "Gas_turbine_1.Q");
   getEbsvar(gt2, "Gas_turbine_2.Q");
```

```
   getEbsvar(gt1mode, "Gas_turbine_1.FLOAD");
   getEbsvar(gt2mode, "Gas_turbine_2.FLOAD");
   getEbsvar(steamT, "Controller.SCV");
   steamT := 480;
   gt1mode := 0;
   gt2mode := 0;
   simulate;
   gt1base := p_gt1_out.Q;
   gt2base := p_gt2_out.Q;
   gt1mode := 1;
   gt2mode := 5;
   gt1:=gt1base*1.1-sparepower;
   simulate;
   powerreal:=(p_gt1_out.Q+p_gt2_out.Q+p_st_out.Q-pu_2.Q-pu_3.Q-
pu_4.Q);

   CCcase := 1;
   if powergoal < powerreal then
      begin
      CCcase := 1;
      end
   else
      begin
      gt1mode := 0;
      gt2mode := 1;
      gt2 := gt2base*minpartload;
      simulate;
      powerreal:=(p_gt1_out.Q+p_gt2_out.Q+p_st_out.Q-pu_2.Q-pu_3.Q-
pu_4.Q);
      if powergoal < powerreal then
         begin
         CCcase := 2;
         end
      else
         begin
         CCcase := 3;
         end;
      end;
   println(" ");
   println("------Base power GT1: " + printtostring(gt1base) + "---
---");
   println("------Max case power: " + printtostring(powerreal) + "-
-----");
   println("------Power goal: " + printtostring(powergoal) + "-----
-");
   println("------CC case: " + printtostring(CCcase) + "------");
   //Correct power output
   for jj:=0 to 30 do
      begin
      //gt2_p-(real-goal)*0,7=new_gt2_p
      println("Power error: " + printtostring(powerreal-
powergoal));
      steamT := min(480,Fluegas.T-15);
      println("Steam temperature set to: "
+printtostring(Controller.SCV));
```

```
     if (jj<6) then //check major error
        begin
        if CCcase = 1 then
           begin
           gt2 := 0;
           gt2mode :=5; //bypass
           gt1mode :=1; //desired power
           gt1 := p_gt1_out.Q + (p_gt2_out.Q-(powerreal-
powergoal)*((p_gt1_out.Q+p_gt2_out.Q)/powerreal));
           end;
        if CCcase = 2 then
           begin
           gt1mode :=1;
           gt2mode :=1;
           gt1 := p_gt1_out.Q -(powerreal-
powergoal)*((p_gt1_out.Q+p_gt2_out.Q)/powerreal);
           gt2 :=gt2base*minpartload;
           end;
        if CCcase = 3 then
           begin
           gt1 := gt1base;
           gt1mode :=0; //baseload
           gt2mode :=1; //desired power
           gt2 := (p_gt2_out.Q-(powerreal-
powergoal)*((p_gt1_out.Q+p_gt2_out.Q)/powerreal));
           end;
        //println("GT1 and GT2: " + printtostring(Gas_turbine_1.Q)
+ " & " + printtostring(Gas_turbine_2.Q));
        end
     else //check minor   error
        begin
        if CCcase = 1 then
           begin
           println(printtostring(p_gt1_out.Q) +", "
+printtostring(gt1base) +", " +printtostring(p_gt2_out.Q) +", "
+printtostring(jj)+", " +printtostring( (2490 > p_gt2_out.Q >
2510) or jj<10 or (p_gt1_out.Q < (gt1base - gt2base*minpartload))
) );
           gt2 := 0;
           gt1mode :=1;
           gt2mode :=5; //bypass
           gt1 := p_gt1_out.Q + (p_gt2_out.Q-(powerreal-
powergoal)*0.4);
           if jj>14  then
              begin
              gt1mode :=1;
              gt2 := 0;
              gt2mode :=5;
              gt1 := p_gt1_out.Q + (p_gt2_out.Q-(powerreal-
powergoal)*0.2);
              end;
           //println("Is equal?: " +printtostring(p_gt1_out.Q) +" "
+printtostring(Gas_turbine_1.Q) +" " +printtostring(gt1));
           end;
        if CCcase = 2 then
           begin
```

```
           gt1mode := 1;
           gt2mode := 1;
           gt1 := p_gt1_out.Q -(powerreal-powergoal)*0.4;
           gt2 :=gt2base*minpartload;
           if jj>14 then
              begin
              gt1mode := 1;
              gt2mode := 1;
              gt1 := p_gt1_out.Q -(powerreal-powergoal)*0.2;
              gt2 :=gt2base*minpartload;
              end;
           end;
        if CCcase = 3 then
           begin
           gt1 := gt1base;
           gt1mode :=0;
           gt2mode :=1; //desired power
           gt2 := (p_gt2_out.Q-(powerreal-powergoal)*0.4);
           if jj>14 then
              begin
              gt1 := gt1base;
              gt1mode := 0;
              gt2mode := 1;
              gt2 := (p_gt2_out.Q-(powerreal-powergoal)*0.2);
              end;
           end;
        //println("GT1 and GT2: " + printtostring(Gas_turbine_1.Q)
+ " & " + printtostring(Gas_turbine_2.Q));
        end;
     simulate;
     println("GT1 and GT2: " + printtostring(p_gt1_out.Q) + " & "
+ printtostring(p_gt2_out.Q));
     powerreal:=(p_gt1_out.Q+p_gt2_out.Q+p_st_out.Q-pu_1.Q-pu_2.Q-
pu_3.Q-pu_4.Q);
     println("Power out, goal and error: "
+printtostring(powerreal) +", " +printtostring(powergoal) +" & " +
printtostring(powerreal-powergoal));
     println("---------------|||||-------------- END of (" +
printtostring(i) + "," + printtostring(jj) +")");
     if (abs(powerreal-powergoal) < powergoal/10000) then
        begin
        println("Unusually low error, break.");
        break;
        end;
     end;
     //Gather results in string arrays before writing to excel
     arA[i+1]:=printToString(p_gt1_out.Q);
     arB[i+1]:=printToString(p_gt2_out.Q);
     arC[i+1]:=printToString(p_st_out.Q);
     arD[i+1]:=printToString(p_h_out.Q);
     arF[i+1]:=printToString(Air.T);
     arG[i+1]:=printToString(air_RH.MEASM);
     arH[i+1]:=printToString(m_f_in.M);
     arJ[i+1]:=printToString(Stack.M*Stack.XCO2);
     arK[i+1]:=printToString(m_f_in.NCV);
     arL[i+1]:=printToString((m_f_in.M*m_f_in.NCV) / 1000);
```

```
     arM[i+1]:=printToString((p_gt1_out.Q+p_gt2_out.Q+p_st_out.Q-
pu_2.Q-pu_3.Q-pu_4.Q) / 1000);

   arO[i+1]:=printToString((p_gt1_out.Q+p_gt2_out.Q+p_st_out.Q+p_h_
out.Q-pu_2.Q-pu_3.Q-pu_4.Q) / 1000);
     arP[i+1]:=printToString((p_gt1_out.Q) /
(m_f1_in.M*m_f1_in.NCV));
     if p_gt2_out.Q <> 0 then
        arQ[i+1]:=printToString((p_gt2_out.Q) /
(m_f2_in.M*m_f2_in.NCV));
     arR[i+1]:=printtostring((p_st_out.Q) / (m_f_in.M*m_f_in.NCV-
(p_gt1_out.Q+p_gt2_out.Q)));//steam cycle efficiency
     arS[i+1]:=printtostring((p_gt1_out.Q+p_gt2_out.Q+p_st_out.Q)
/ (m_f_in.M*m_f_in.NCV));

   arT[i+1]:=printtostring((p_gt1_out.Q+p_gt2_out.Q+p_st_out.Q+p_h_
out.Q) / (m_f_in.M*m_f_in.NCV));
     arU[i+1]:=printtostring((Stack.M*Stack.XCO2)*3600*1000 /
(p_gt1_out.Q+p_gt2_out.Q+p_st_out.Q));
     arV[i+1]:=printtostring((Stack.M*Stack.XCO2)*3600*1000 /
(p_gt1_out.Q+p_gt2_out.Q+p_st_out.Q+p_h_out.Q));
     arW[i+1]:=printtostring((Stack.M*Stack.XCO2)*3600*8410 /
1000);
     if inputressult[0] = "val_power.P" then
        arW[i+1]:=printtostring((Stack.M*Stack.XCO2)*3600*8410 /
4000);
     arX[i+1]:=printtostring(h_steam.T);
     arY[i+1]:=printtostring(h_steam.P);
     arZ[i+1]:=printtostring(l_steam.X);
     arZ2[i+1]:=printtostring(pu_2.Q+pu_3.Q+pu_4.Q);
     if i > 0 then
        arZ3[i+1]:=printtostring(atof(arW[i+1])+atof(arZ3[i]));
     if i = 0 then
        arZ3[i+1]:=printtostring(atof(arW[i+1]));
     arZ6[i+1]:=printtostring(st1.M1M1N);
     arZ7[i+1]:=printtostring(st2.M1M1N);
     arZ8[i+1]:=printtostring(Condenser1.M1M1N);
     arZ9[i+1]:=printtostring(Steam.P);

   end;

//Writing to excel document

end;
```